

ชีวสังเคราะห์ของไฟโตสเตอรอลในเซลล์เพาะเลี้ยงของเป็ดน้ำน้อย



นายดำรง ก่องดวง

สถาบันวิทยบริการ

จุฬาลงกรณ์มหาวิทยาลัย

วิทยานิพนธ์นี้เป็นส่วนหนึ่งของการศึกษาตามหลักสูตรปริญญาวิทยาศาสตรดุษฎีบัณฑิต

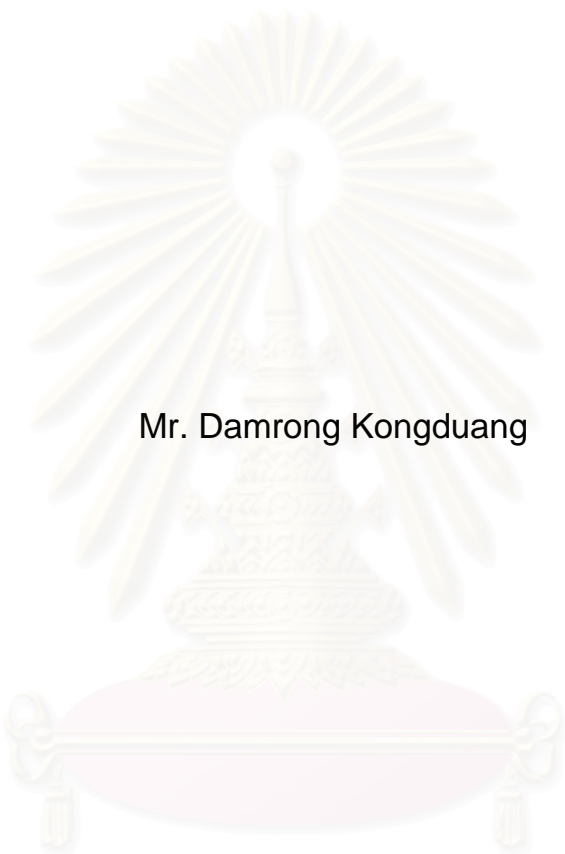
สาขาวิชาเภสัชเคมีและผลิตภัณฑ์ธรรมชาติ

คณะเภสัชศาสตร์ จุฬาลงกรณ์มหาวิทยาลัย

ปีการศึกษา 2550

ลิขสิทธิ์ของจุฬาลงกรณ์มหาวิทยาลัย

BIOSYNTHESIS OF PHYTOSTEROLS IN CELL SUSPENSION CULTURES
OF *CROTON STELLATOPILOSUS*



Mr. Damrong Kongduang

A Dissertation Submitted in Partial Fulfillment of the Requirements for the Degree of
Doctor of Philosophy Program in Pharmaceutical Chemistry and Natural Products
Faculty of Pharmaceutical Sciences

Chulalongkorn University

Academic year 2007

Copyright of Chulalongkorn University

Thesis Title BIOSYNTHESIS OF PHYTOSTEROLS IN CELL SUSPENSION
 CULTURES OF *CROTON STELLATOPILOSUS*
By Mr. Damrong Kongduang
Field of Study Pharmaceutical Chemistry and Natural Products
Thesis Advisor Associate Professor Wanchai De-Eknamkul, Ph.D.
Thesis Co-advisor Assistant Professor Juraithip Wungsintaweekul, Ph.D.

Accepted by the Faculty of Pharmaceutical Sciences, Chulalongkorn University in
Partial Fulfillment of the Requirements for the Doctoral Degree

..... *Pornpen Pramyoti* Dean of the Faculty of Pharmaceutical Sciences
(Associate Professor Pornpen Pramyothin, Ph.D.)

THESIS COMMITTEE

..... *K. Kittisak* Chairman
(Associate Professor Kittisak Likhitwitayawuid, Ph.D.)

..... *Wanchai De-Eknamkul* Thesis Advisor
(Associate Professor Wanchai De-Eknamkul, Ph.D.)

..... *J. Wungsintaweekul* Thesis Co-advisor
(Assistant Professor Juraithip Wungsintaweekul, Ph.D.)

..... *Khanit Suwanborirux* Member
(Khanit Suwanborirux, Ph.D.)

..... *Rutt Suttisri* Member
(Associate Professor Rutt Suttisri, Ph.D.)

..... *Aran Incharoensakdi* Member
(Professor Aran Incharoensakdi, Ph.D.)


..... *Worapan Sitthithaworn* Member
(Assistant Professor Worapan Sitthithaworn, Ph.D.)

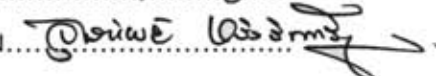
ตำรา ค ก่องดวง : ชีวสังเคราะห์ของไฟโตสเตอรอลในเซลล์เพาะเลี้ยงของเปล้าน้อย
(BIOSYNTHESIS OF PHYTOSTEROLS IN CELL SUSPENSION CULTURES OF
CROTON STELLATOPILOSUS) อ. ที่ปรึกษา : รศ.ดร. วันชัย ดีเอกนามกุล, อ. ที่ปรึกษาร่วม
: ผศ.ดร. จุไรทิพย์ หวังสินทวีกุล, 142 หน้า.

การศึกษาในครั้งนี้ เป็นการใช้เทคนิคการบ่อนสารติดตามเพื่อหาองค์ความรู้ใหม่เกี่ยวกับ วิถีชีวสังเคราะห์ของสารเทอปีนอยด์และไฟโตสเตอรอลในเซลล์เพาะเลี้ยงของเปล้าน้อย ซึ่งจะทำให้เข้าใจถึงแหล่งต้นกำเนิดของหน่วยไอโซพรีนของสารกลุ่มดังกล่าว การทดลองได้ดำเนินการโดยการบ่อนน้ำตาลให้เซลล์เพาะเลี้ยงด้วยกลูโคสที่ติดฉลากด้วยสารรังสีที่คาร์บอนตำแหน่งที่ 1 คือ $[1-^{14}\text{C}]$ glucose ซึ่งพบว่าเซลล์สามารถรับเอาสารติดตามเข้าสู่โมเลกุลของสารไฟโตสเตอรอลได้ สารไฟโตสเตอรอลที่แยกได้พบว่าเป็นสารผสมระหว่าง เบตา-ซิโตสเตอรอลและสตีกลมาสเตอรอล ซึ่งถูกสร้างขึ้นมากในวันที่ 4 หลังการบ่อนสารติดตาม ข้อมูลที่ได้จากการทดลองเบื้องต้นได้นำไปสู่การทดลองหลักที่บ่อนด้วย $[1-^{13}\text{C}]$ glucose และ $[2-^{13}\text{C}]$ sodium acetate ซึ่งพบว่าเซลล์เพาะเลี้ยงสามารถรับเอาคาร์บอนไอโซโทปเข้าสู่โมเลกุลของสารไฟโตสเตอรอลทั้งสองชนิดได้ในระดับสูงเมื่อทำการสกัดแยกสารติดตาม และวิเคราะห์โครงสร้างโมเลกุลของสารด้วยวิธีคาร์บอน 13 นิวเคลียร์แมกเนติกเรโซแนนซ์สเปกโตรสโกปี พบว่าสารผสมไฟโตสเตอรอลที่ได้มีรูปแบบการติดตามของคาร์บอน 13 เป็นไปตามแบบที่สอดคล้องกับการสร้างสารโดยใช้วิถีชีวสังเคราะห์ของ mevalonate โดยไม่พบว่ามีส่วนที่ติดฉลากมาจากการใช้วิถีชีวสังเคราะห์ของ deoxyxylulose phosphate (DXP) เลย จากนั้นได้ทำการศึกษาองค์ประกอบของเซลล์พืชในพืชและเซลล์เพาะเลี้ยงของเปล้าน้อยด้วยกล้องจุลทรรศน์อิเล็กตรอนแบบส่องผ่าน ซึ่งพบว่าในส่วนใบพบคลอโรพลาสต์ ที่มีโครงสร้างที่สมบูรณ์อยู่ในกลุ่มเซลล์พาลีเสด ขณะที่ในเซลล์เพาะเลี้ยงสีเขียว จะพบคลอโรพลาสต์บ้างเล็กน้อยซึ่งมีโครงสร้างยังไม่สมบูรณ์ ส่วนในเซลล์เพาะเลี้ยงไม่พบว่ามีคลอโรพลาสต์ในองค์ประกอบของเซลล์เลย นอกจากนี้ยังได้ทำการศึกษาการแสดงออกของยีน ด้วยเทคนิค semiquantitative RT-PCR ที่เกี่ยวข้องกับวิถีชีวสังเคราะห์ของ DXP คือยีน *dxs*, *dxr* และ *ggpps* พบว่าทั้งสามยีนมีการแสดงออกที่สูงมากเฉพาะในใบและเซลล์เพาะเลี้ยงสีเขียวเท่านั้น แต่ไม่พบการแสดงออกในเซลล์เพาะเลี้ยง ดังนั้นจึงสรุปว่าวิถีชีวสังเคราะห์ของไฟโตสเตอรอลในเซลล์เพาะเลี้ยงเปล้าน้อยที่มาจาก วิถีชีวสังเคราะห์ของ mevalonate แต่เพียงเส้นทางเดียวนั้น จะมีความเกี่ยวข้องกับการไม่แสดงออกของยีนที่เกี่ยวข้องกับวิถีชีวสังเคราะห์ของ DXP ในเซลล์เพาะเลี้ยงเปล้าน้อยซึ่งไม่มีคลอโรพลาสต์อยู่

สาขาวิชา เกษษเคมีและผลิตภัณฑ์ธรรมชาติ ลายมือชื่อนิสิต..... อังรค์ ก่องดวง.....

ปีการศึกษา 2550

ลายมือชื่ออาจารย์ที่ปรึกษา..... 

ลายมือชื่ออาจารย์ที่ปรึกษาร่วม..... 

4376952433: MAJOR PHARMACEUTICAL CHEMISTRY AND NATURAL PRODUCTS
 KEY WORD: BIOSYNTHESIS/ SUSPENSION CULTURES /*CROTON STELLATOPILOSUS*
 / PHYTOSTEROLS / β -SITOSTEROL / STIGMASTEROL / THE MEVALONATE PATHWAY
 / TRANSMISSION ELECTRON MICROSCOPY / TRANSCRIPTION PROFILE

DAMRONG KONGDUANG: BIOSYNTHESIS OF PHYTOSTEROLS IN CELL
 SUSPENSION CULTURES OF *CROTON STELLATOPILOSUS*. THESIS ADVISOR:
 ASSOC. PROF. WANCHAI DE-EKNAMKUL, Ph.D., THESIS CO-ADVISOR: ASST.
 PROF. JURAITHIP WUNGSINTAWEEKUL, Ph.D., 142 pp.

This study aimed to use the techniques of feeding experiments to understand the biosynthetic process of terpenoids and phytosterols with respect to their origin of isoprene units in *Croton stellatopilosus* cell suspension cultures. Feeding experiments with labeled glucose was first optimized for feeding conditions by using radioactively labeled [1-¹⁴C]glucose followed by monitoring its radiolabel uptake. The preliminary results showed that the highest incorporation of the labeled glucose occurred after 4 days of the feedings. Under the optimized conditions, [1-¹³C]glucose and [2-¹³C]sodium acetate were then fed into the cell suspension cultures of *C. stellatopilosus*. β -Sitosterol and stigmasterol, the two major phytosterols produced, were isolated and their ¹³C-labeling patterns elucidated using quantitative NMR spectroscopy. Analysis of the ¹³C-enrichment patterns revealed that the components of all isoprene units of the phytosterols were supplied exclusively from the mevalonate pathway. No isoprene units originated from the alternative deoxyxylulose phosphate (DXP) pathway were detected in this study. Transmission electron micrographs (TEM) showed that there were different developmental stages of chloroplasts in different *C. stellatopilosus* tissues. In leaf, the chloroplasts were fully developed in palisade cells, the green callus contained a few chloroplasts with partial development, whereas no chloroplasts were found in the suspension cultured cells. Molecular analysis on the transcription level of these different types of tissues by using semi-quantitative RT-PCR technique revealed that the three genes (*dxs*, *dxr* and *ggpps*) involved in the isoprenoid biosynthetic route of the DXP pathway were strongly expressed in the plant leaf and green callus culture but rarely expressed in the suspension culture. This study indicated that the operation of either the DXP pathway or MVA pathway for the isoprene formation in *C. stellatopilosus* is dependent upon types of cultures and ability of chloroplast-forming cells in the tissues of *C. stellatopilosus*.

Field of study Pharmaceutical Chemistry
 and Natural Products
 Academic year 2007

Student's signature... *Damrong Kongduang*
 Advisor's signature... *Wanchai De Eknamkul*
 Co-advisor's signature... *J. Wung-sintaweekul*

ACKNOWLEDGEMENTS

I would like to express my sincere gratitude and deep appreciation to my advisor Associate Professor Dr. Wanchai De-Eknamkul, for his concern, guidance, encouragement and suggestion throughout the research study.

I sincerely acknowledge Assistant Professor Dr. Juraithip Wungsintaweekul, my co-advisor, for her valuable advice, supervision and understanding throughout my work, especially in the feeding and the molecular cloning experiments.

I would like to thank Assistant Professor Dr. Worapan Sitthithaworn for the information of *ggpps* and gift of *ggpps* specific primers.

I am grateful to laboratory assistants, colleagues and friends at the Faculty of Pharmaceutical Sciences, Chulalongkorn University, and also the staffs, postgraduates and friends at tissue culture laboratory, Department of Pharmacognosy and Pharmaceutical Botany, Faculty of Pharmaceutical Sciences, Prince of Songkla University and the staffs of the Scientific Equipment Center, Prince of Songkla University for suggestions on Gel Document, NMR, GC and GC-MS instruments.

I would like to thank the Royal Golden Jubilee (RGJ) Ph.D. Program. Thailand Research Fund (TRF) for financial support, the Faculty of Pharmaceutical Sciences, Chulalongkorn University and Department of Pharmacognosy and Pharmaceutical Botany, Faculty of Pharmaceutical Sciences, Prince of Songkla University, for providing laboratory facilities, equipments and chemical compounds.

Finally, I am grateful to my parents, my wife and my family for their love, encouragement, support and care. The usefulness of this dissertation, I dedicate to my parents and all my teachers.

CONTENTS

	Page
ABSTRACT (Thai).....	iv
ABSTRACT (English).....	v
ACKNOWLEDGEMENTS.....	vi
CONTENTS.....	vii
LIST OF TABLES.....	xii
LIST OF FIGURES.....	xiv
LIST OF SCHEMES.....	xx
ABBREVIATIONS.....	xxi
CHAPTER I INTRODUCTION.....	1
CHAPTER II LITERATURE REVIEW.....	6
1. <i>Croton stellatopilosus</i> Ohba.....	6
1.1 Botanical description of <i>Croton stellatopilosus</i> Ohba.....	6
1.2 The evidence of changing name from <i>Croton sublyratus</i> Kurz to <i>Croton stellatopilosus</i> Ohba.....	8
1.3 Medicinal uses of <i>C. stellatopilosus</i>	9
1.3.1 Thai folk medicinal uses.....	9
1.3.2 Therapeutic uses of Plaunoi.....	9
1.4 Chemical constituents of <i>C. stellatopilosus</i>	10
2. Plaunotol.....	14
2.1 Physicochemical properties.....	14
2.2 Various techniques used for obtaining plaunotol.....	15
2.2.1 Plaunotol isolation	15
2.2.2 Plaunotol extraction and purification	15
2.2.3 Determination of plaunotol content by thin-layer chromatography (TLC) densitometric.....	16
2.2.4 Determination of plaunotol content by gas chromatography method.....	17

	Page
2.2.5 Chemical synthesis of plaunotol.....	17
2.3 Biosynthesis.....	17
2.4 Antipeptic ulcer activity.....	18
2.5 Production of plaunotol in tissue culture techniques.....	20
3. The biosynthetic pathway of terpenoids.....	20
3.1 The classical mevalonate (MVA) pathway.....	21
3.2 The deoxyxylulose phosphate (DXP) pathway.....	24
3.3 Cross-talk between MVA and DXP pathways in plants.....	26
4. Previous biosynthetic studies in <i>C. stellatopilosus</i>	28
4.1 Feeding experiments (incorporation experiment).....	28
4.2 Cell-free extracts.....	29
CHAPTER III MATERIALS AND METHODS.....	30
1. Materials.....	30
1.1 Plant materials.....	30
1.2 Chemicals, kits and enzymes.....	30
1.3 Instrumentations.....	31
1.4 Solution preparations.....	34
2. Methods.....	34
2.1 Tissue culture techniques.....	34
2.1.1 Nutrient media.....	34
2.1.2 Induction of callus culture.....	36
2.1.3 Induction of green callus culture.....	36
2.1.4 Induction of suspension culture.....	37
2.1.5 Time-course study of <i>C. stellatopilosus</i> suspension cultures...	37

	Page
2.2 Phytochemical studies	37
2.2.1 Sample extraction.....	37
2.2.2 Screening of secondary metabolites.....	38
2.2.3 Isolation of secondary metabolites.....	39
2.3 Feeding experiments.....	42
2.3.1 Feeding with [1- ¹⁴ C]glucose.....	42
2.3.2 Feeding with [U- ¹³ C]glucose.....	42
2.3.3 Feeding with [1- ¹³ C]glucose.....	43
2.3.4 Feeding with [2- ¹³ C]sodium acetate.....	43
2.4 Semi-quantitative RT-PCR technique.....	43
2.4.1 RNA isolation.....	43
2.4.2 cDNA preparation.....	45
2.4.3 DNA fragment amplification.....	45
2.4.4 Agarose gel electrophoresis.....	48
2.5 Thin layer chromatography (TLC) analysis.....	49
2.5.1 TLC-radioscanning.....	49
2.5.2 Detection of terpenoids and steroids on TLC plates.....	49
2.6 Gas chromatographic analysis.....	50
2.7 High performance liquid chromatography (HPLC) analysis.....	51
2.8 Gas chromatographic – mass spectrometric (GC-MS) analysis.....	52
2.9 Gel documentation.....	52
2.10 Quantitative ¹³ C NMR analysis.....	53
2.11 Transmission electron microscopy.....	53

	Page
CHAPTER IV RESULTS.....	55
1. Establishment of <i>Croton stellatopilosus</i> cell suspension cultures and their terpenoid and steroid biosynthetic potential	55
1.1 Establishment of callus culture.....	55
1.2 Establishment of green callus cultures.....	55
1.3 Establishment of suspension cultures.....	57
1.4 Detection of secondary metabolites by gas chromatography and gas chromatography – mass spectrometry	58
1.4.1 Detection of secondary metabolites by gas chromatography..	58
1.4.2 Identification of terpenoids and phytosterols by GC–MS.....	61
1.5 Time-course study of <i>C. stellatopilosus</i> cell suspension cultures...	67
2. Phytochemical studies.....	73
2.1 Isolation and purification of terpenoids and phytosterols.....	73
2.2 Identification of phytosterols	77
3. Feeding and incorporation experiments.....	85
3.1 Feeding with radioactively labeled [1- ¹⁴ C]glucose for system optimization.....	85
3.2 Feeding with [U- ¹³ C]glucose and analysis by GC-MS.....	88
3.3 Feeding with [1- ¹³ C]glucose and quantitative analysis by ¹³ C NMR	88
3.4 Feeding with [2- ¹³ C]sodium acetate and quantitative ¹³ C NMR analysis of phytosterols.....	94
3.5 Summary of quantitative ¹³ C NMR analysis of phytosterols.....	100

	Page
4. Transmission electron microscopic analysis.....	106
5. Comparative analysis of <i>dxs</i> , <i>dxr</i> and <i>ggpps</i> genes expression profiles of <i>C. stellatopilosus</i> plant and cell cultures.....	108
5.1 cDNA preparation of <i>C. stellatopilosus</i> leaf, green callus and suspension cultures.....	108
5.2 Transcription profiles analyses of <i>dxs</i> , <i>dxr</i> and <i>ggpps</i> genes.....	109
CHAPTER V DISCUSSION.....	112
1. <i>Croton stellatopilosus</i> suspension cultures	112
1.1 Establishment of cell suspension cultures of <i>C. stellatopilosus</i>	112
1.2 Detection of terpenoids and phytosterols by gas chromatography and gas chromatography – mass spectrometry.....	113
1.3 [1- ¹³ C]Glucose and [2- ¹³ C]sodium acetate feeding experiments on cell suspension cultures of <i>C. stellatopilosus</i>	114
2. The origin of isoprene blocks of phytosterol skeleton	115
2.1 Conversion of [1- ¹³ C]glucose to pyruvate by glycolytic pathway	117
2.2 Biosynthesis of IPP from pyruvate <i>via</i> the mevalonate pathway...	118
2.3 Biosynthesis of β -sitosterol and stigmasterol from IPP	119
3. Possible explanation on the sole operation of the MVA pathway in <i>C. stellatopilosus</i> cell suspension cultures.	120
4. Comparative analysis of <i>dxs</i> , <i>dxr</i> and <i>ggpps</i> gene expression profiles of <i>C. stellatopilosus</i> plant and cell cultures.....	124
5. Conclusions.....	125
REFERENCE.....	127
VITA.....	142

LIST OF TABLES

	Page
Table 1	Chemical constituents of <i>C. stellatopilosus</i>11
Table 2	Composition and preparation of MS agar.....35
Table 3	Contents of secondary metabolites in the crude extract of suspension culture of <i>C. stellatopilosus</i> on day 4.....69
Table 4	Contents of terpenoids and phytosterols isolated from feeding experiment of suspension cultures of <i>C. stellatopilosus</i> 74
Table 5	125 MHz ¹³ C NMR spectral data of the isolated major labeled compound (in CDCl ₃) in comparison with reported values (Wright et al., 1978) of β-sitosterol and stigmasterol.84
Table 6	¹³ C NMR analysis and relative ¹³ C-enrichment of β-sitosterol and stigmasterol from <i>C. stellatopilosus</i> cell suspension cultures fed with [1- ¹³ C]glucose and unlabeled glucose (control) under the same condition..... 92
Table 7	¹³ C NMR analysis and relative ¹³ C-enrichment of β-sitosterol and stigmasterol from <i>C. stellatopilosus</i> cell suspension cultures fed with [2- ¹³ C]sodium acetate and unlabeled glucose (control) under the same condition.....98
Table 8	Relative ¹³ C enrichment in carbons of β-sitosterol and stigmasterol derived from suspension cultures of <i>C. stellatopilosus</i> administered with [1- ¹³ C]glucose and [2- ¹³ C]acetate..... 101
Table 9	Average ¹³ C enrichment in carbon atom of the C ₅ isoprenic skeleton of stigmasterol and β-sitosterol incorporating [1- ¹³ C]glucose and [2- ¹³ C]sodium acetate 102

	Page
Table 10	Average relative ^{13}C -abundance of β -sitosterol and stigmasterol after feeding with $[1-^{13}\text{C}]$ glucose and $[2-^{13}\text{C}]$ sodium acetate102
Table 11	^{13}C -Enrichment of some carbon atoms in the molecules of stigmasterol and β -sitosterol fed with $[1-^{13}\text{C}]$ glucose <i>via</i> the mevalonate pathway 105
Table 12	^{13}C -Enrichment of some carbon atoms in the molecules of stigmasterol and β -sitosterol fed with $[2-^{13}\text{C}]$ sodium acetate <i>via</i> the mevalonate pathway 105
Table 13	The relative ^{13}C -enrichment of the two sterols. The values were calculated based on ^{13}C -NMR signal intensities of some relevant carbon atoms106
Table 14	The concentration and purity of the isolated total RNA108
Table 15	Expression profiles of genes from different sources of <i>C. stellatopilosus</i>110

LIST OF FIGURES

	Page
Figure 1	Two possible biosynthetic pathways of IPP based on the well-known mevalonate pathway (A) and the newly found non-mevalonate pathway (B) 2
Figure 2	<i>Croton stellatopilosus</i> Ohba (Euphorbiaceae) (A), Inflorescences (B), Leaves and fruits (C)..... 7
Figure 3	The chemical structure of plaunotol..... 14
Figure 4	Biosynthetic pathway of plaunotol..... 18
Figure 5	The classical mevalonate (MVA) pathway..... 22
Figure 6	The deoxyxylulose phosphate (DXP) pathway..... 25
Figure 7	Overview of isoprenoid metabolic pathways localized in the cytosol and in the plastids of plant cells..... 28
Figure 8	(A) Induction of callus from the leaf explants of <i>C. stellatopilosus</i> on MS agar medium containing 2.0 mg/l 2,4-D, 1.0 mg/l kinetin and 0.8% (w/v) plant agar. (B) Callus cultures of <i>C. stellatopilosus</i> obtained from the induction and were maintained on MS agar medium containing 1.0 mg/l 2,4-D, 1.0 mg/l BA and 0.8% (w/v) plant agar. 56
Figure 9	Green callus cultures grown on MS medium containing 1% (w/v) sucrose, 2.0 mg/l NAA, 2.0 mg/l BA and 2 g/L gellan gum. 56
Figure 10	(A) Cell suspension cultures of <i>C. stellatopilosus</i> maintained in MS liquid medium containing 3% (w/v) sucrose, 2.0 mg/L 2,4-D and 2.0 mg/L BA. (B) Cell suspension cultures after being harvested and washed thoroughly with distilled water for analysis of terpenoid and steroid formation. 57

	Page
Figure 11 First GC trial showing the GC chromatogram of crude hexane extract of the cell suspension cultures of <i>C. stellatopilosus</i> , 1= phytol and 2= GGOH	59
Figure 12 Second GC trial showing the GC chromatogram of crude hexane extract of the cell suspension cultures of <i>C. stellatopilosus</i> , 1= phytol, 2= GGOH, 3= campesterol, 4= stigmasterol and 5= β -sitosterol.....	59
Figure 13 Final GC optimization showing the GC chromatogram of crude hexane extract of the cell suspension cultures of <i>C. stellatopilosus</i> A; authentic compounds, B; suspension extract day 4, 1= phytol, 2= plaunotol, 3= GGOH, 4= campesterol, 5= stigmasterol and 6= β -sitosterol.....	60
Figure 14-1 Mass spectral data of phytol (A) from crude hexane extract of the cell suspension cultures of <i>C. stellatopilosus</i> comparison with the pattern of WILEY275 database library (B).	62
Figure 14-2 Mass spectral data of geranylgeraniol (C) from crude hexane extract of the cell suspension cultures of <i>C. stellatopilosus</i> comparison with the pattern of WILEY275 database library (D).	63
Figure 14-3 Mass spectral data of campesterol (E) from crude hexane extract of the cell suspension cultures of <i>C. stellatopilosus</i> comparison with the pattern of WILEY275 database library (F).	64
Figure 14-4 Mass spectral data of stigmasterol (G) from crude hexane extract of the cell suspension cultures of <i>C. stellatopilosus</i> comparison with the pattern of WILEY275 database library (H).	65

	Page
Figure 14-5 Mass spectral data of β -sitosterol (I) from crude hexane extract of the cell suspension cultures of <i>C. stellatopilosus</i> comparison with the pattern of WILEY275 database library (J).	66
Figure 15 Growth curve (A) and product formation curves (B) during a 14-day culture cycle of <i>C. stellatopilosus</i> cell suspension culture.	67
Figure 16 Calibration curve of authentic compounds.....	69
Figure 17 GC chromatograms (A); Authentic compounds, (B-F); crude hexane extract cell suspension cultures of <i>C. stellatopilosus</i> on day 0-day 14, 1=phytol, 2=GGOH, 3=campesterol, 4=stigmasterol and 5= β -sitosterol... ..	71
Figure 18 HPLC chromatograms of terpenoids isolated cell suspension cultures of <i>C. stellatopilosus</i> feeding with $[1-^{13}\text{C}]$ glucose, 1=Fr. 4.1 and 2=Fr. 4.2.	74
Figure 19 GC-MS chromatograms of phytol isolated from cell suspension cultures of <i>C. stellatopilosus</i> , feeding experiment with $[1-^{13}\text{C}]$ glucose (A) and $[2-^{13}\text{C}]$ sodium acetate (B)	75
Figure 20 Mass spectral data of (A) phytol isolated from cell suspension cultures of <i>C. stellatopilosus</i> , feeding experiment with $[1-^{13}\text{C}]$ glucose, (B) with $[2-^{13}\text{C}]$ sodium acetate, (C) standard phytol	76
Figure 21 Chemical structures of campesterol, stigmasterol and β -sitosterol	77
Figure 22 GC-MS chromatogram of phytosterols isolated from cell suspension cultures of <i>C. stellatopilosus</i>	78

	Page
Figure 23 Mass spectral data of phytosterols isolated from the cell suspension cultures of <i>C. stellatopilosus</i> . (A) campesterol, (B) stigmasterol and (C) β -sitosterol	79
Figure 24 500 MHz ^1H NMR spectrum (in CDCl_3) of the major compounds found in suspension cultures of <i>C. stellatopilosus</i>	80
Figure 25 125 MHz ^{13}C NMR spectrum (in CDCl_3) of the major compound found in suspension cultures of <i>C. stellatopilosus</i>	82
Figure 26 125 MHz ^{13}C NMR spectrum (in CDCl_3) of the major compound found in suspension cultures of <i>C. stellatopilosus</i> expanded from 10 to 31 ppm (A), 31 to 58 ppm (B) and 68-146 ppm (C).	83
Figure 27 Radio-uptake of $[1-^{14}\text{C}]$ glucose and growth curve during a 14-day culture cycle of <i>C. stellatopilosus</i> cell suspension cultures.....	86
Figure 28 Preliminary studies on feeding of $[1-^{14}\text{C}]$ glucose into <i>C. stellatopilosus</i> suspension cultures: (A). TLC plate detected under I_2 vapor, (B). TLC radiochromatograms using TLC-radioscanner, 1, 2 indicate the positions of GGOH and β -sitosterol, respectively.....	87
Figure 29 Comparison of 125 MHz ^{13}C NMR spectra of a mixture of phytosterols (β -sitosterol and stigmasterol) obtained from suspension cultures of <i>C. stellatopilosus</i> (A) unlabeled glucose incorporation, and (B) $[1-^{13}\text{C}]$ glucose incorporation.	90

	Page
Figure 30 ¹³ C-labeling patterns of <i>C. stellatopilosus</i> phytosterols obtained from the incorporation experiments using [1- ¹³ C]glucose. The value indicated at a particular carbon is the ¹³ C-enrichment ratio obtained from Table 6. The value of the carbon with * is the summation of NMR-signal overlapping of different carbons.	93
Figure 31 Comparison of 125 MHz ¹³ C NMR spectra of a mixture of phytosterols (β-sitosterol and stigmasterol) obtained from suspension cultures of <i>C. stellatopilosus</i> (A) unlabeled acetate incorporation, and (B) [2- ¹³ C]sodium acetate incorporation.....	95
Figure 32 ¹³ C-labeling patterns of <i>C. stellatopilosus</i> phytosterols obtained from the incorporation experiments using [2- ¹³ C]sodium acetate. The value indicated at a particular carbon is the ¹³ C-enrichment ratio obtained from Table 7. The value of the carbon with * is the summation of NMR-signal overlapping of different carbons.	99
Figure 33 Summary of the degree of ¹³ C-enrichment at various carbon atoms of β-sitosterol and stigmasterol.	104
Figure 34 Electron micrograph images of different tissues of <i>C. stellatopilosus</i> : (A) leaves, (B) palisade mesophyll cells in leaf, (x 3,800) and (C) its magnified palisade mesophyll cells in chloroplast, (x 15,200), (D) green callus, (E) a callus cell, (x 4,000) and (F) its magnified chloroplast (x 60,000), (G) cell suspension cultures and (H) suspension cultured cells (x 1,500). v=vacuole, n=nucleus, c=chloroplast and g=oil globule.....	107

	Page
Figure 35 Agarose gel electrophoresis of total RNA from leaves (L), green callus (C) and suspension cultures (S) of <i>C. stellatopilosus</i> , M; DNA ladder (SibEnzyme).....	109
Figure 36 The mRNA expression profiles of <i>dxs</i> , <i>dxr</i> and <i>ggpps</i> genes in plant leaves, green callus and suspension cultures: (A). 1.2% agarose gel electrophoresis of gene transcripts in comparison with the <i>18S rRNA</i> ; (B). relative intensity to <i>18S rRNA</i> of genes after gel documentation.....	111
Figure 37 ¹³ C-labeling patterns of β-sitosterol and stigmasterol after feeding with [1- ¹³ C]glucose (●) and [2- ¹³ C]sodium acetate (■)	120
Figure 38 Proposed relationship between the DXP pathway and MVA pathway occurring in whole leaf (A), callus culture (B) and cell suspension culture (C) of <i>C. stellatopilosus</i>	123

LIST OF SCHEMES

	Page
Scheme 1	
Separation of crude hexane extract of <i>C. stellatopilosus</i> suspension culture fed with [1- ¹³ C]glucose.....	40
Scheme 2	
Separation of crude hexane extract of <i>C. stellatopilosus</i> suspension culture fed with [2- ¹³ C]sodium acetate.....	41



สถาบันวิทยบริการ
จุฬาลงกรณ์มหาวิทยาลัย

ABBREVIATIONS AND SYMBOLS

β	=	beta
δ	=	chemical shift
μCi	=	microCurie
μg	=	microgram
μl	=	microliter
[1- ¹³ C]	=	carbon position 1 of the molecule is labeled with carbon 13
[1- ¹⁴ C]	=	carbon position 1 of the molecule is labeled with carbon 14
[2- ¹³ C]	=	carbon position 2 of the molecule is labeled with carbon 13
[U- ¹³ C]	=	all carbons of the molecule are uniformly labeled with carbon 13
¹ H-NMR	=	proton nuclear magnetic resonance
¹³ C-NMR	=	carbon 13 nuclear magnetic resonance
2,4-D	=	2,4-dichlorophenoxyacetic acid
AcCoA	=	acetyl coenzyme A
BA	=	6-benzylaminopurine
bp	=	base pair
°C	=	degree Celsius
cDNA	=	complementary deoxyribonucleic acid
CHCl ₃	=	chloroform
cm	=	centimeter
conc	=	concentration
cpm	=	count per minute
DEPC	=	diethyl pyrocarbonate
DMAPP	=	dimethylallyl pyrophosphate

DNA	=	deoxyribonucleic acid
dNTP	=	deoxynucleoside triphosphate
dpm	=	disintegration per minute
DXP	=	1-deoxy-D-xylulose-5-phosphate
DXR	=	1-deoxy-D-xylulose 5-phosphate reductoisomerase
<i>dxr</i>	=	1-deoxy-D-xylulose 5-phosphate reductoisomerase gene
DXS	=	1-deoxy-D-xylulose-5-phosphate synthase
<i>dxs</i>	=	1-deoxy-D-xylulose-5-phosphate synthase gene
eV	=	electron volt
FID	=	flame ionization detector
Fig	=	Figure
fw	=	fresh weight
g	=	gram
GAP	=	D-glyceraldehyde 3-phosphate
GC	=	gas chromatography
GGOH	=	geranylgeraniol
GGPPS	=	geranylgeranyl pyrophosphate synthase
<i>ggpps</i>	=	geranylgeranyl pyrophosphate synthase gene
HCl	=	hydrochloric acid
HMG-CoA	=	3-hydroxy-3-methylglutaryl-CoA
HMGR	=	3-hydroxy-3-methylglutaryl-CoA reductase
HPLC	=	high performance liquid chromatography
h	=	hour
H ₂ SO ₄	=	sulfuric acid
I ₂	=	iodine

IPP	=	isopentenyl pyrophosphate
kb	=	kilobase
kV	=	kilovolt
L	=	liter
lb	=	pound
M	=	molar
ME	=	2-C-methyl-D-erythritol
MeOH	=	methanol
MEP	=	2-C-methyl-D-erythritol 4-phosphate
mg	=	milligram
ml	=	milliliter
mM	=	millimolar
mRNA	=	messenger ribonucleic acid
MS	=	mass spectrometry
MS	=	Murashige and Skoog medium
MVA	=	mevalonic acid
MW	=	molecular weight
m/z	=	mass to charge ratio
N	=	normality
NAA	=	α -naphthaleneacetic acid
NaOH	=	sodium hydroxide
nm	=	nanometer
OD	=	optical density
pH	=	hydrogen ion concentration

ppm	=	part per million
Rf	=	retention factor
RNA	=	ribonucleic acid
RNase A	=	ribonuclease A
rpm	=	revolutions per minute
RT-PCR	=	Reverse Transcriptase Polymerase Chain Reaction
sec	=	second
TAE	=	tris acetate EDTA
TEM	=	transmission electron microscopy
temp.	=	temperature
TLC	=	thin-layer chromatography
UV	=	ultraviolet
UV-VIS	=	ultraviolet-visible
V	=	volt
v/v	=	volume by volume
WHO	=	World Health Organization
wt	=	weight
w/v	=	weight by volume
w/w	=	weight by weight

CHAPTER I

INTRODUCTION

Terpenoids and steroids are groups of natural products that play important roles in all living organisms. They function as steroid hormones in mammals, carotenoids in plants and ubiquinones in bacteria. Terpenoids, when considered together with the steroids, constitute the largest class of secondary metabolites comprising more than 30,000 known compounds (Hill, 2000). Many terpenoid compounds possess therapeutic activities such as paclitaxel (Taxol[®]) from *Taxus brevifolia*, ginkgolides from *Ginkgo biloba*, eleutherobin from a soft coral, etc.

Common biosynthetic building block of this group of compounds is the so-called isoprene unit, which is the metabolic form of isopentenyl diphosphate (IPP). It has been well established that the biosynthesis of IPP can proceed via two different pathways, namely the mevalonate (MVA) pathway and the non-mevalonate pathway. The mevalonate pathway has long been assumed to be the exclusive biosynthetic route used in all organisms for the biosynthesis of IPP (Spurgeon and Porter, 1981). The enzymology and regulation of this pathway have been well studied, particularly in mammalian systems where it is responsible for the biosynthesis of cholesterol (Sakakura, Shimano and Sone, 2001; Horton, 2002; Weber, Boll and Stampfl, 2004).

Recently, the existence in nature of the non-mevalonate pathway (Fig. 1) for the biosynthesis of certain terpenoids has been demonstrated (Lichtenthaler *et al.*, 1997). This finding was based on ¹³C-labelling patterns that are incompatible with the operation of the acetate-mevalonate pathway. Administration experiments with ¹³C-acetate and bacteria (Flesch and Rohmer, 1988) or ¹³C-glucose and *Ginkgo biloba* leaves (Schwarz, 1994) showed that their isolated terpenoids having labeling patterns that are not consistent with the MVA-origin.

This mevalonate-independent pathway (Fig. 1) starts from the condensation of pyruvate and glyceraldehyde-3-phosphate to form 1-deoxy-D-xylulose-5-phosphate (DXP) (Rohmer *et al.*, 1993, 1996). The latter is then rearranged and reduced to the key intermediate 2-C-methyl-D-erythritol-4-phosphate (MEP) (Takahashi *et al.*, 1998). Transformation of MEP to IPP proceeds via reductive elimination of a cyclic diphosphate intermediate (Rohdich *et al.*, 2000)

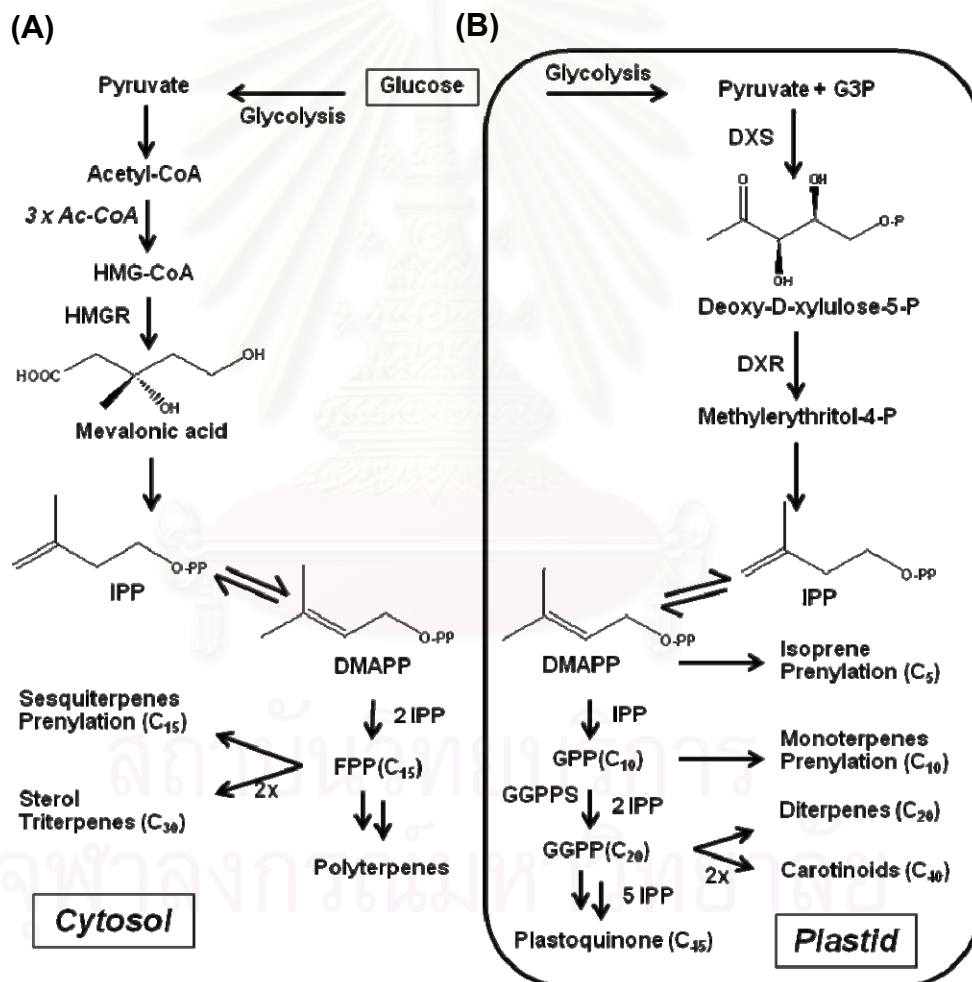


Figure 1 Two possible biosynthetic pathways of IPP based on the well-known mevalonate pathway (A) and the newly found non-mevalonate pathway (B) (Stefan *et al.*, 2006)

It has been proposed that in plants, the non-mevalonate pathway is generally operative for formation of monoterpenoids, diterpenoids, phytols and carotenoids (Hirai *et al.*, 2000; Umlauf *et al.*, 2004; Bouvier, Rahier and Camara, 2005) whereas the mevalonate pathway served for the skeletons of phytosterols, sesquiterpenes, triterpenes and polyterpenes. The two pathways leading to IPP are thus compartmentalized in the plastid and the cytosol, respectively. However, both pathways may function in the formation of certain isoprenoids, in a cooperative process that results from metabolic cross-talk within the plastidic envelope membrane (Enfissi *et al.*, 2005). For this aspect, a quantitative assessment of the differential contribution of the two IPP pathways in the biosynthesis of an individual isoprenoid may be deduced from the ^{13}C -labelling pattern, as determined by ^{13}C NMR spectroscopy, following incorporation of $[1-^{13}\text{C}]$ -D-glucose into product (Rohmer *et al.*, 1993; Umlauf *et al.*, 2004).

Confirmation of the presence of the non-mevalonate pathway will require characterization of the intermediates and enzymatic steps of this novel pathway. Although the non-mevalonate labelling patterns of terpenoids have been demonstrated in plants as mentioned above, these studies have been carried out only in a limited taxonomically families of plants. So far, only a few tropical plants have been investigated. Furthermore, several findings have suggested that plants contain multiple, parallel pathways for terpenoid biosynthesis, and the subcellular compartmentation of these pathways (i.e. in plastids) plays a central role in regulating the biosynthesis of a wide variety of terpenoids (McCaskill and Croteau, 1998). Therefore, more information from other sources of plants is still needed for a better understanding of terpenoid metabolism in plants.

Among Thai medicinal plants, *Croton stellatopilosus* Ohba (formerly named *C. sublyratus* Kurz.) or plau-noi is the only source of plaunotol, which is a potent

cytoprotective antipeptic ulcer (Ogiso *et al.*, 1978) and is particularly interesting. Presently, the leaves of *C. stellatopilosus* are well-known as being the raw material for manufacturing an antipeptic-ulcer drug, namely, Kelnac[®] which contains plaunotol as an active ingredient (Ogiso *et al.*, 1985). It acts by inhibiting the growth of *Helicobacter pylori* (Koga *et al.*, 1996).

Plaunotol is an acyclic diterpene alcohol and consists of four isoprene units attached in head to tail fashion (Ogiso *et al.*, 1978). It has been found to be accumulated in the leaves at up to 0.5% (w/w) of dry weight (Vongchareonsathit and De-Eknamkul, 1998). The isoprene units of plaunotol skeleton are originated from the DXP pathway (Wungsintaweekul and De-Eknamkul, 2005). The biosynthesis of plaunotol was first studied by De-Eknamkul and his co-workers in 1997. The enzyme geranylgeraniol 18-hydroxylase catalyzes the final committed step from the molecule of geranylgeraniol to plaunotol (Tansakul and De-Eknamkul, 1998). Recently, a phosphatase was reported to catalyze the step of dephosphorylation yielding geranylgeraniol from geranylgeranyl diphosphate (Nualkaew *et al.*, 2006). However, for the early step in the plaunotol biosynthesis, there is unfortunate lack of reported knowledge.

The structure of plaunotol is ideal for studying the biosynthesis of IPP in Plaunoi plant. Its acyclic diterpenoid molecule allows easy interpretation of ¹³C-labelling patterns to indicate whether the precursor IPP is formed *via* mevalonate or non-mevalonate pathway. However, the success will depend very much on the efficiency of ¹³C-incorporation experiments. The incorporation rate of ¹³C-precursors into plaunotol must be high enough so that the enrichment of ¹³C in particular atoms of plaunotol molecule is detectable by ¹³C-NMR. Low ¹³C-incorporation is usually a problem for experiments with intact plants or differentiated parts (i.e. leaves, roots, etc.). With tissue (*in vitro*) cultures, on the other hand, high incorporation of a

precursor into the product is normally observed, and it is obviously the material of choice.

Plant tissue and cell cultures of *C. stellatopilosus* have been established previously to study their potential to produce plaunotol. It has been shown that callus cultures of this plant could accumulate plaunotol under the presence of gelling agents in the medium (Morimoto and Murai, 1989). For cell suspension culture, it has been reported to produce geranylgeraniol (Kitaoka, Nagashima and Kamimura, 1989). Although the results appear to support my proposal, I have never repeated these experiments and both plaunotol and geranylgeraniol have not been found in my *C. stellatopilosus in vitro* cultures.

In the present study, suspension cultures of *C. stellatopilosus* reestablished in our laboratory were used for ^{13}C -incorporation experiments in order to demonstrate possible biosynthetic pathway of terpenoids operating in this plant. Therefore, this work aims to study the terpenoid biosynthetic pathway in the suspension cultures of *C. stellatopilosus* by $[1-^{13}\text{C}]$ glucose and $[2-^{13}\text{C}]$ acetate feeding experiments and quantitative ^{13}C NMR spectroscopy. Comparative analyses of the organelle-forming abilities, as well as mRNA expression of chloroplastidic genes in plant cells from leaf, green callus and suspension cultures, would be investigated. The results obtained from this study will be useful for understanding the terpenoid biosynthetic pathway, leading to enhancement of the terpenoid production in plant cell culture by metabolic engineering.

CHAPTER II

LITERATURE REVIEW

1. *Croton stellatopilosus* Ohba

1.1 Botanical description of *Croton stellatopilosus* Ohba

Croton stellatopilosus Ohba, formerly known as *Croton sublyratus* Kurz (Fig. 2), is a tropical plant belonging to the family Euphorbiaceae. This plant has been called in Thai as “Plaunoi”. It is a kind of shrub up to 6 m tall, branching from base; younger parts are distinctly pubescent; flowering with mature leaves. *Indumentum* consists of stellate-dendritic, yellowish to brown hairs with a slightly darker center, not flat, 0.2–0.8 mm in diameters. *Stipules* are 3-4 mm long, densely pubescent. *Leaves* are crowded but not pseudo-verticillate; petiole is 0.5–2.5 cm long, distinctly but not densely pubescent at least on younger leaves; leaf blade is obovate and sometimes constricted near base, rarely nearly elliptic, 6–18 by 3–7 cm, chartaceous, leaf base is attenuate, margin is serrate (teeth c. 5 mm apart), apex is acute to short-acuminate, The leaf is glabrous above, with scattered and distinct but not dense hairs below, basal glands are sessile, flat, 0.8–1 mm in diam. and often elongate-narrowed, partly to completely on the blade very close to the petiole rather than on the petiole, few marginal glands are sometimes present, small (c. 0.3 mm diameters), sessile; side veins are 8–14 pairs, the basal pair is slightly different (angle more acute), tertiary veins are visible. *Inflorescences* are whitish, 7–10 cm long, most often collected as stiff and dense, erect buds sometimes on a bent stalk of 1–2.5 cm long, distinctly proterogynous and often the apical, shorter staminate part is still in bud when the lower pistillate part is already in flower or even in fruit (precocious fruiting),

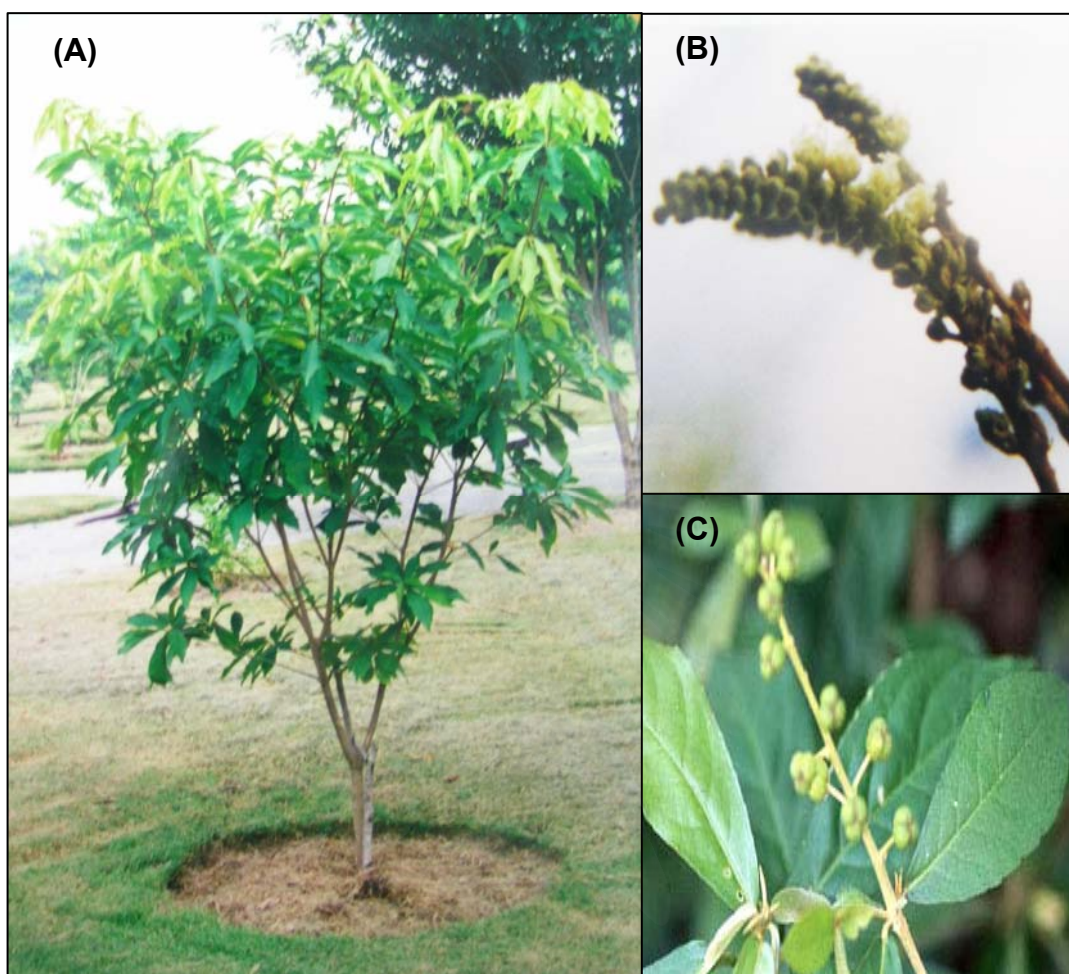


Figure 2 *Croton stellatopilosus* Ohba (Euphorbiaceae) (A), Inflorescences (B), Leaves and fruits (C).

with 4–10 pistillate flowers, without bisexual bracts; with scattered and distinct indumentum on all parts, slowly glabrescent; bracts are 1.5–2 mm long, eglandular, is pubescent, caducous. *Staminate flowers* are densely pubescent throughout; pedicel 2–6 mm long; sepals and petals are both 2.5 by 1 mm; stamens are 10, glabrous or with few hairs at base. *Pistillate flower* is densely pubescent throughout; pedicel 4–6 mm long (–8 mm in fruit); sepals are 3 by 1.5 mm, as long as the ovary; petals are not seen; stigmas are 3 mm long, free, undivided in the lower half and once divided apically. *Fruits* are 5 by 6 mm, smooth to very slightly muriculate,

sulcate, quite thin-walled, sparsely pubescent to subglabrous. *Seeds* are 4 by 2.5 mm, with a very small caruncle. Flowering and fruiting on December to February. Distribution areas of this plants in Thailand appear to be in Lop Buri (Khao Thungna), Sa Kaeo, Prachin Buri (Kabinburi), Chachoengsao, Chon Buri (Khao Khieo). This information was cited in the web site of Flora of Thailand Euphorbiaceae (<http://www.nationaalherbarium.nl/thaieuph/ThSearchSc/ThSearchScT.htm>)

1.2 The evidence of changing name from *Croton sublyratus* Kurz to *Croton stellatopilosus* Ohba

The botanical name of “Plaunoi” has been changed recently based on its taxonomic characteristics. It was originally identified as *C. sublyratus* by Airy Shaw (1972) by comparing with the collections from the Andaman Island of India. However, the samples of Thai collections differ in at least two characters from the Andaman plants. First, the basal leaf glands are sessile and flat (distinctly protruding to nearly stipitate in *C. sublyratus*), and peculiarly cone-like, dense, pyramidal inflorescence buds (not found on the Andaman Island samples). Second, the leaves of the Thai collections are generally slightly smaller. These differences have been used as the major points to differentiate the two species. *C. stellatopilosus* has, therefore, been described for the samples from south-eastern Thailand and is the correct name for the source plant of plaunotol in the strictest sense as described by Esser and Chayamarit (2001).

1.3 Medicinal uses of *C. stellatopilosus*

1.3.1 Thai folk medicinal uses

C. stellatopilosus (Plaunoi) is a Thai medicinal plant used as anthelmintic for the treatment of skin diseases (จุฬาลงกรณ์มหาวิทยาลัย, คณะเภสัชศาสตร์, ภาควิชาเภสัชพฤกษศาสตร์, 2530; Ponglux, *et al*, 1987). Stem, bark and leaf have been used as an antidiarrheal and to normalize menstruation, whereas its flower has been used as an anthelmintic (มหาวิทยาลัยมหิดล, คณะเภสัชศาสตร์, 2523). Firewood of Plaunoi has been used for postpartum (เปรมจิต นาคประสิทธิ์, บรรณารักษ์, 2526). In addition, Plaunoi and Plau-yai (*C. oblongifolius* Roxb.) have been used together for various purposes such as stomachic, anthelmintic, emmenagogue, digestant, transquillizer and carminative. Both have also been used for the treatment of lymphatic, pruritic, leprosy, tumor and yaws (ประเสริฐ พรหมมณี และคณะ , 2531; นันทวัน บุญยะประภัศร, 2532).

1.3.2 Therapeutic uses of Plaunoi

The leaves of *C. stellatopilosus* have been used as the raw material for extracting plaunotol, the anti-peptic ulcer substance. Plaunotol has been registered with the World Health Organization (WHO) under the code CS-684. Its tradename is Kelnac[®] which has been manufactured by Sankyo Co., Ltd. (Ogiso *et al.*, 1985). Kelnac[®] has been reported to enhance the mucosal protective factors by increasing gastric mucosal blood flow, promoting mucous and prostaglandin production in the gastric mucosa and increasing gastric mucosal resistance. Furthermore, it has been

found to exert a profound therapeutic effect in gastric ulcer (Department of Medical Information, Sankyo Co., Ltd, 1993).

1.4 Chemical constituents of *C. stellatopilosus*

In 1978, Ogiso and coworkers have isolated and identified plaunotol as an antipeptic ulcer substance from the acetone extract of stem of *C. stellatopilosus* (Ogiso *et al.*, 1978). Other compounds with antiulcer activity were isolated by Kitazawa and his co-workers in 1980, they are diterpene lactones, namely, plaunol A, plaunol B, plaunol C, plaunol D and plaunol E. This made it interesting to continue research on the isolation of chemical constituents from *C. stellatopilosus* (Kitazawa and Ogiso, 1981; Kitazawa, Kurabayashi, Kasuga, Oda and Ogiso, 1982; Takahashi, Kurabayashi, Kitazawa, Haruyama and Ogiso, 1983). The list of these compounds and their chemical structures are shown in Table 1

สถาบันวิทยบริการ
จุฬาลงกรณ์มหาวิทยาลัย

Table 1 Chemical constituents of *C. stellatopilosus*

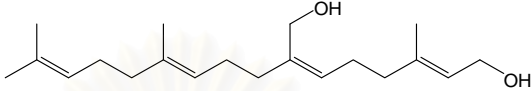
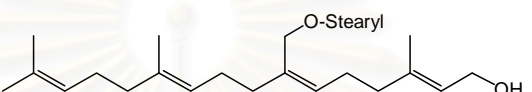
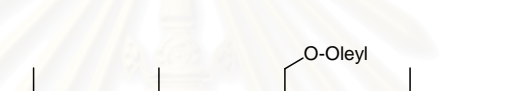
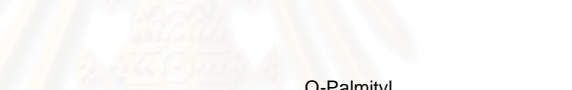
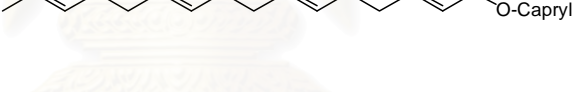
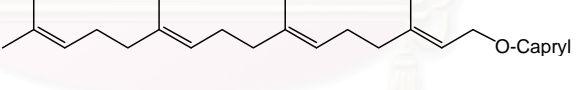
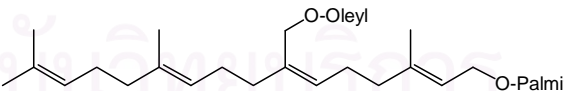
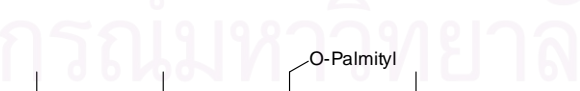
Chemical group/ Name	Chemical structure	References
Acyclic diterpene/ Plaunotol (18-hydroxy geranyl geraniol)		Kitazawa <i>et al.</i> , 1982
Geranylgeraniol Ester A		Kitazawa <i>et al.</i> , 1982
Geranylgeraniol Ester B		Kitazawa <i>et al.</i> , 1982
Geranylgeraniol Ester C		Kitazawa <i>et al.</i> , 1982
Geranylgeraniol Ester D		Kitazawa <i>et al.</i> , 1982
Geranylgeraniol Ester E		Kitazawa <i>et al.</i> , 1982
Geranylgeraniol Ester F		Kitazawa <i>et al.</i> , 1982
Geranylgeraniol Ester G		Kitazawa <i>et al.</i> , 1982

Table 1 Chemical constituents of *C. stellatopilosus* (continued)

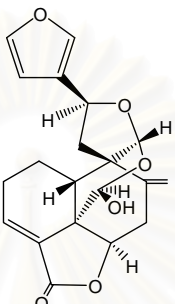
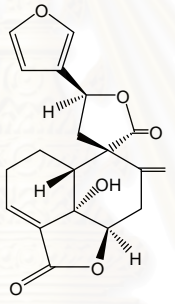
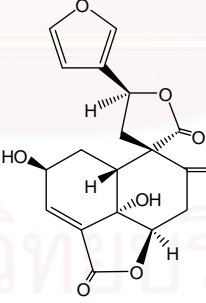
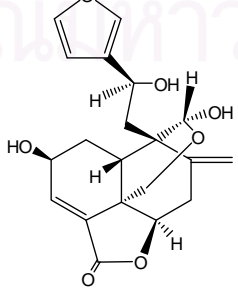
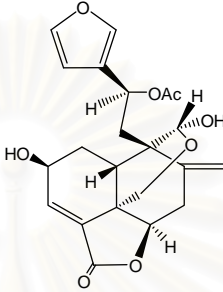
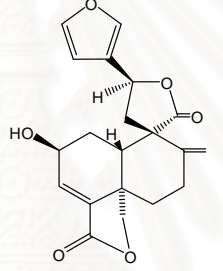
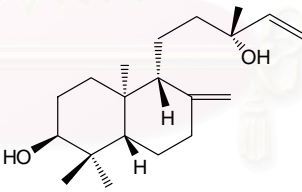
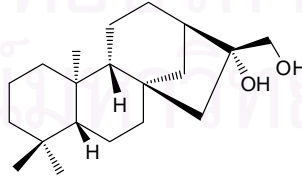
Chemical group/Name	Chemical structure	References
Clerodane diterpene /		
Plaunol A		Kitazawa <i>et al.</i> , 1979; Kitazawa <i>et al.</i> , 1980
Plaunol B		Kitazawa <i>et al.</i> , 1979; Kitazawa <i>et al.</i> , 1980
Plaunol C		Kitazawa <i>et al.</i> , 1980
Plaunol D		Kitazawa <i>et al.</i> , 1980

Table 1 Chemical constituents of *C. stellatopilosus* (continue)

Chemical group/ Name	Chemical structure	References
Clerodane diterpenes/ Plaunol E		Kitazawa <i>et al.</i> , 1980
Plaunolide		Takahashi <i>et al.</i> , 1983
Labdane diterpene / ent-13 α -hydroxy-13- epimanool		Ogiso <i>et al.</i> , 1978
Kaurane diterpene / ent-16 β , 17- dihydroxykaurane		Kitazawa and Ogiso, 1981

2. Plaunotol

2.1 Physicochemical properties

Generic name : Plaunotol (CS-684)

Chemical name : (2*E*,6*Z*,10*E*)-7-hydroxymethyl-3,11,15-trimethyl-2,6,10,14-hexadecatetraen-1-ol or 18-hydroxygeranylgeraniol

Molecular formula : $C_{20}H_{34}O_2$

Molecular mass : 306.255

The structure of plaunotol is shown in Figure 3

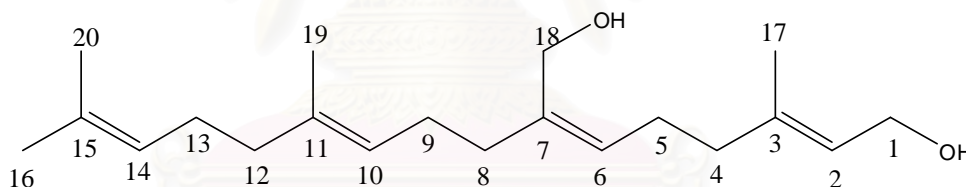


Figure 3 The chemical structure of plaunotol

Plaunotol occurs as pale yellow to light brown viscous liquid, having a slightly characteristic odor and a bitter taste. It is soluble in methanol, ethanol, acetone, ethyl acetate, dioxane, ether, chloroform, toluene or vegetable oil, but is practically insoluble in water (Department of Medicinal Information, Sankyo Co., Ltd., 1993).

For spectroscopy, plaunotol shows its infrared spectrum with absorption bands at 3300, 1665, 1440, 1380 and 1000 cm^{-1} . The proton magnetic resonance (PMR) spectrum of plaunotol shows signals due to four vinyl methyl groups at δ 1.58

(6H, s) and δ 1.66 (6H, s), six allyl methylene groups at δ 1.9-2.3 (12H, m), two hydroxymethyl groups at δ 3.94 (2H, s) and δ 3.97 (2H, d), and four olefinic protons at δ 5.0-5.3 (4H, m). For mass spectrum, plaunotol shows the molecular ion at m/e 306.255 (M^+ , calculated for $C_{20}H_{34}O_2$ 306.256) and also other main peaks at m/e 288, 270, 121, 81 and 69 (100) (Ogiso *et al.*, 1978, 1985).

2.2 Various techniques used for obtaining plaunotol

Different processes for obtaining plaunotol have been reported by various research groups as follows:

2.2.1 Plaunotol isolation (Ogiso *et al.*, 1978)

In 1978, Ogiso and coworkers reported a method to isolate plaunotol from a crude drug of *C. stellatopilosus*. The crude drug (81.5 kg) was first extracted three times with acetone under reflux. After evaporation of the solvent, the residue was dissolved in 10 L of 80% aqueous methanol and washed with *n*-hexane. The concentrated methanol layer was poured into 40 L benzene under vigorous stirring. After washing with an aqueous sodium hydrogen carbonate solution, the benzene solution was evaporated and the residue was extracted with ether. The ether soluble fraction was isolated by column chromatography on silica gel (3 kg) using benzene and ethyl acetate as eluent. Plaunotol (53 g) was isolated by this procedure.

2.2.2 Plaunotol extraction and purification (Nilubol, 1992)

In 1992, Nilubol *et al* patented a technique for extraction and purification of plaunotol. Six kg of dried ground leaves of Plaunoi was refluxed with 40 L of

methanol. The methanol extract was evaporated leaving a crude extract which was then dissolved in 1.0 L of 90% methanol and washed with n-hexane. The methanol layer was evaporated and the residue was suspended in 0.5 L of water and extracted with diethyl ether. The ether layer was washed with a 5% solution of aqueous sodium carbonate and dried over anhydrous sodium sulphate. The solvent was evaporated leaving an oily residue which was purified by column chromatography over silica gel, eluting with ethyl acetate/benzene (10% by volume) and later with ethyl acetate/benzene (30% by volume). Fractions containing the active compound were combined and the solvent was distilled off to give 3.4 g of pure plaunotol. This protocol was patented in the USA (patented No. 826702).

2.2.3 Determination of plaunotol content by thin-layer chromatography (TLC) densitometric

TLC densitometric method was developed for rapid and precise measurement of plaunotol. This method allows the active constituent to be determined in unpurified plant extracts and therefore allows a large-scale screening of a plant population to be performed. TLC is performed on silica gel 60 F254 plate using benzene: ethyl acetate (1:1) (Ogiso *et al.*, 1981) or 20% ether in chloroform or chloroform: *n*-propanol (96:4) (Vongchareonsathit and De-Eknamkul, 1998) as developer with 10 cm height of the solvent front. The TLC plate is then scanned with a TLC densitometer under the wavelength of 220 nm.

2.2.4 Determination of plaunotol content by gas chromatography method

Gas chromatography method can be used for determining the plaunotol content in the microgram range. This method is performed by using a glass column packed with 2% OV17 on 60/80 Supelcoport, flow rate: 30 ml/min N₂, temperature program: from 235 °C (hold 2 min) to 250 °C (temperature rate 15 °C/min) and hold 10 min, injector temperature: 300°C, sample size 2 µl (Vongchareonsathit and De-Eknamkul, 1998).

2.2.5 Chemical synthesis of plaunotol

The total synthesis of plaunotol bearing an (*E*, *Z*, *E*)-configuration has been successfully achieved by application of the method developed by Corey and Yamamoto (1970). This synthesis route involves a stereospecific sequence for trisubstituted olefin having an allylic alcohol via β-oxido phosphonium ylide. Reaction of phosphonium iodide, prepared by Coates' procedure (Coates and Robinson, 1971), with aldehyde obtained by ozonolysis of geranyl-2-tetrahydropyranyl ether, gives a Wittig betadine. Subsequent reaction of the betadine with paraformaldehyde followed by treatment of the resulting tetrahydropyranyl ether with acid furnishes the desired compound bearing (*E*, *Z*, *E*)-configuration. (Ogiso *et al.*, 1978, 1985).

2.3 Biosynthesis

Plaunotol biosynthesis has been firstly reported by the group of De-Eknamkul and his coworkers in 1998. Plaunotol is derived from four isoprene units. One molecule of DMAPP and three molecules of IPP were attached by head to tail

condensation, catalyzed by prenyltransferases (Spurgeon and Porter, 1981). Geranylgeranyl diphosphate (GGPP) is formed. GGPP is then dephosphorylated to geranylgeraniol (GGOH) by geranylgeranyl diphosphate phosphatase enzyme (Nualkaew *et al.*, 2005, 2006). Finally, GGOH is hydroxylated at C-18 position, catalyzed by GGOH 18-hydroxylase (Fig. 4) (Tansakul and De-Eknamkul, 1998).

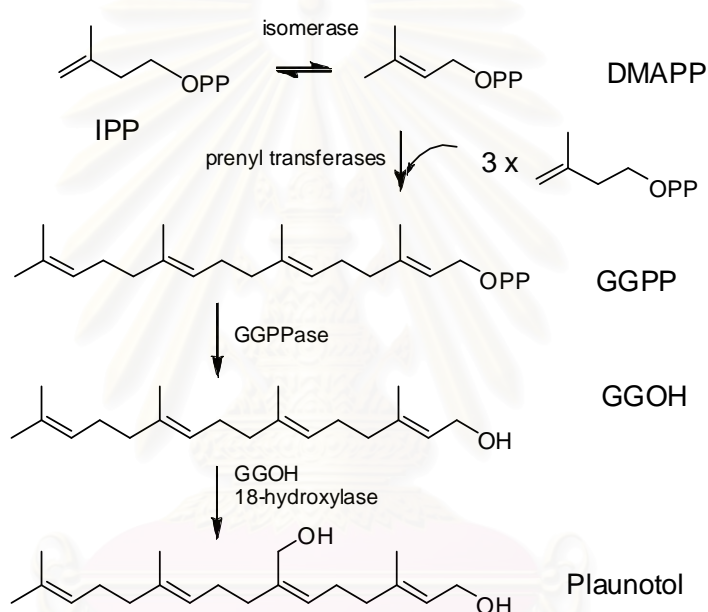


Figure 4 Biosynthetic pathway of plaunotol

2.4 Antipeptic ulcer activity

Plaunotol is widely used in the treatment of peptic ulcers including *Helicobacter pylori*-associated and non-steroidal anti-inflammatory drug induced ulcers in Japan. The mechanism underlying the anti-ulcer effects of plaunotol includes the increase of prostaglandin production in gastric mucosa (Ushiyama *et al.*, 1987). On the other hand, Shiratori and coworkers (1993) reported that plaunotol

released endogenous secretin, and that secretin is a potential mediator of the anti-ulcer actions of mucosal protective agents. Furthermore, they have demonstrated that endogenous prostaglandin has a significant role in the inhibitory action of exogenous and plaunotol-released endogenous secretin in rats. In animal experiments, plaunotol prevented indomethacin-induced gastric mucosal injury by inhibiting neutrophil activation (Murakami *et al.*, 1999). Takagi and coworkers reported that gastric mucosal injury induced by *H. pylori* infection is mediated by interleukin-8 (IL-8). IL-8 was inhibited by plaunotol in a dose-dependent manner and suggested that plaunotol is a useful anti-ulcer drug that also exhibits an additional efficacy for *H. pylori*-induced gastric mucosal injury (Takagi *et al.*, 2000). Thus, plaunotol prevents gastric mucosal injury and has gastroprotective actions through various mucosal defensive factors.

In 2002, Koga and coworkers investigated the effect of plaunotol when combined with clarithromycin or amoxicillin against *H. pylori* *in vitro* and *in vivo*. For *in vitro*, when combined with clarithromycin, plaunotol was shown to have synergistic activity. When combined with amoxicillin, plaunotol showed additive activity against 10 out of 14 strains of *H. pylori*. In a C57BL/6 mouse gastritis model infected with *H. pylori* SS1, the plaunotol-clarithromycin and plaunotol-amoxicillin combinations both exhibit synergistic effects, which allow the effective dose of clarithromycin to be reduced when co-administered with plaunotol. These results suggest that plaunotol may have a useful role in combination with anti *H. pylori* drugs in the treatment of *H. pylori*-associated diseases (Koga *et al.*, 2002).

2.5 Production of plaunotol in tissue culture techniques

Plant tissue and cell culture techniques have been used to study the production of plaunotol in *in vitro* cultures of *C. stellatopilosus* (Morimoto, 1989; Morimoto and Murai 1989; စာအုပ် နမူနာ, 2534). There has been only one report on callus cultures that showed plaunotol accumulation at 0.17% of dry weight (Morimoto, 1989). Geranylgeraniol has also been found to accumulate in the suspension cultures of *C. stellatopilosus* in the lag or stationary phase of cell growth at 0.05% of dry weight (Kitaoka *et al.*, 1989).

3. The Biosynthetic Pathway of Terpenoids

Terpenoids play important roles in all living organisms; they function as steroid hormones in mammals, carotenoids in plants and ubiquinones in bacteria. All of these terpenoids are biosynthesized by starting with isopentenyl diphosphate (IPP) which is transformed by IPP-isomerase to dimethylallyl diphosphate (DMAPP), IPP and DMAPP are then condensed by prenyltransferases to geranyl diphosphate (GPP). A consecutive condensation of GPP with IPP yields farnesyl diphosphate (FPP) and a third generates geranylgeranyl diphosphate (GGPP). GPP is the precursor of all monoterpenes (C₁₀). FPP furnishes the sesquiterpenes (C₁₅) and GGPP the diterpenes (C₂₀). Typical structures contain carbon skeletons represented by (C₅)_n, and are classified as hemiterpenes (C-5), monoterpenes (C-10), sesquiterpenes (C-15), diterpenes (C-20), sesterterpenes (C-25), triterpenes (C-30) and tetraterpenes (C-40) (Dewick, 2002). IPP and DMAPP are biosynthesized either via the classical mevalonate (MVA) pathway or the non-mevalonate pathway in which

2-C-methyl-D-erythritol 4-phosphate (MEP) is the first committed intermediate (Duvold *et al.*, 1997; Takahashi *et al.*, 1998). In higher plants and several algae there is a compartmentation of isoprenoid biosynthesis (Arigoni *et al.*, 1997; Lichtenthaler *et al.*, 1997; Schwender *et al.*, 1997). The MVA pathway is used to produce triterpenes or sterols in the cytosol, whereas the non-mevalonate pathway is used for the production of isoprenoids like carotenoids and phytol in the plastid.

3.1 The classical mevalonate (MVA) pathway

The classical route for the formation of the C₅ building blocks of terpenoid biosynthesis in plants via the reactions of the mevalonate pathway was first demonstrated in yeast and mammals (for review see Spurgeon and Porter, 1981). This well-characterized sequence (Fig. 5) starts from acetyl-CoA as precursor. Sequentially, two molecules of acetyl-CoA are condensed to form acetoacetyl CoA by thiolase. The latter compound is then condensed with another molecule of acetyl-CoA to 3-hydroxy-3-methylglutaryl-CoA (HMG-CoA) by HMG-CoA synthase (HMGS). Later, HMG-CoA is reduced to mevalonic acid in the presence of NADPH by HMG-CoA reductase (HMGR). This enzyme has been of great interest since it catalyzes the rate-limiting step in MVA pathway and thus becomes a key target for interruption of cholesterol biosynthesis. The series of HMG-CoA reductase inhibitors such as mevastatin, lovastatin, simvastatin and pravastatin are highly effective hypocholesterolemic agents (Spurgeon and Porter, 1981). HMGR is the rate-limiting enzyme of the mevalonate pathway (Goldstein and Brown, 1990). In the absence of sterol isoprenoids in the cell, HMGR gene transcription is directly activated by a family of transcription factors, namely sterol regulatory element binding proteins

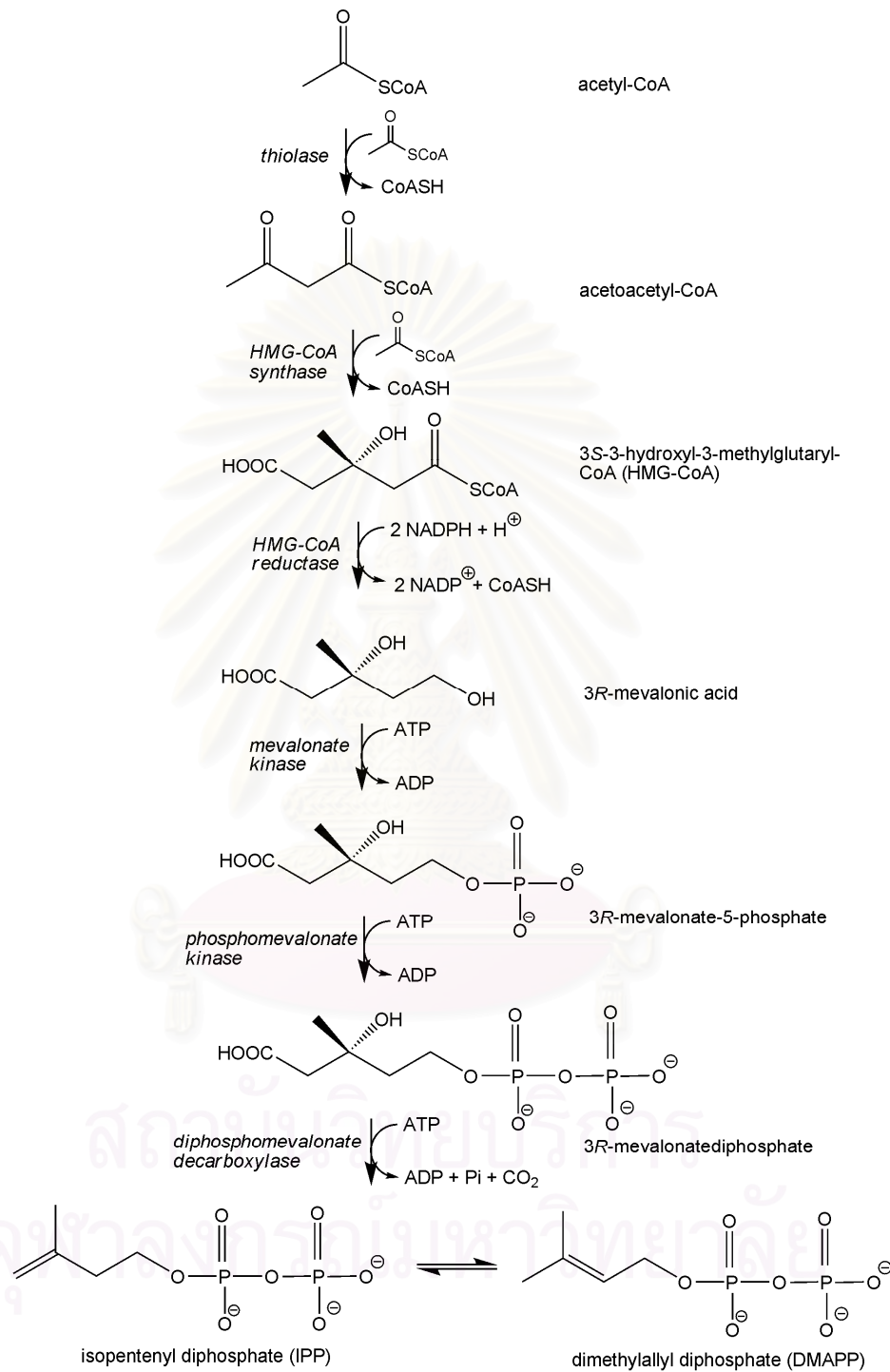


Figure 5 The classical mevalonate (MVA) pathway

(SREBPs) (Horton, 2002; Weber *et al.*, 2004). There is evidence that SREBPs activate not only HMGR gene transcription, but also every step of cholesterol synthetic pathway by increasing gene expression of all the enzymes acting in the mevalonate pathway (Sakakura *et al.*, 2001). Additionally, other regulatory mechanisms can influence the activity of HMGR. The degradation rate of HMGR protein is influenced by cell's requirements for both sterol and nonsterol isoprenoids. Cell's requirements for nonsterol isoprenoids will determine the rate of translation of HMGR mRNA. Mevalonic acid is phosphorylated twice to form mevalonic 5-diphosphate via mevalonic monophosphate by mevalonate kinase (MK) and phosphomevalonate kinase (PMK), respectively. MK is the second essential enzyme of the terpenoid biosynthetic pathway after HMGR catalyzes the phosphorylation of mevalonic acid into phosphomevalonate. Although MK has no rate-limiting properties, it has been demonstrated that MK activity is regulated via feedback inhibition by intermediates of the MVA pathway, including geranylpyrophosphate, farnesylpyrophosphate and geranylgeranylpyrophosphate (Hinson *et al.*, 1997). PMK catalyzes the next step in the isoprenoid/sterol biosynthesis, converting mevalonate 5-phosphate and ATP to mevalonate 5-diphosphate and ADP. Recent functional investigations of the recombinant human enzyme have shown that the reaction catalyzed by PMK is a reversible reaction; kinetic constants of human PMK have been determined for both its forward (formation of mevalonate 5-diphosphate) and reverse (formation of mevalonate 5-phosphate) reactions (Bonetti *et al.*, 2003).

Mevalonic 5-diphosphate is then decarboxylated and dehydrated to form isopentenyl diphosphate by mevalonate-5-diphosphate decarboxylase (MDD). Isopentenyl diphosphate is isomerized to dimethylallyl diphosphate by isopentenyl diphosphate isomerase (IPI) (Spurgeon and Porter, 1981).

3.2 The deoxyxylulose phosphate (DXP) pathway

The existence of the alternative pathway for IPP biosynthesis was first demonstrated by Rohmer in different bacterial species (Rohmer, 1999). Recently, the DXP pathway has been completely elucidated in *Escherichia coli*. The initial step in the DXP pathway is the formation of 1-deoxy-D-xylulose 5-phosphate (DXP) by the condensation of pyruvate and D-glyceraldehyde 3-phosphate (Fig. 6), catalyzed by 1-deoxyxylulose-5-phosphate synthase (DXS) (Broers, 1994; Schwarz, 1994). The *dxs* gene encoding this enzyme was first cloned from *E. coli* (Sprenger *et al.*, 1997; Lois *et al.*, 1998). This enzyme has a typical thiamine-binding motif and needs both thiamine and a divalent cation such as Mg^{2+} or Mn^{2+} for enzyme activity. In the second step, DXP is transformed into 2C-methyl-D-erythritol-4-phosphate (MEP). The formation of MEP from DXP occurs in a single step by rearrangement of DXP to an intermediate with a branched carbon skeleton, 2C-methyl-D-erythrose-4-phosphate (MEOP), followed by reduction using NADPH (Takahashi *et al.*, 1998). The enzyme catalyzing this first committed step of DXP pathway is called 1-deoxyxylulose-5-phosphate reductoisomerase which is encoded by the *ispC* gene (formerly called *dxr*). This enzyme requires Mg^{2+} or Mn^{2+} as cofactor (Rohdich *et al.*, 2006). The next step of the DXP pathway is the conversion of MEP to 4-(diphosphocytidyl)-2C-methyl-D-erythritol in a cytidine triphosphate (CTP) dependent reaction which is catalyzed by 4-diphosphocytidyl-2-C-methyl-D-erythritol synthase. This enzyme is encoded by *ygbP* gene (now designated *ispD*), which is present in many bacteria as well as in *Arabidopsis thaliana* (Rohdich *et al.*, 1999). The further step in the pathway is the ATP-dependent phosphorylation of the 2-hydroxy group of 4-(diphosphocytidyl)-2C-methyl-D-erythritol converting into 4-(diphosphocytidyl)-2C-

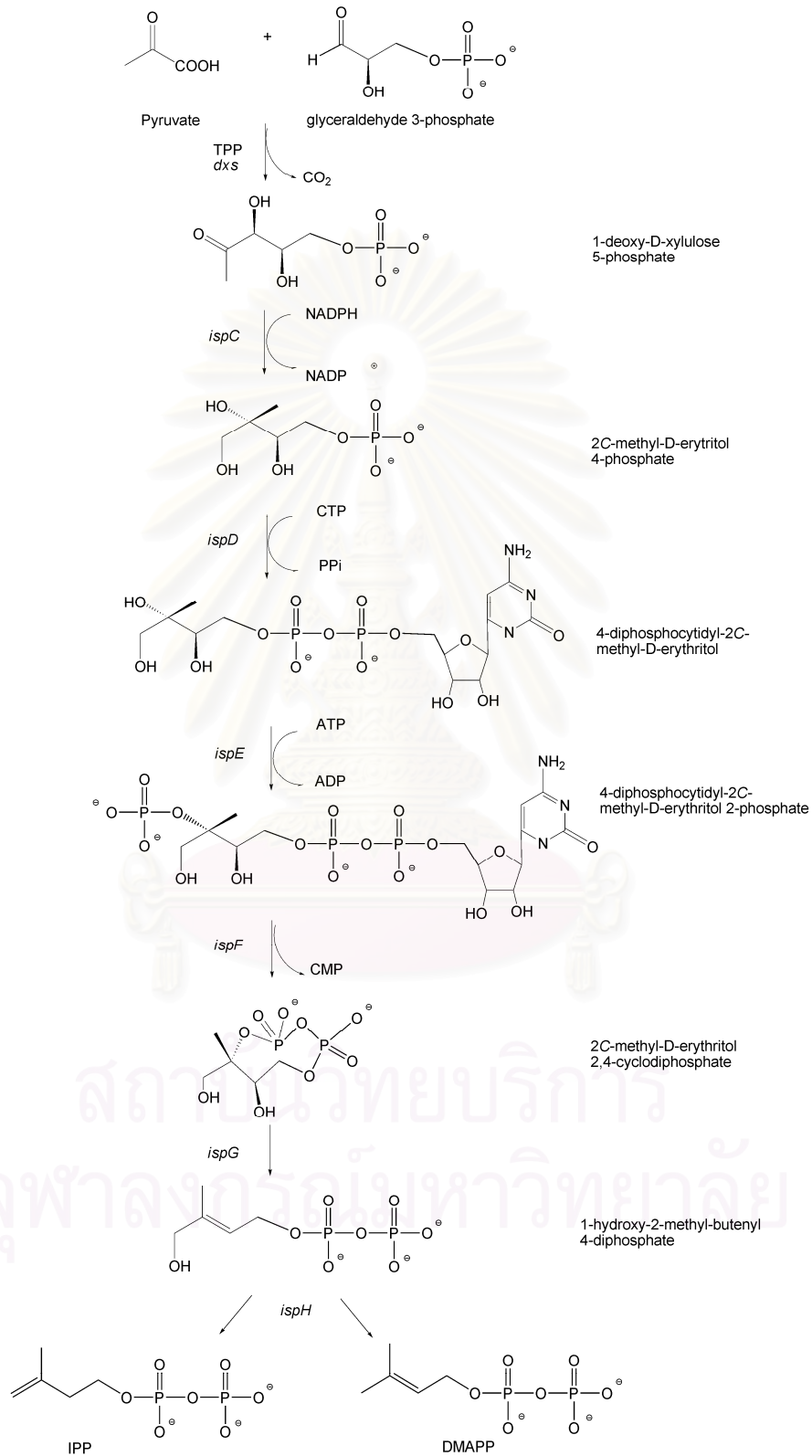


Figure 6 The deoxyxylulose phosphate (DXP) pathway

methyl-D-erythritol-2-phosphate by an enzyme, namely, 4-(diphosphocytidyl)-2C-methyl-D-erythritol kinase, encoded by the *ychB* gene (now designated *ispE*), which has been identified in the genome of *E. coli* and many other organisms (Lüttgen *et al.*, 2000).

The next step in the DXP pathway has also been identified using bioinformatics. Genome analyses have shown that many putative orthologues of the *E. coli ygbB* gene (now designated *ispF*) are linked or fused to putative orthologues of *ispD* (Rohdich *et al.*, 1999; Herz *et al.*, 2000). Based on these findings, the *E. coli ispF* gene has been expressed and the recombinant protein shown to catalyze the conversion of 4-(diphosphocytidyl)-2C-methyl-D-erythritol-2-phosphate into 2C-methyl-D-erythritol 2,4-cyclodiphosphate (Herz *et al.*, 2000). The next enzyme has been studied, *IspG* (formerly *GcpE*) gene of *E. coli* has been expressed and this protein has been shown to catalyze the conversion of 2C-methyl-D-erythritol 2,4-cyclodiphosphate into 1-hydroxy-2-methyl-2-(*E*)-butenyl 4-diphosphate. In the dark, the plant *GcpE* catalysis requires, in addition to ferredoxin, NADP⁺/ferredoxin oxidoreductase and NADPH as electron shuttle (Seemann *et al.*, 2006). The last step, *LytB* (*IspH*) protein catalyzes the subsequent transformation of 1-hydroxy-2-methyl-2-(*E*)-butenyl 4-diphosphate into a mixture of IPP and DMAPP (Rohdich *et al.*, 2003).

3.3 Cross-talk between MVA and DXP pathways in plants

In higher plants, the biosynthesis of the different terpenoid classes is located in different subcellular compartments. Whereas mono- and diterpenes are synthesized in the plastids, the production of sesquiterpenes and sterols is located in the cytosol (McGarvey and Croteau, 1995). Accordingly, the enzymes of the MVA or

DXP pathway are also located in different compartments. Enzymes of the MVA pathway have been isolated from the cytosol, whereas genes coding for enzymes of the DXP pathway possess typical plastid-targeting sequences (Lange *et al.*, 1998; Lange and Croteau, 1999). This differential allocation of the early pathways to certain terpenoid classes has also been observed for stress-induced isoprenoids after wounding or treatment of plants with elicitors. It can be suggested that exchange of common intermediates such as IPP, DMAPP, GPP and FPP might occur between the two compartments as described by the "Cross-talk Theory" (Fig. 7). The extent of this cross-talk or exchange depends on the species as well as on the presence and concentration of exogenous precursors.

A powerful strategy for quantitative assessment of the differential contribution of the two isoprenoid pathways has been established using the labeled glucose as well as labeled 1-deoxy-D-xylulose and mevalonate as precursors in whole plants, plant tissue cultures or cultured plant cells (Schuhr *et al.*, 2003). An understanding of the correlations between isotopic fractionations and biochemical processes is, therefore, essential in the elucidation of biosynthetic pathways and for the discrimination among alternative pathways (Chikaraishi, Naraoka and Poulson, 2004). Moreover, mixed biosynthesis with contributions from both pathways may be determined from such studies (Adam *et al.*, 1998; Bergamo *et al.*, 2005). In continuation of previous studies concerning IPP biosynthesis in plant isoprenoids are reviewed. (Schwender *et al.*, 1996; Knoss, Reuterand and Zapp, 1997; Thiel *et al.*, 1997; Adam and Zapp, 1998; Adam *et al.*, 1998, Adam, Thiel and Zapp, 1999; Hirai *et al.*, 2000; Barlow, Becker and Adam, 2001; Hertewich *et al.*, 2001; Thiel and Adam, 2002; Masse, Belt and Rowland, 2004; Umlauf *et al.*, 2004; Bergamo *et al.*, 2005; Wungsintaweekul and De-Eknamkul, 2005). Those studies have revealed the

actual contribution of the MVA and DXP pathways, which in agreement with the explanation of “Cross-talk theory” (Fig. 7).

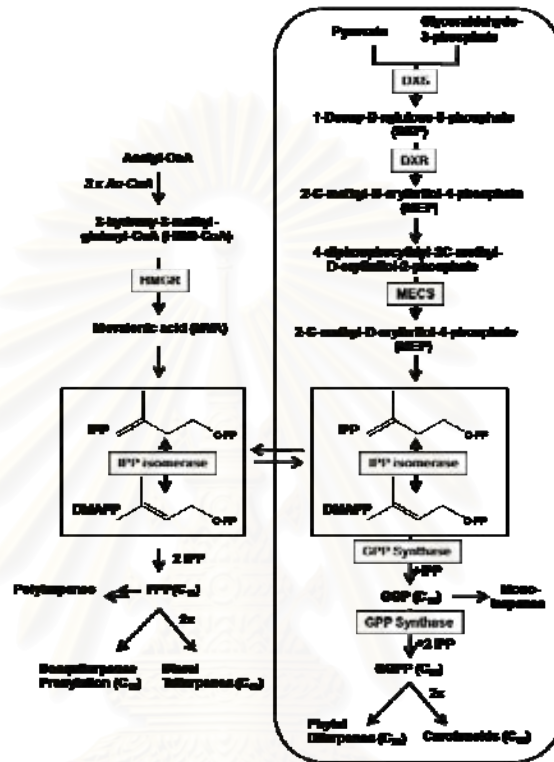


Figure 7 Overview of isoprenoid metabolic pathways localized in the cytosol and in the plastids of plant cells (Burlat *et al.*, 2004)

4. Previous Biosynthetic Studies in *C. stellatopilosus*

4.1 Feeding experiments (incorporation experiments)

Feeding of [^{14}C]glucose into the leaves of *C. stellatopilosus* has been shown to have low incorporation of the label into plaunotol (Potduang, 2000). This may be due to the complication of site in the chloroplast. Feeding of *C. stellatopilosus* callus with [$1\text{-}^{13}\text{C}$]glucose has shown that the incorporation of the label into phytosterol

occurs in a manner of mixed origin of isoprene units from both mevalonate and non-mevalonate pathways (De-Eknamkul and Potduang, 2003). Subsequent feeding of *C. stellatopilosus* whole leaf with [1-¹³C] and [U-¹³C]glucose has shown that the incorporation of the label in to plaunotol proceeds exclusively by the DXP pathway (Wungsintaweekul and De-Eknamkul, 2005).

4.2 Cell-free extracts

The fraction of 20,000 g pellet from fresh leaves of *C. stellatopilosus* has been used in the studies of enzyme activities utilizing [1-³H]GGDP as substrate (Tansakul and De-Eknamkul, 1998). It was clearly shown that the amount of GGOH is formed and utilized in plaunotol formation. Therefore, the biosynthetic pathway of plaunotol has been proposed to involve two enzymes, namely, geranylgeranyl diphosphatase and GGOH-18-hydroxylase.

In 2005 Nualkaew and coworkers, studied the process of catalytic dephosphorylation of geranylgeranyl diphosphate (GGPP) to give geranylgeraniol (GGOH) in *C. stellatopilosus* leaves by *in vivo* chloroplast feedings with [1-³H]GGPP and [1-³H]GGMP and *in vitro* enzyme catalyzed reactions. The results strongly suggested that the formation of GGOH from GGPP proceeds in the chloroplasts via two successive monodephosphorylation reactions. Hence, the enzyme was named geranylgeranyl diphosphate phosphatase, rather than geranylgeranyl diphosphatase based on its catalytic mechanism (Nualkaew *et al.*, 2005, 2006).

CHAPTER III

MATERIALS AND METHODS

1. Materials

1.1 Plant materials

Young leaves of *Croton stellatopilosus* Ohba (Euphorbiaceae) used in this study were collected from trees growing in the open field of the Faculty of Pharmaceutical Sciences, Chulalongkorn University and the Herb Garden of the Faculty of Pharmaceutical Sciences, Prince of Songkla University, Hat Yai Campus. A voucher specimen (no. 21867) is deposited in the Herbarium, Royal Forest Department in Bangkok, Thailand.

1.2 Chemicals, kits and enzymes

[1- ¹³ C]glucose	Cambridge Isotope Laboratories, Inc, USA.
[1- ¹⁴ C]glucose (56.0 mCi/mmol , 308 μCi/ml)	Amersham, England.
[U- ¹³ C]glucose	Cambridge Isotope Laboratories, Inc, USA.
[2- ¹³ C]sodium acetate	Cambridge Isotope Laboratories, Inc, USA.
Gellan gum	Sigma Aldrich Chemie, Germany
Geranylgeraniol (GGOH)	Sigma-Aldrich Pte Ltd, Singapore.
Phytol	Sigma-Aldrich Pte Ltd, Singapore.
Plant agar	Duchefa Biochemie, The Netherlands.
Sucrose	Mitropol Co. Ltd., Thailand.

Supplemented plant growth regulators were purchased from Gibco Laboratories, USA as follows:

Auxin:	2,4-dichlorophenoxyacetic acid (2,4-D)
	α -naphthaleneacetic acid (NAA)
Cytokinin:	kinetin-6-furfurylaminopurine (Kinetin)
	6-benzylaminopurine (BA)

The compounds used in the preparation of MS stock solutions were purchased from Sigma Chemical Co., USA.

Analytical grade organic solvents used in this study [benzene, chloroform, dichloromethane, ethanol, ethyl acetate, *n*-hexane, methanol, *n*-propanol] were purchased from Labscan, Thailand.

Kits and enzymes

RNeasy Plant Mini Kit	Qiagen, Germany
SuperScript TM III RT	Invitrogen, USA
<i>taq</i> PCR core kit	Qiagen, Germany

1.3 Instrumentations

1.3.1 Equipment

GC-FID	HP6850 Hewlett Packard, USA
	Flame ionization detector
	Auto sampler 7683B series

GC-MS	HP6890 GC-HP5972 MSD Hewlett Packard, USA HP5972 MSD detector
Gel documentation	Gel Doc model 1000, BIO-RAD, USA Molecular Analyst® Software, Windows Software for BioRad's Image Analysis Systems Version 1.4
HPLC	Waters 600E, UV detector, Milford, USA Waters 600PF pump Waters 484 tunable absorbance detector 807-IT Jasco integrator
NMR	UNITY INNOVA, Varian Inc., USA
Transmission Electron Microscope	JEM 2010, JEOL, USA
TLC radio scanner	Linear analyzer, LB 284/285; Berthold, Germany

1.3.2 Instruments

Autoclave	HA-3D, Hirayama, Tokyo, Japan
Balances	Explorer, Ohaus, USA Avery Berkel, USA Sartorius TE 3102S, USA
Centrifuges	Safeguard, Clay Adum, USA Denver Instrument, USA Hermle Z 323 K, Germany Kubota 5922, Japan
Electrophoresis	Mupidα Mini electrophoresis system, Japan
Heater	Isopad, Germany
Heater block	DRI-BATH, Thermolyne corporation, USA

Heating mantles	Barnstead Electrothermal, Southend, UK
Hot air oven	Memmert, Schwubuch, Germany
Hot plate	PC101, Corning, USA
Laminar air flow	Holten HV2448, Allerod, Denmark
Liquid scintillation counter	WALLAC 1409, Perkin Elmer, Turku, Finland
Micropipettes	0.1-2.0 μ l, 2-20 μ l, 20-200 μ l, 100-1000 μ l, Socorex, Switzerland
Microwave oven	LG, Thailand
Mini shaker	MS1, IKA, Staufen, Germany
pH-meter	Orion Research Inc., USA
Refrigerators	For 4°C, Sanden Intercool, Thailand; for -20°C, Whirlpool, Thailand; Deep-freezer (-80°C), Forma Scientific, USA
Rotary Evaporator	Eyela, Tokyo Rikakikai Co LTD, Japan
Shaker	Innova2300, New Brunswick Scientific, Illinois, USA
Speed vac	Plus SC 210A, Savant, USA
Sonicate	Crest Ultrasonic Corporation, USA
UV chromatography viewer	Camag, UV-cabinet II, Switzerland
UV-Transluminator (312 nm)	Camag, USA
UV-VIS spectrophotometer	Labomed, Inc., USA
Vacuum pump	Cacuubrand, Wertheim, Germany
Vortex	Vortex-Genie 2, USA
Water bath	WB14 Memmert, Schwubuch, Germany

1.4 Solution preparations

Anisaldehyde spray reagent	Anisaldehyde (5 ml) was mixed with acetic acid (10 ml) and conc HCl (5 ml) and distilled water was added to 80 ml.
Ethidium bromide solution	Ethidium bromide 10 μ l was dissolved in 100 ml distilled water.
TAE buffer (50x)	Tris (121 g), EDTA.3Na (19.7 g) and acetic acid (35 ml) were dissolved with distilled water to make 500 ml and pH was adjusted with conc HCl to 8.0

2. Methods

2.1 Tissue culture techniques

2.1.1 Nutrient media

A standard basal medium used in this study was MS medium (Murashige and Skoog, 1962). Its composition is shown in Table 2. Plant growth regulators (2,4-D, BA, kinetin and NAA) were used as required. Plant agar and gellan gum were added to solidify the culture medium. All stocks were kept at 4 °C, except vitamin stock was kept in -20 °C. KI stock solution was kept in bottle and protected from light.

For MS medium preparation, all stocks were pipetted to flask and volume was adjusted by deionized or redistilled water. The pH of the medium was adjusted to 5.8 with 1N sodium hydroxide solution or 1N hydrochloric acid solution. For solid medium, agar was added. The mixture was heated while stirring until the agar

Table 2 Composition and preparation of MS agar (Murashige and Skoog, 1962)

MS	Concentration in stock solution	Amount of stock solution in used (ml)
Stock 1 (Macronutrients)	g/1000 ml	50
NH ₄ NO ₃	33.0	
KNO ₃	38.0	
MgSO ₄ .7H ₂ O	7.4	
KH ₂ PO ₄	3.4	
Stock 2 (Micronutrients)	mg/100 ml	1
H ₃ BO ₃	620	
MnSO ₄ . H ₂ O	1,690	
ZnSO ₄ .7H ₂ O	860	
Na ₂ MoO ₄ .2H ₂ O	25	
CuSO ₄ .5H ₂ O	2.5	
CoCl ₂ .6H ₂ O	2.5	
Stock 3	g/100 ml	5
CaCl ₂ .2H ₂ O	8.7	
Stock 4	mg/100 ml	1
KI	75	
Stock 5 (Vitamins)	mg/100 ml	1
Nicotinic acid	5	
Pyridoxine HCl	5	
Thiamine HCl	5	
Inositol	10,000	
Stock 6 (Fe-EDTA stock)	g/500 ml	5
Na ₂ EDTA	3.73	
Fe ₂ SO ₄ .7H ₂ O	2.78	
Plant growth regulators		as required
Distilled water		adjusted to 1,000
Sucrose		30 g
Plant agar (Gellan gum)		8 g (2 g)
pH		5.8

was dissolved and clear solution was obtained. The medium (20 ml of each) was then transferred to culture bottles, tightly closed the lids and sterilized by autoclaving at 121°C at 15 lb/inch² for 15-20 minutes. The medium was cooled down to room temperature and kept until used.

2.1.2 Induction of callus culture

Young fully expanded leaves of *C. stellatopilosus* were washed under tap water, then soaked in 70% (v/v) ethanol for 3 minutes followed by surface sterilization in 0.5% (v/v) sodium hypochlorite for 5 minutes and washing 5 times with sterile distilled water. Sterilized leaves were excised into pieces, 5 x 5 mm² and placed on MS medium supplemented with 2.0 mg/l 2,4-D, 1.0 mg/l kinetin, 3% w/v sucrose and 0.8 % (w/v) plant agar. The culture was maintained at 25 ± 2 °C under control condition at 16 h of photo-period (2000 lux). Under culture condition, the callus was formed within 2 weeks.

For callus proliferation, the calli formed were subcultured 2-3 times, every 3 weeks, on MS medium supplemented with 1.0 mg/l 2,4-D, 1.0 mg/l BA, 3% (w/v) sucrose and 0.8% (w/v) plant agar. The calli appeared as friable, soft and yellowish tissues.

2.1.3 Induction of green callus culture

Three week-old proliferated calli were placed on MS medium supplemented with 2 mg/l BA, 2 mg/l NAA, 1% (w/v) sucrose and 0.2% (w/v) gellan gum. Green callus culture was kept at 25 ± 2 °C under light 16 h/day

2.1.4 Induction of suspension culture

Cell suspension cultures of *C. stellatopilosus* were initiated from the green callus cultures (2.1.3). Calli were transferred into a 250-ml erlenmeyer flask containing 50 ml of MS liquid medium supplemented with 2.0 mg/l 2,4-D, 2.0 mg/l BA and 3% (w/v) sucrose (Wungsintaweekul *et al.*, 2007). Suspension culture was shaken on a rotary shaker at 120 rpm, at 25 ± 2 °C, under fluorescent lamps 16 h/day. Cell suspensions were subcultured on the same medium every 2 weeks. Inoculation size was 20 ml.

2.1.5 Time-course study of *C. stellatopilosus* suspension cultures

Suspension culture maintained in MS medium supplemented with 2.0 mg/l 2,4-D, 2.0 mg/l BA and 3% (w/v) sucrose was investigated for time course study. For growth curve, fresh weight of each sample was determined by weighing cells after removing the medium completely. For production curve, contents of GGOH, phytol and phytosterols (β -sitosterol, stigmasterol, campesterol) were determined by gas chromatographic analysis (2.6). Samples were taken every day after subculture and were analyzed in triplicate.

2.2 Phytochemical studies

2.2.1 Sample extraction

2.2.1.1 GC analysis

Fresh cell suspension cultures (2 g) were harvested and extracted with 5 ml of 95% (v/v) ethanol under reflux at 60 °C for 1 h. The filtrate was evaporated under vacuum and further re-dissolved in 2 ml of 50% (v/v) ethanol in the presence of 1%

(v/v) NaOH. The solution was heated for 30 min and cooled. The lipophilic fraction was partitioned 5 times with 3 ml of *n*-hexane. The *n*-hexane fractions were pooled and dried under vacuum. The residue was further dissolved in 100 μ l of *n*-hexane and subjected to gas chromatography for secondary metabolite analysis.

2.2.1.2 Isolation by column chromatography

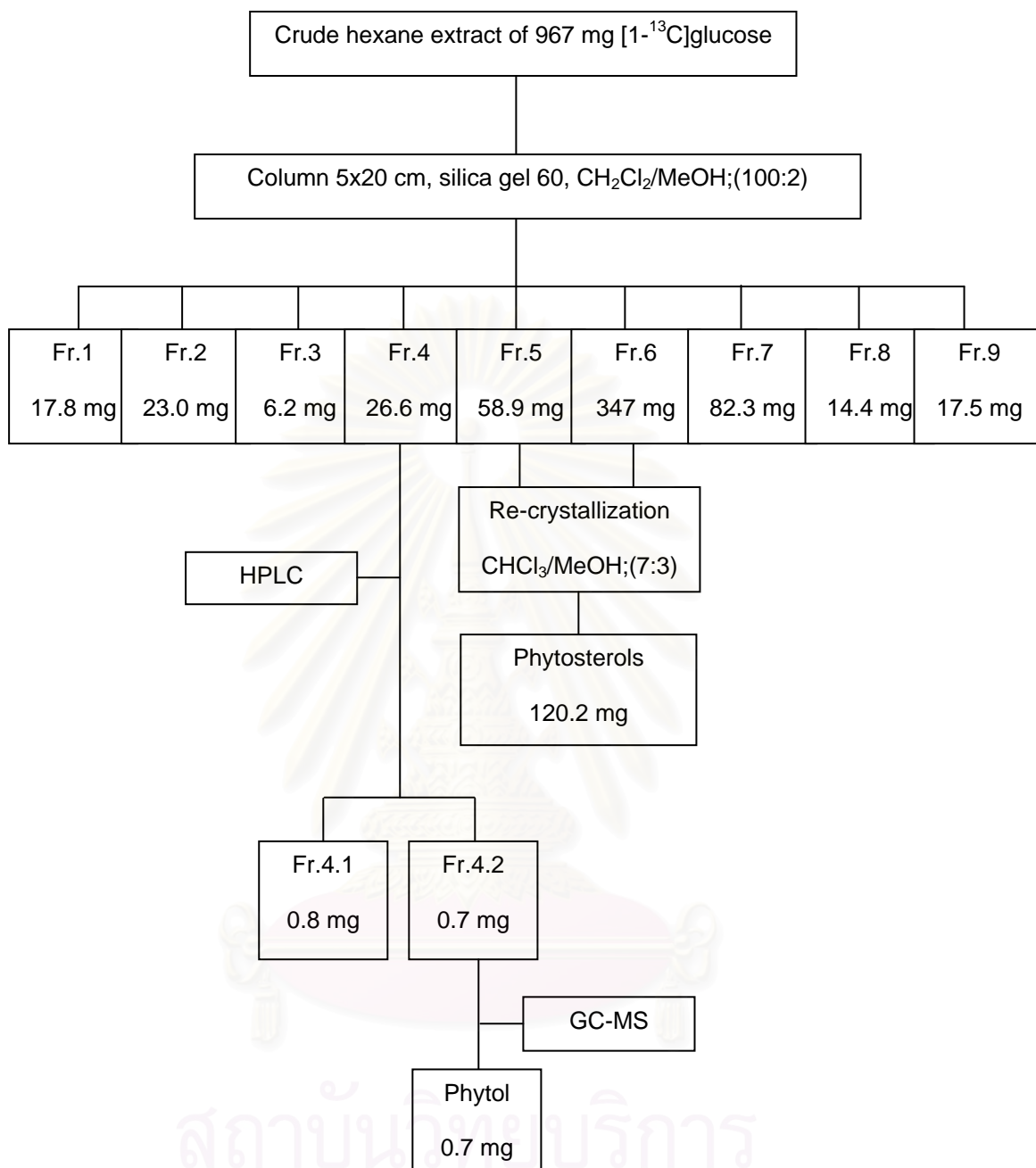
Isolation of terpenoids containing β -sitosterol and stigmasterol was performed. Cells, 835 g and 750 g, from feeding experiments with [1-¹³C]glucose and [2-¹³C]sodium acetate, respectively, were extracted separately with 700 ml of 95% (v/v) ethanol under reflux at 60 °C for 1 h. The extracts were filtered and evaporated to dryness under vacuum. The residues were then re-dissolved in 50% (v/v) ethanol in the presence of 1% (v/v) NaOH and heated at 60 °C for 30 min. After cooling at room temperature, the extracts were partitioned 5 times with 150 ml of *n*-hexane. The *n*-hexane layers were combined and concentrated to dryness under reduced pressure.

2.2.2 Screening of secondary metabolites

Accumulation of secondary metabolites in the cell suspension culture was evaluated using gas chromatography. GC separation was achieved in a chemically bonded fused-silica capillary column using an Agilent 6850 gas chromatograph equipped with flame ionization detector as described in 2.6

2.2.3 Isolation of secondary metabolites

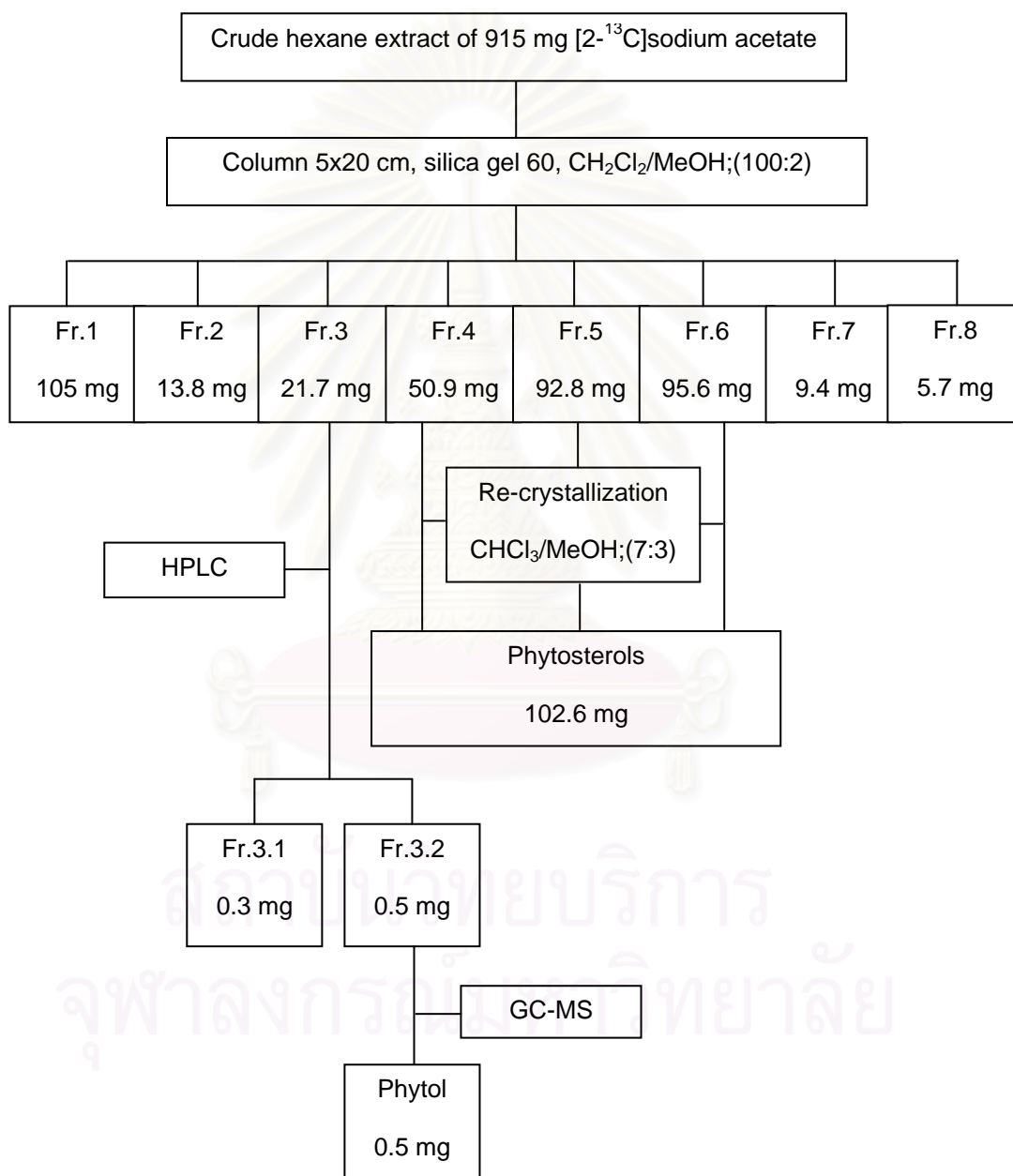
In all experiments, the extraction of terpenoids and steroids were performed as described in section 2.2.1.2. The crude extracts obtained from both labeled glucose and labeled sodium acetate feedings (967 and 915 mg, respectively) were dissolved in *n*-hexane and separated by column chromatography with silica gel 60 (Scharlau GE0048, Spain; column size 5x20 cm) eluted with dichloromethane/methanol (100:2) separately (Scheme 1 and 2). Fractions of 10 ml were collected and examined by TLC (dichloromethane/methanol (100:2; anisaldehyde/H₂SO₄ as visualization reagent). Fractions of similar chromatographic patterns were combined together. Finally, nine fractions were obtained from the crude hexane extract of [1-¹³C]glucose feeding (Scheme 1). Fraction 4 (26.6 mg) was subsequently purified by normal phase HPLC to give 2 fractions (Fr. 4.1 and Fr. 4.2). Fraction 4.2 (0.7 mg) was analyzed by GC-MS. Fraction 5 and fraction 6 were analyzed by TLC on silica gel 60 F₂₅₄ (Merck KGaA) using dichloromethane/methanol (100:2) as mobile. The *R_f* value of these fractions (fraction 5 and fraction 6) was 0.42. Fraction 5 and fraction 6 were combined and re-crystallized with chloroform/methanol (7:3) to afford 120.2 mg.



Scheme 1 Separation of crude hexane extract of *C. stellatopilosus* suspension culture fed with [1-¹³C]glucose

As the crude hexane extract of [1-¹³C]glucose feeding, eight fractions were obtained from the crude hexane extract of [2-¹³C]sodium acetate feeding (Scheme 2). Fraction 3 (21.7 mg) was subsequently purified by normal phase HPLC to give 2 fractions (Fr. 3.1 and Fr. 3.2). Fraction 3.2 (0.5 mg) was analyzed By GC-MS. Fractions 4-6 were analyzed by TLC on silica gel 60 F₂₅₄ (Merck KGaA) using

dichloromethane/methanol (100:2) as mobile. The R_f value of these fractions (fractions 4-6) was 0.42. Fractions 4-6 were combined and re-crystallized with chloroform/methanol (7:3) to afford 102.6 mg.



Scheme 2 Separation of crude hexane extract of *C. stellatopilosus* suspension culture fed with [2- 13 C]sodium acetate

2.3 Feeding experiments

2.3.1 Feeding with [1-¹⁴C]glucose

The cell suspension cultures of *C. stellatopilosus* (7-day old) were subcultured freshly on MS medium supplemented with 2.0 mg/l 2,4-D, 2.0 mg/l BA and 3% (w/v) sucrose. Later, [1-¹⁴C]glucose was dissolved in water at the concentration of 3.3×10^{-3} $\mu\text{Ci/ml}$ and then transferred into cell culture. The mixture was incubated at culture condition. In order to monitor the uptake of [1-¹⁴C]glucose into cells, the culture was sampled everyday. One milliliter of the cell suspension was centrifuged at 5,000 rpm for 10 min. The cells were ground before radio detection. The radio-uptake rate could be calculated based on the radioactivity present in the cells and in the medium by liquid scintillation counter. The harvested cells were then dried at 55 °C for 12 h. The dried cells were ground and extracted as described previously (2.2.1.1) and applied onto a pre-coated TLC plate (2.5.1) to be analyzed for radioactivity by TLC-radioscanner.

2.3.2 Feeding with [U-¹³C]glucose

From section 2.3.1, the optimal radioactive uptake appeared to be at day 4 after subculturing. Therefore, the cell suspension cultures of *C. stellatopilosus* (7-day old) were transferred into 250-ml erlenmeyer flasks and cultured for 4 days on a rotary shaker (120 rpm) at 25 ± 2 °C, under 16 h of photo-period (2000 lux). MS medium containing 2 mg/l 2,4-D, 2 mg/l BA and supplemented by [U-¹³C]glucose (25% w/v, 99% ¹³C enrichment in 75% w/v of unlabeled D-glucose) was used as culture medium. Fresh cells (2.6 g of fresh weight) were harvested and extracted as described in 2.2.1.1. The crude hexane extract (0.5 mg) was dissolved in 100 μl of

n-hexane and subjected to gas chromatograph-mass spectrometer for ^{13}C incorporative analysis.

2.3.3 Feeding with [1- ^{13}C]glucose

Cell suspension cultures of *C. stellatopilosus* (7-day old) were transferred into 250-ml erlenmeyer flasks (100 flasks) and grown for 4 days on a rotary shaker (120 rpm) at 25 ± 2 °C, under 16 h of photo-period (2000 lux), in MS medium containing 2 mg/l 2,4-D, 2 mg/l BA and supplemented by [1- ^{13}C]glucose (20% w/v, 99% ^{13}C enrichment in 80% w/v of unlabeled D-glucose).

2.3.4 Feeding with [2- ^{13}C]sodium acetate

For labeling studies with acetate, cell suspension cultures were grown in the medium similar to the glucose medium but containing [2- ^{13}C]sodium acetate (50% w/v, 99% ^{13}C enrichment in 50% w/v of unlabeled sodium acetate).

2.4 Semi-quantitative RT-PCR technique

Determination of the mRNA transcription levels using semi-quantitative RT-PCR technique was performed by conducting parallel reactions on each RNA sample. The first reaction used specific primers for *dxs*, *dxr*, *ggpps* and the other used primer for a house-keeping gene (*18S rRNA*).

2.4.1 RNA isolation

For the study on mRNA expression of *dxs*, *dxr*, *ggpps* genes using semiquantitative RT-PCR, total RNA was prepared from RNeasy Plant Mini Kit. The leaves (300 mg), green callus (150 mg) and suspension culture (150 mg) were separately ground into powder in the presence of liquid N_2 . The powder was

transferred to an RNase-free microcentrifuge tube, 450 μ l of buffer RLT was added, then vortexed vigorously. The lysate was transferred to QIAshredder spin column and centrifuged at 14,000 rpm for 2 min. The supernatant of the flow-through was transferred to a new microcentrifuge tube without disturbing the cell-debris pellet in the collection tube. A half volume of absolute ethanol was added to the clear lysate, mixed by pipetting and transferred to an RNeasy spin column, and centrifuged at 10,000 rpm for 15 s. The flow-through was discarded, and 700 μ l of buffer RW1 was added onto the RNeasy spin column, centrifuged at 8000 rpm for 15 s in order to wash the spin column membrane. Buffer RPE (500 μ l) was added and centrifuged at 10,000 rpm for 15 s. After drying the membrane by centrifuging at 10,000 rpm for 2 min, the RNeasy spin column was removed, placed on a new microcentrifuge tube and 30 μ l RNase-free water was added and incubated on ice for 1 min. The total RNA was eluted after centrifugation at 10,000 rpm for 1 min. The total RNA solution was stored at -20°C until used.

The concentration and purity of the total RNA were measured by a spectrophotometer. The concentration of the total RNA was analyzed by dilution of the total RNA solution with distilled water to 100-200 times and determined using the A_{260} nm with the following equation:

$$\text{Concentration of total RNA } (\mu\text{g}/\mu\text{l}) = (A_{260}) (\text{dilution factor}) (40 \mu\text{g}/\mu\text{l})$$

The purity of total RNA was analyzed by spectrophotometer, the purity of total RNA was judged by the ratio of A_{260}/A_{280} , of which has a ratio of 1.4-1.5. The pattern of intact RNA was evaluated by agarose gel electrophoresis.

2.4.2 cDNA preparation

The first-strand cDNA of *C. stellatopilosus* was synthesized using the SuperscriptTMIII reverse transcriptase and RACE32 primer (RACE32: 5'-GACTCGAGTCGACATCGATTTTTTTTTTTTTTTT-3'). According to manufacturer instruction, the cDNA synthesis mixture contained solutions as followed.

	Volume	Final concentration
	8 μ l	0.24 μ g (leaves)
Total RNA	8 μ l	0.08 μ g (green callus)
	8 μ l	1.68 μ g (suspension cultures)
RACE32 primer, 50 μ M	1 μ l	2.5 μ M
dNTP mix, 2.5 mM each	4 μ l	0.5 mM
Sterile distilled water	varied	to 13 μ l

The solution was incubated at 65°C for 5 min, then quickly chilled on ice for 1 min. Four μ l of 5x First strand buffer, 1 μ l of 0.1 M DTT and 1 μ l of SuperscriptTMIII RT were added into the solution and incubated at 50°C for 1 h. The reaction was inactivated by heating at 70°C for 15 min. After that adding RNase H (1 μ l) was then added to the reaction and incubated at 37°C for 20 min to afford the cDNA solution. The resulting cDNA was stored at -20°C until used.

2.4.3 DNA fragment amplification

The DNA fragment was amplified using Taq PCR core kit. The standard mixture was composed of primers and cDNA template according to the instruction manual.

Component (Master mix)	Volume/reaction	Final concentration
10x PCR Buffer	5 μ l	1x
dNTP mix, 2.5 mM each	4 μ l	200 μ M of each dNTP
Primer A	varied	0.1-0.5 μ M
Primer B	varied	0.1-0.5 μ M
<i>Taq</i> DNA Polymerase	0.25 μ l	2.5 units/reaction
Distilled water	varied	-
Template cDNA	varied	\leq 1 μ g/reaction
Total volume	50 μ l	

The *dxs*, *dxr* and *ggpps* genes transcription profiles were determined using semi-quantitative RT-PCR technique, in comparison with the house-keeping gene (*18Sr RNA*). Scheme of amplifications and the thermal profile were as shown below:

2.4.3.1 Specific Primers for Semi Quantitative RT-PCR

Designated	T _m (°C)	Sequence	Remark
18s-0.5F	62.45	5'-CAAAGCAAGCCTACGCTCTG-3'	For <i>18Sr</i>
18s-0.5R	62.45	5'-CGCTCCACCAACTAAGAACG-3'	<i>RNA</i>
FCS6-N	66.12	5'-CTTTTTGGTACCATGGCTCTCTCTGCA-3'	For
256A	58.66	5'-GCTCCCACAGGTGGTATTGTTCCATCAA-3'	<i>dxs</i>
PDXRF-S2	63.08	5'-AATTGGGGTACCATGGCTCTTAATTTG-3'	For
PDXR-A1	58.66	5'-TGCAAGTGCCACCACTTTAAA-3'	<i>dxr</i>
CS-S380	66.40	5'-GCGTGTGAACTTGTTGGCGGAG-3'	For
CS-A1048	66.47	5'-CAATGGAGCCGCCTTCTCAGG-3'	<i>ggpps</i>

2.4.3.2 PCR Parameters for the *18Sr RNA* Amplification

Segment	Step	Temperature (°C)	Time (min)	Number of cycles
1	Denaturing	95	3	1
2	Denaturing	95	1	35
	Annealing	58	2	
	Extension	72	3	
3	Extension	72	10	1
	Holding	4	∞	

2.4.3.3 PCR Parameters for the *dxs* Amplification

Segment	Step	Temperature (°C)	Time (min)	Number of cycles
1	Denaturing	95	3	1
2	Denaturing	95	1	30
	Annealing	58	2	
	Extension	72	3	
3	Extension	72	10	1
	Holding	4	∞	

2.4.3.4 PCR Parameters for the *dxr* Amplification

Segment	Step	Temperature (°C)	Time (min)	Number of cycles
1	Denaturing	95	3	1
2	Denaturing	95	1	35
	Annealing	48	2	
	Extension	72	3	
3	Extension	72	10	1
	Holding	4	∞	

2.4.3.5 PCR Parameters for the *ggpps* Amplification

Segment	Step	Temperature (°C)	Time (sec)	Number of cycles
1	Denaturing	95	30	1
2	Denaturing	95	30	30
	Annealing	50	30	
	Extension	72	60	
3	Extension	72	60	1
	Holding	4	∞	

2.4.4 Agarose gel electrophoresis

Agarose gel electrophoresis was used to analyze the PCR products. Agarose gel 1.2% (w/v) was prepared. The mixture was boiled using microwave oven until cleared solution was obtained. The solution was poured into the tray and a comb was placed in the agarose gel. The gel was placed at room temperature for 30 min for gel setting. The agarose gel tray was carefully removed and placed on the platform in the electrophoresis tank containing 1x TAE buffer. The RNA or DNA sample was mixed with loading buffer and slowly loaded into the slots of the submerged gel using the micropipette. Electrophoresis was carried out at a constant 100 V for 25 min. The gel was stained with ethidium bromide solution for 15 min. The resulting RNA or DNA pattern was observed under UV transilluminator (312 nm) and the picture was developed.

Composition per one gel	For agarose gel (1.2% w/v)
Agarose	0.24 g
TAE (x50)	0.4 ml
dH ₂ O	20 ml
Total volume	20 ml

2.5 Thin layer chromatography (TLC) analysis

Technique	: one dimension, ascending, single development
Stationary phase	: pre-coated TLC plate of silica gel 60 F ₂₅₄ on aluminum sheets
Layer thickness	: 0.2 mm
Solvent system	: benzene/ethyl acetate (4:1, v/v) dichloromethane/methanol (100:2, v/v)
Temperature	: 25-30 °C
Detection	: ultraviolet light at 254 and 365 nm, Iodine vapor, a mixture of anisaldehyde/H ₂ SO ₄ , TLC-radioscanner

2.5.1 TLC-radioscanning

The dried extracts (2.3.1) were dissolved in 40 µl of *n*-hexane and applied onto a pre-coated TLC plate of silica gel 60 F₂₅₄ on aluminum sheets. The plate was developed in a solvent system of benzene/ethyl acetate (4:1, v/v). TLC plate was visualized under I₂ vapor. The R_f value of dried extracts compared with authentic GGOH and β-sitosterol were 0.62 and 0.58, respectively. The TLC plate was then analyzed for radioactivity by TLC-radioscanner. The incorporation rates were calculated based on the results of radioactivity present in the cells and medium.

2.5.2 Detection of terpenoids and steroids on TLC plates

I collected fractions from column chromatography with silica gel 60 as described in 2.2.3. Then the collected fractions were analyzed by TLC on silica gel 60 F₂₅₄ (Merck KGaA) using dichloromethane/methanol (100:2, v/v) as mobile phase and a mixture of anisaldehyde/H₂SO₄ as visualization reagent for detection of terpenoids and steroids.

2.6 Gas chromatographic analysis

Accumulation of secondary metabolites in the cells was evaluated by gas chromatography. GC separation was achieved in a chemically bonded fused-silica capillary column using an Agilent 6850 gas chromatograph equipped with flame ionization detector, with setting parameters as follows.

Instrument model	Hewlett Packard HP6850 Series GC System	
Detector	FID (Flame Ionization Detector)	
Column	HP1 Methylsiloxane size 30 m, 0.32 mm x 0.25 μ m film thickness	
Column temperature		
Gradient	Initial temp.	220 °C, hold 3 min.
	Gradient	220-280 °C, 10 °C/min.
	Final temp.	280 °C, hold 16 min.
	Total time	25 min.
Injector temperature	280 °C	
Oven temperature	300 °C	
Helium carrier gas	flow rate 1.0 ml/min.	
Hydrogen supply	flow rate 30.0 ml/min	
Nitrogen supply	flow rate 30.0 ml/min	
Air flow	flow rate 300 ml/min	
Sample size	1 μ l	

The calibration curve was constructed using the authentic phytol, GGOH and phytosterols. The stock solutions of the authentic compounds were prepared in volumetric flask to obtain 1.56 mg/ml, 1.34 mg/ml and 3 mg/ml stock solutions of

phytol, GGOH and phytosterols, respectively. The stock solutions were diluted by half-dilution technique and the concentration ranges of 0.039-0.312 mg/ml and 0.084-0.67 mg/ml were used to construct the calibration curves of phytol and GGOH, respectively. The analysis of phytosterols by gas chromatography could be deduced to be a mixture of campesterol, stigmasterol and β -sitosterol in a ratio of 1:2:7. By analysis of the peak areas of phytosterols, the concentration range of campesterol, stigmasterol and β -sitosterol were 0.05-0.40 mg/ml, 0.075-0.60 mg/ml, and 0.25-2.0 mg/ml, respectively.

2.7 High performance liquid chromatography (HPLC) analysis

Selective fractions from column chromatography were subsequently purified by analytical normal phase HPLC. The conditions of HPLC were described below.

Instrument model: Waters600E, UV detector, Milford, MA, USA
- 600PF pump
- 484 tunable absorbance detector
- 807-IT Jasco integrator

Chromatographic column: Hypersil silica, 250x46 mm, 5 μ M

Mobile phase : hexane/chloroform (95:5, v/v)

Flow rate : 1.0 ml / min

Detector : UV 235 nm

Injection volume : 10 μ l

2.8 Gas chromatographic – mass spectrometric (GC-MS) analysis

Selective fractions from 2.2.3 (Isolation of secondary metabolite) and the crude hexane extract of cell suspension culture fed with [U-¹³C]glucose (2.3.2) were analyzed by GC-MS. Electron impact (70 eV) using a Hewlett Packard HP6890 GC-HP5972 MSD gas chromatograph-mass spectrometer with setting parameters as follows.

Instrument model	Hewlett Packard HP6890 GC-HP5972 MSD	
Detector	HP5972 MSD	
Column	HP1 Methylsiloxane size 30 m, 0.32 mm x 0.25 µm film thickness	
Column temperature		
Gradient	Initial temp.	220 °C, hold 3 min.
	Gradient	220-280 °C, 10 °C/min.
	Final temp.	280 °C, hold 16 min.
	Total time	25 min.
Injector temperature	280 °C	
Oven temperature	300 °C	
Helium carrier gas	flow rate 1.0 ml/min.	
Sample size	1 µl	

2.9 Gel documentation

The %volume of band intensity of *dxs*, *dxr* and *ggpps* on agarose gel was determined by gel documentation. After staining agarose gel with ethidium bromide solution for 15 min, the agarose gel was destained with distilled water for 30 min. The

bands of *dxs*, *dxr* and *ggpps* were developed and band intensity was measured. For a blank, empty gel was integrated and subtracted from the sample. The relative intensity was calculated as a ratio of intensity of sample and a house-keeping gene (*18S rRNA*).

2.10 Quantitative ^{13}C NMR analysis

The structures of unlabeled and labeled phytosterols were analyzed by ^1H NMR and ^{13}C NMR spectroscopy. NMR spectra were recorded in CDCl_3 , at $25\text{ }^\circ\text{C}$, using the INOVA-500 NMR spectrometer Varian, USA of the Scientific Equipment Center, Prince of Songkhla University. The ^{13}C NMR spectra of the isolated compounds were identical with those of β -sitosterol and stigmasterol as described previously. (Arigoni *et al.*, 1997 and Adam *et al.*, 1998) ^{13}C -NMR spectra from incorporation experiments with $[1\text{-}^{13}\text{C}]\text{glucose}$ and $[2\text{-}^{13}\text{C}]\text{sodium acetate}$ (99% ^{13}C abundance) and unlabeled sodium acetate and glucose (1.1% ^{13}C natural abundance) were recorded under identical conditions. The NMR signals were separately integrated for each carbon atom. The intensity of each signal was normalized with the intensity of C20. Relative ^{13}C -abundance of individual carbon atoms was calculated as a ratio of ^{13}C -labeled and unlabeled materials.

2.11 Transmission electron microscopy

Plant cells from leaf, green callus and suspension cultures of *C. stellatopilosus* were prepared for electron micrograph in order to perceive the cell organelles. Samples for electron microscopic observation were prepared according to the method described previously (Glauert, 1984; Sitthithaworn *et al.*, 2006). Young fresh

leaves, green callus and suspension cultures of *C. stellatopilosus* were cut into small pieces (1.0 x 1.0 mm) and fixed in a solution of 2.5% glutaraldehyde in 0.1 M phosphate buffer, pH 7.2, at 4°C for 2 h. The specimens were post fixed in 1% osmium tetroxide at 4°C for 2 h, and then washed with distilled water for 5 min 3 times. After staining with 2% uranyl for 20 min they were dehydrated in a graded series of ethanol solutions (70%, 80%, and 90% 5 min 3 times each, and 100% 10 min 2 times) and infiltrated using 100% propylene oxide for 15 min twice and a mixture of propylene oxide and epoxy resin at the ratios of 1:1 for 2 h, 1:2 for 2 h, and in pure epoxy resin for another 3 h. The resulting samples were embedded in liquid paraffin wax for at least 16 h at 70°C. Blocks of specimens were sectioned at 80-90 nm thickness with an ultramicrotome. The sections were viewed and photographed under a JEOL JEM-2010 CX Transmission electron microscopy at 80 kV.

CHAPTER IV

RESULTS

1. Establishment of *Croton stellatopilosus* Cell Suspension Cultures and Their Terpenoid and Steroid Biosynthetic Potential

1.1 Establishment of callus culture

Young leaves were used as explants to initiate callus culture in petri dishes containing solid MS medium supplemented with 1.0 mg/L 2,4-D, 0.1 mg/L kinetin and 3% (w/v) sucrose. The petri dishes were maintained at 25 ± 2 °C under photo-period of 16/8 h. Subsequent manipulation of plant growth regulator was carried out on MS agar medium supplemented with the combination of 2,4-D (from 1.0 to 2.0 mg/l) and kinetin (from 0.5 to 1.0 mg/l). It was found that the combination of 2.0 mg/l 2,4-D and 1.0 mg/l kinetin appeared to be the best for callus formation. As shown in Figure 8A, the calli were initiated at the edge of leaf segments and formed as compact yellowish nodules after 2 weeks of incubation. The induced calli were subcultured successfully on MS agar medium containing 3% (w/v) sucrose, 1.0 mg/l 2,4-D and 1.0 mg/l BA with subculturing passage every three weeks. In this medium the callus had a high growth rate resulting in friable, soft and yellowish tissues (Fig. 8B).

1.2 Establishment of green callus cultures

To obtain green callus cultures, the normal callus tissues (maintained on MS agar medium containing 1.0 mg/l 2,4-D and 1.0 mg/l BA) were subcultured for a few times (3 weeks each) on MS medium containing 1% (w/v) sucrose, 2.0 mg/l NAA, 2.0 mg/l BA and 2 g/L gellan gum (Morimoto and Murai,1989). Under these conditions,

the yellowish callus gradually produced green pigment in the tissues (Fig. 9). These green calli were subsequently used for the analysis of transcription profile and cellular development.

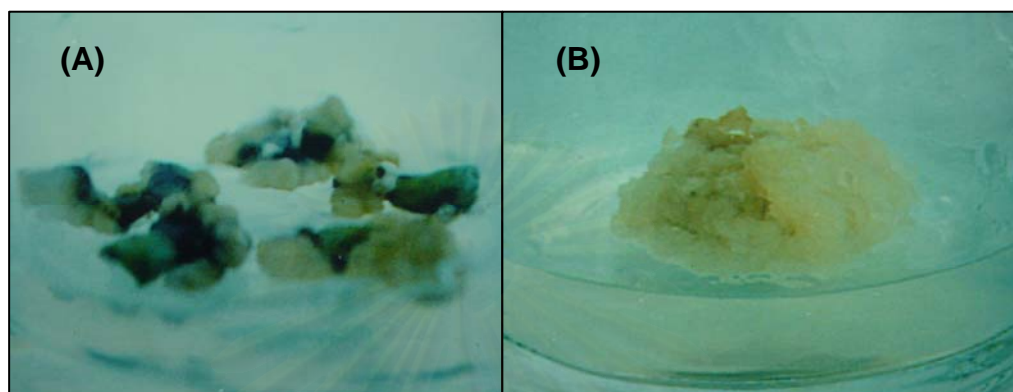


Figure 8 (A) Induction of callus from the leaf explants of *C. stellatopilosus* on MS agar medium containing 2.0 mg/l 2,4-D, 1.0 mg/l kinetin and 0.8% (w/v) plant agar. (B) Callus cultures of *C. stellatopilosus* obtained from the induction and were maintained on MS agar medium containing 1.0 mg/l 2,4-D, 1.0 mg/l BA and 0.8% (w/v) plant agar.



Figure 9 Green callus cultures grown on MS medium containing 1% (w/v) sucrose, 2.0 mg/l NAA, 2.0 mg/l BA and 2 g/L gellan gum.

1.3 Establishment of suspension cultures

The resulting green callus were subcultured every three weeks and transferred to the liquid MS medium containing 3% (w/v) sucrose, 2.0 mg/l 2,4-D and 2.0 mg/l BA (Wungsintaweeikul *et al.*, 2007). The suspension cultures were rotated at 120 rpm on a rotary shaker. During the 1st to 4th subcultures, the undifferentiated cultured cells under these conditions turned pale green. After that, it appeared to be friable, homogeneous and yellowish aggregates with rapid growth (Fig. 10). The established cell suspension cultures were then subcultured every week. These suspension cultures were subsequently used for the analysis of terpenoid and steroid formation and for [1-¹³C]glucose and [2-¹³C]sodium acetate feeding experiments.

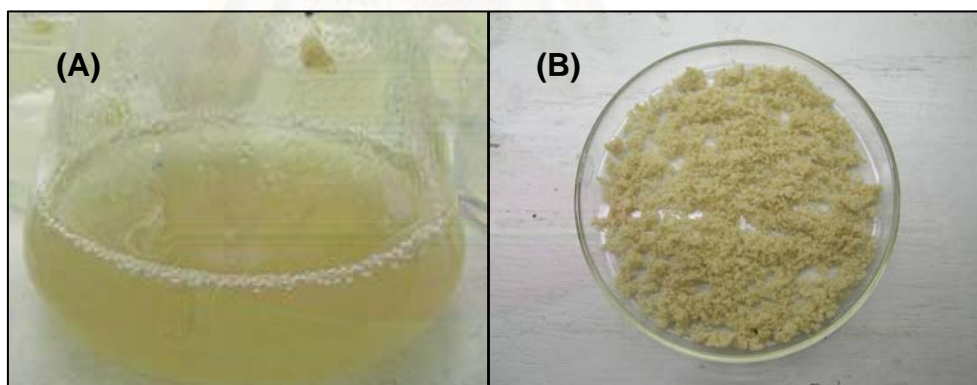


Figure 10 (A) Cell suspension cultures of *C. stellatopilosus* maintained in MS liquid medium containing 3% (w/v) sucrose, 2.0 mg/L 2,4-D and 2.0 mg/L BA. (B) Cell suspension cultures after being harvested and washed thoroughly with distilled water for analysis of terpenoid and steroid formation.

1.4 Detection of secondary metabolites by gas chromatography and gas chromatography – mass spectrometry

1.4.1 Detection of secondary metabolites by gas chromatography

Detection of phytol, GGOH and phytosterols in the crude hexane extracts of *C. stellatopilosus* cell suspension cultures was performed by gas chromatography (GC). Various GC parameters were first set up as follows: column HP1 Methylsiloxane size 30 m, 0.32 mm x 0.25 μ m film thickness, inject temp. 200 °C, temp. program: 200 °C for 3 min then elevated to 280 °C within 13 °C/min, then hold at 280 °C to 14 min. I found phytol and GGOH at the elution times of 7.4 and 7.6 min, respectively, but phytosterols were not detected under this first GC condition (Fig.11). Subsequently, I improved the GC conditions by changing the inject temp. from 200 to 280 °C, and the temperature program: 220 °C for 3 min then elevated to 280 °C within 15 °C/min, then hold at 280 °C to 16 min. The resulting chromatograms showed the presence of the phytosterols i.e. β -sitosterol, stigmasterol and campesterol, whereas the peaks of phytol and GGOH were not separated (Fig.12). Finally, I could optimize the GC conditions (CHAPTER III, 2.6) to detect all of them in a single run with phytol, GGOH, campesterol, stigmasterol and β -sitosterol eluted at 7.8, 8.4, 20.4, 21.2 and 22.8 min, respectively. (Fig.13). Under this GC condition, plaunotol could be eluted at 8.0 min although this diterpene was not detected in the crude hexane extracts of the cell suspension cultures of *C. stellatopilosus*.

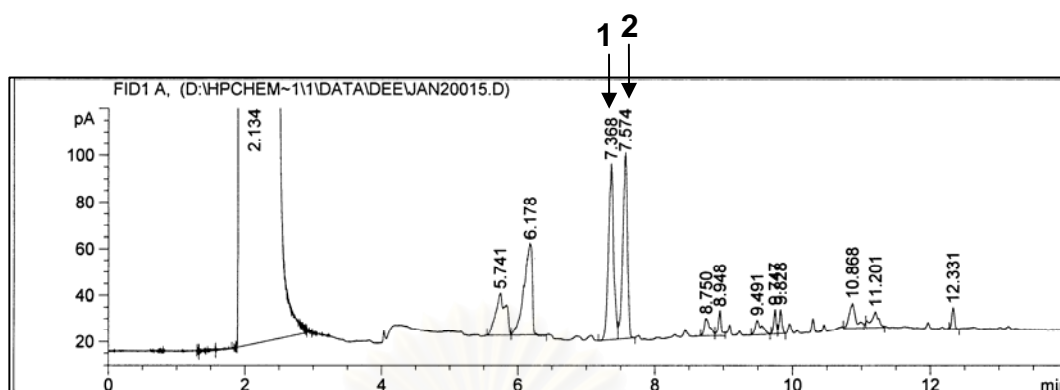


Figure 11 First GC trial showing the GC chromatogram of crude hexane extract of the cell suspension cultures of *C. stellatopilosus*, 1= phytol and 2= GGOH

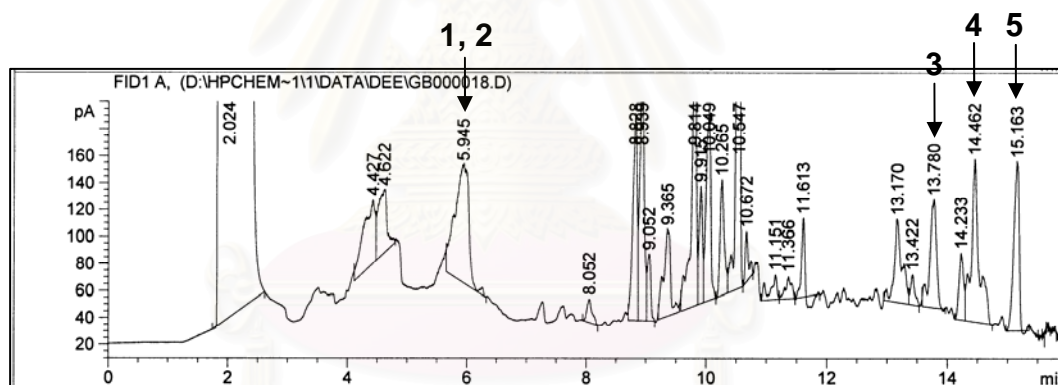


Figure 12 Second GC trial showing the GC chromatogram of crude hexane extract of the cell suspension cultures of *C. stellatopilosus*, 1= phytol, 2= GGOH, 3= campesterol, 4= stigmasterol and 5= β -sitosterol

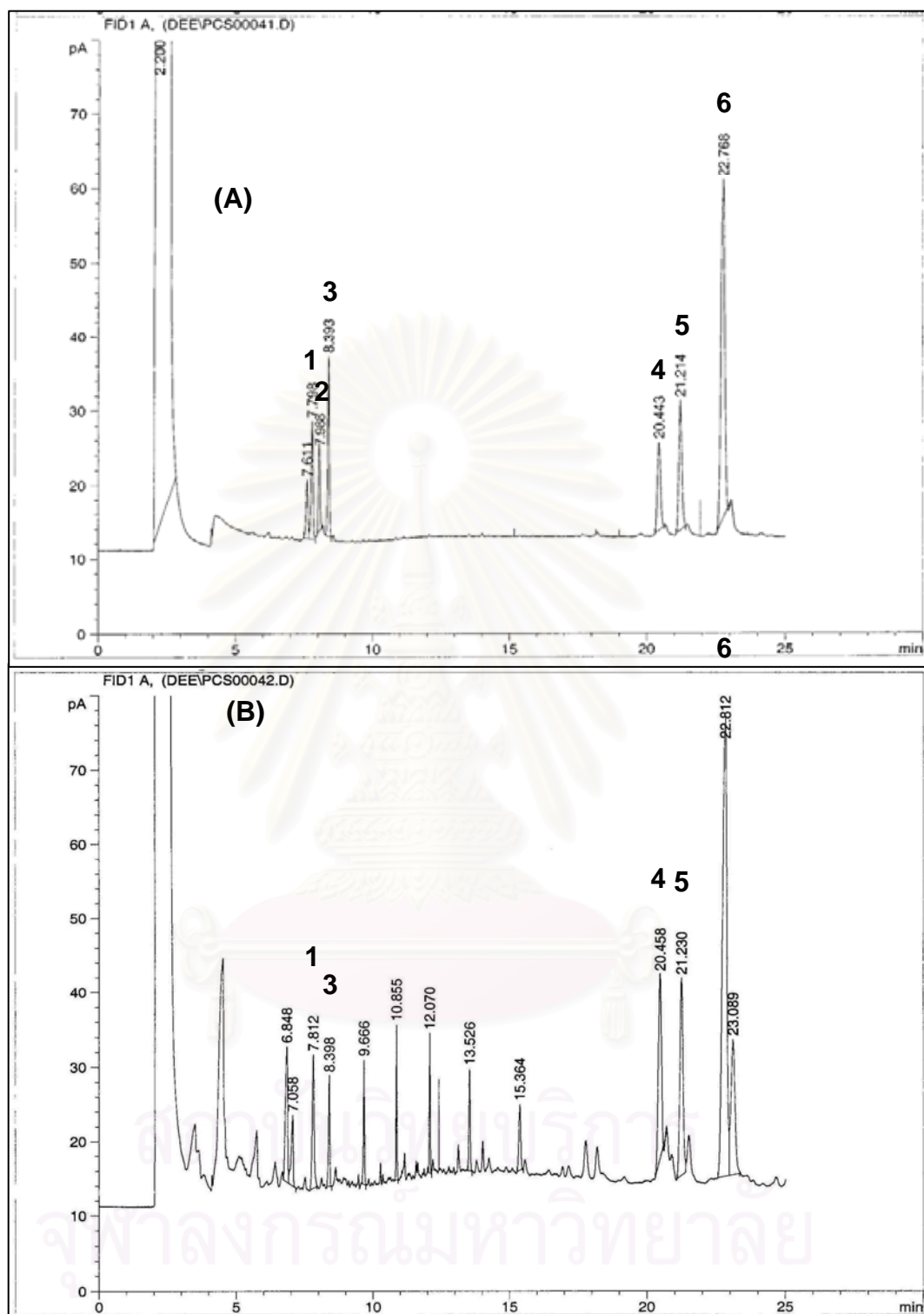


Figure 13 Final GC optimization showing the GC chromatogram of crude hexane extract of the cell suspension cultures of *C. stellatopilosus* A: Authentic compounds; B: suspension extract day 4, 1= phytol, 2= plaunotol, 3= GGOH, 4= campesterol, 5= stigmasterol and 6= β -sitosterol.

1.4.2 Identification of terpenoids and phytosterols by GC–MS

After optimizing the GC condition to detect simultaneously the terpenoids and phytosterols in the crude hexane extract of *C.stellatopilosus* cell suspension cultures, the identity of these compounds further confirmed by GC-MS. It can be seen in Figure 14 that the molecular weights of phytol, GGOH, campesterol, stigmasterol and β -sitosterol were detected to be 296, 290, 400, 412 and 414, respectively. Furthermore, their mass fragmentations were also matched with the pattern of WILEY275 database library.



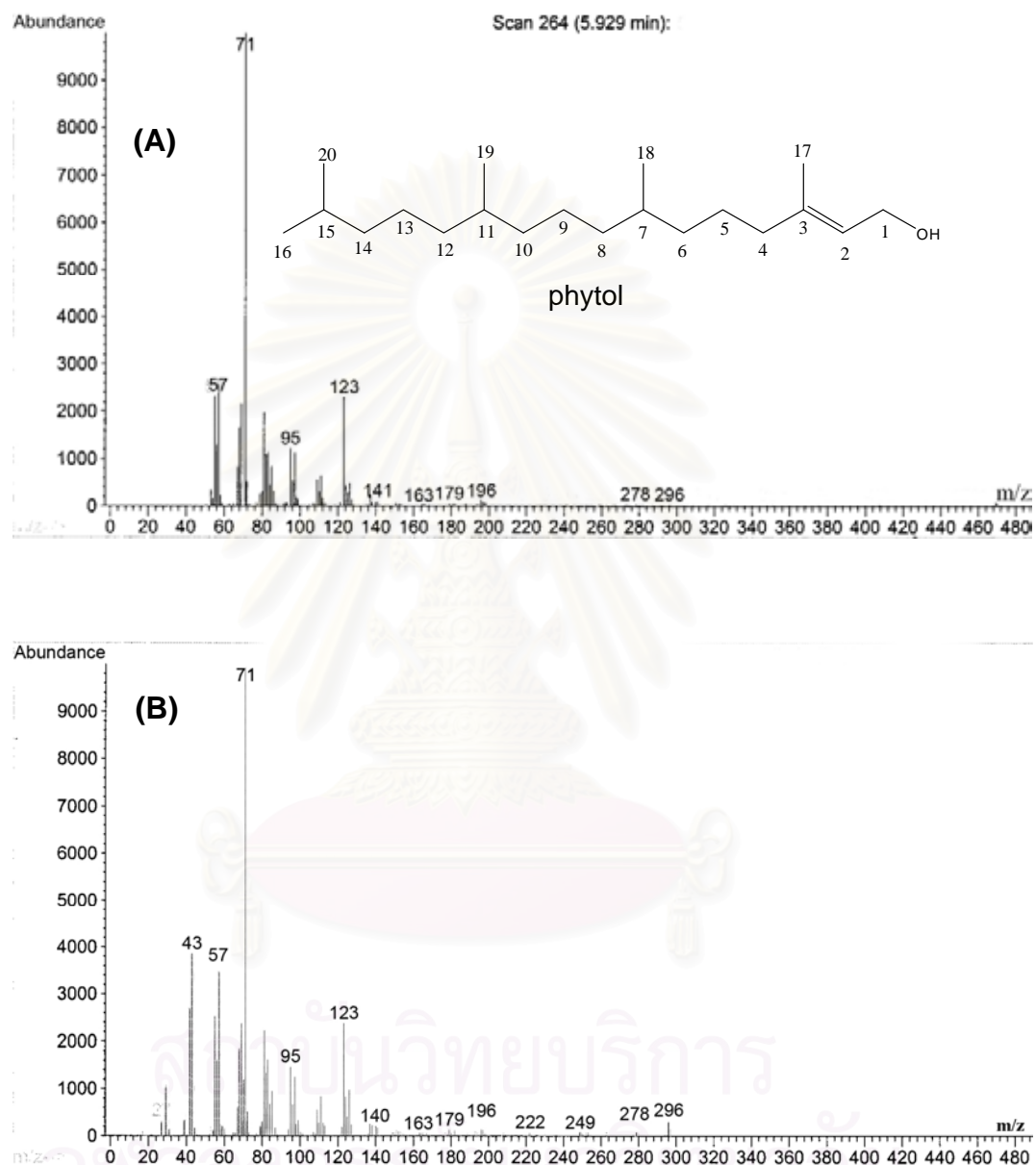


Figure 14-1 Mass spectral data of phytol (A) from crude hexane extract of the cell suspension cultures of *C. stellatopilosus* comparison with the pattern of WILEY275 database library (B).

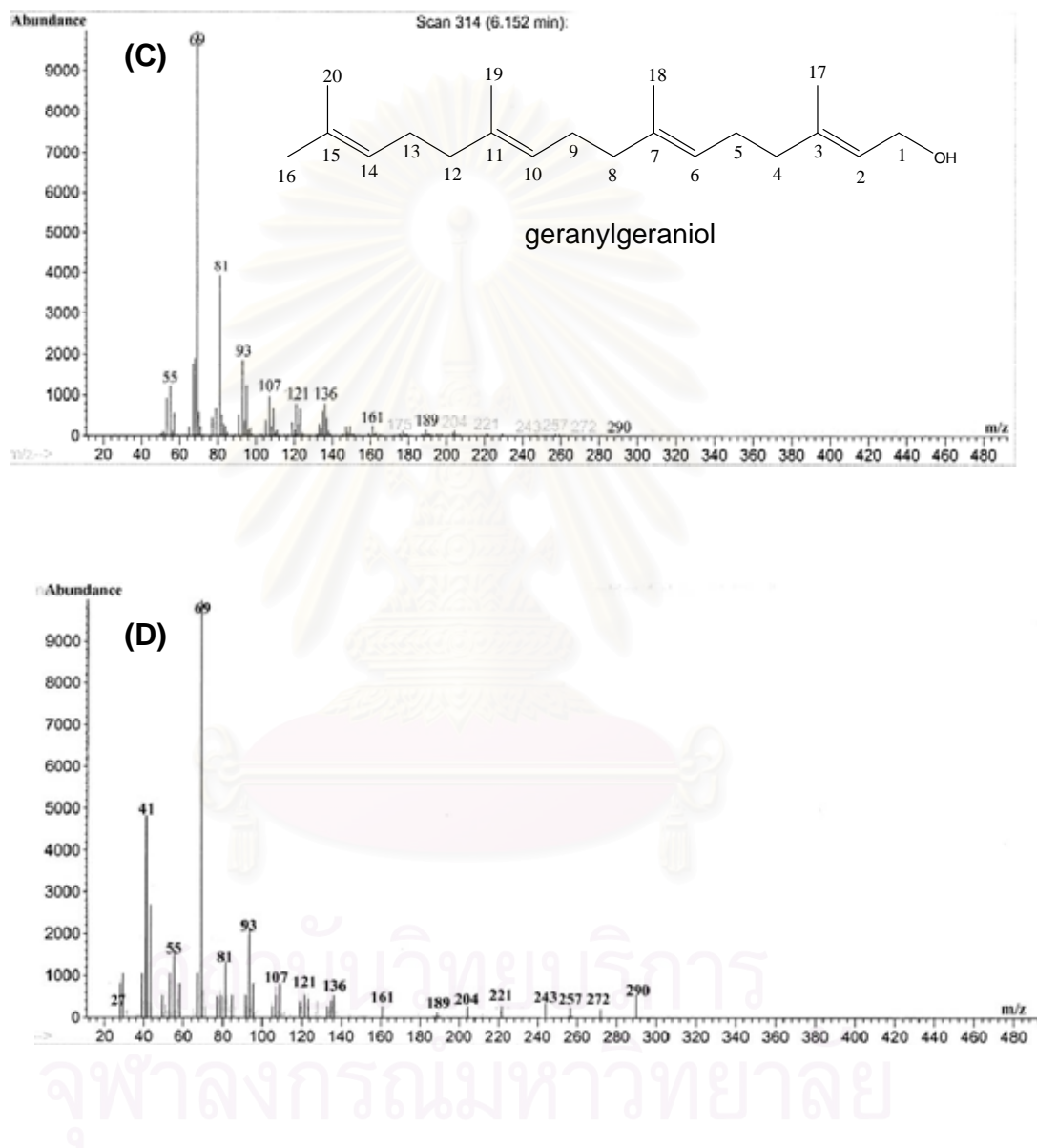


Figure 14-2 Mass spectral data of geranylgeraniol (C) from crude hexane extract of the cell suspension cultures of *C. stellatopilosus* comparison with the pattern of WILEY275 database library (D).

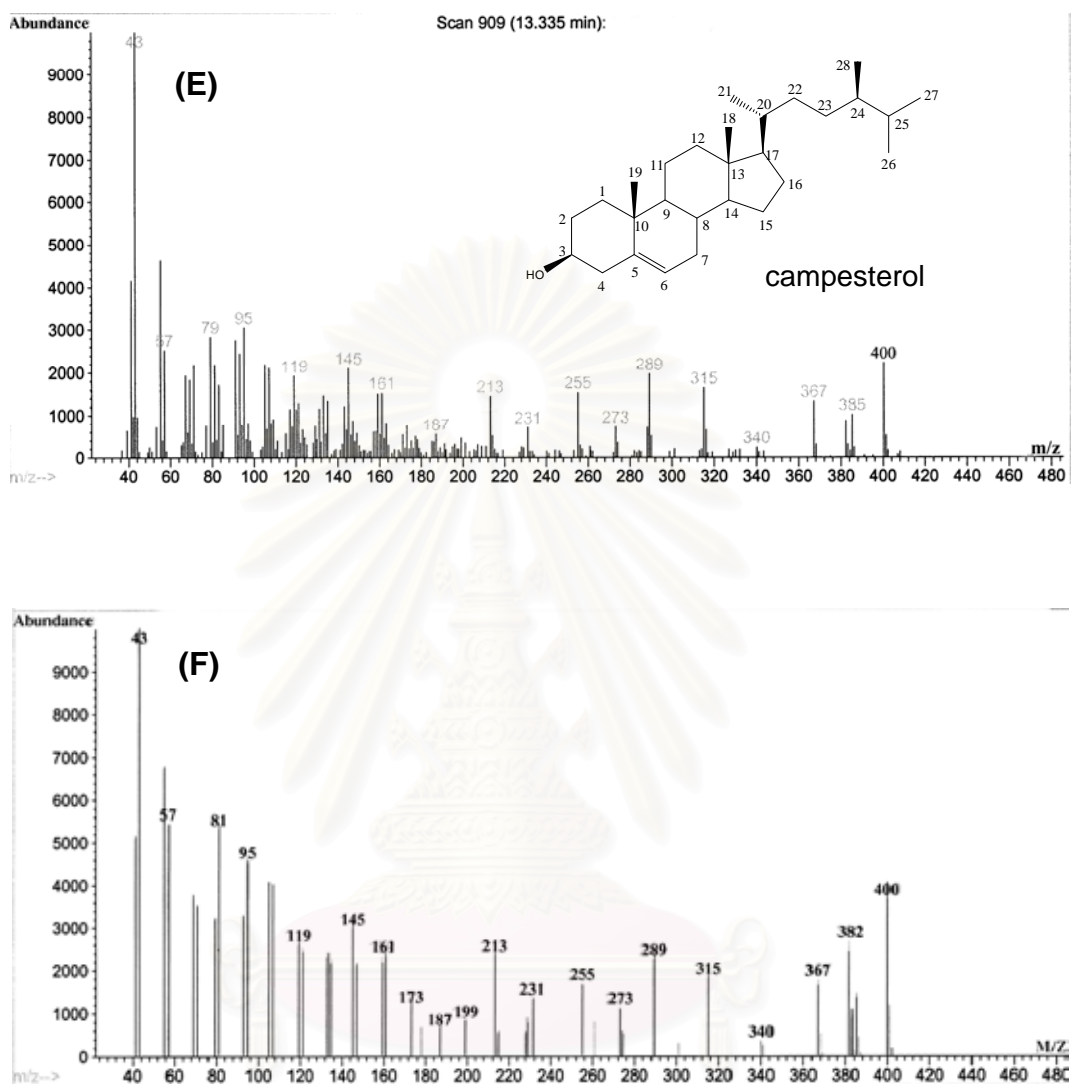


Figure 14-3 Mass spectral data of campesterol (E) from crude hexane extract of the cell suspension cultures of *C. stellatopilosus* comparison with the pattern of WILEY275 database library (F).

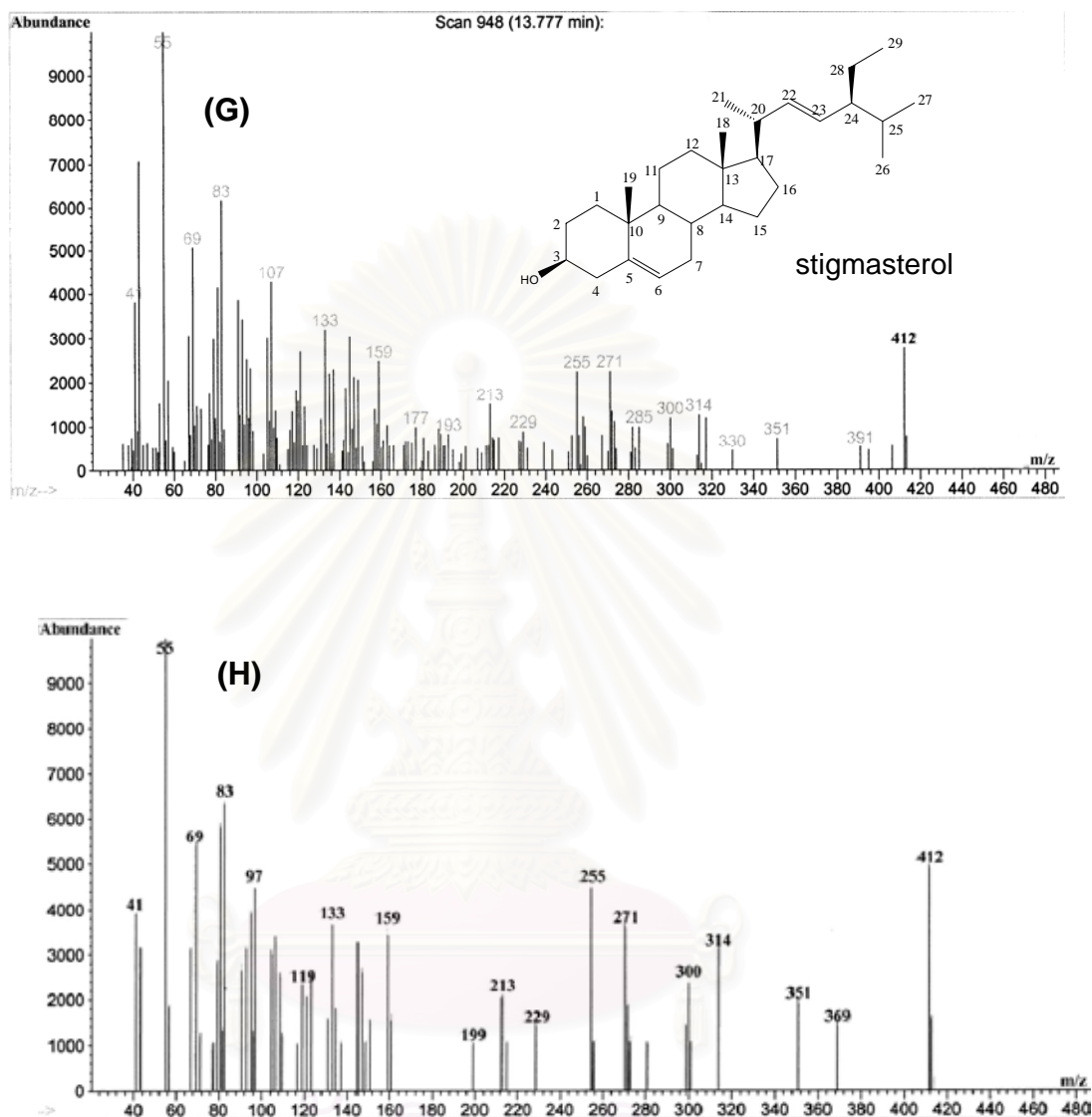


Figure 14-4 Mass spectral data of stigmasterol (G) from crude hexane extract of the cell suspension cultures of *C. stellatopilosus* comparison with the pattern of WILEY275 database library (H).

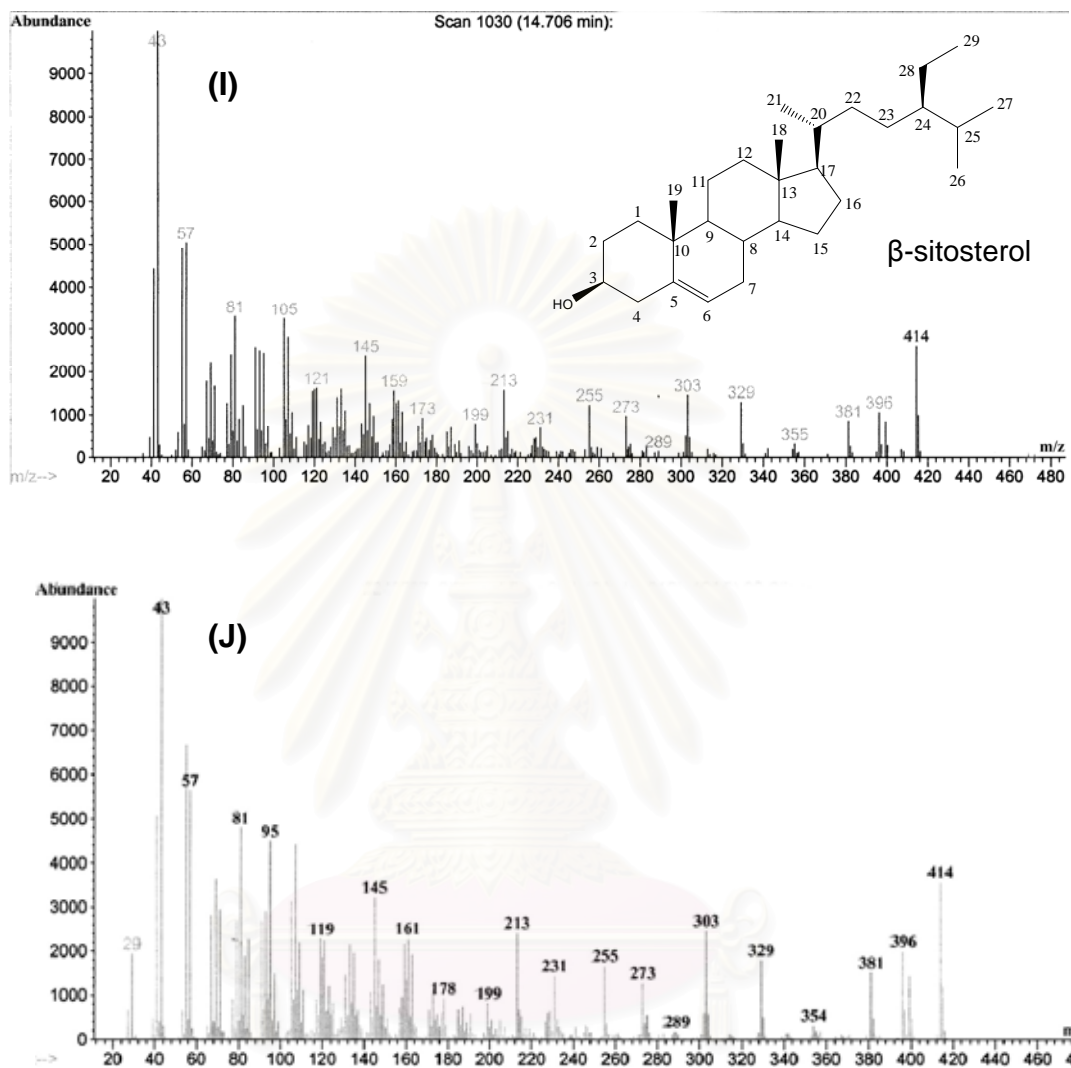


Figure 14-5 Mass spectral data of β -sitosterol (I) from crude hexane extract of the cell suspension cultures of *C. stellatopilosus* comparison with the pattern of WILEY275 database library (J).

1.5 Time-course study of *C. stellatopilosus* cell suspension cultures

Determination of phytol, GGOH and phytosterols (campesterol, stigmasterol, β -sitosterol) produced by *C. stellatopilosus* cell suspension cultures was performed using gas chromatography and calibration curves of standards. The relationship between the age of cultured cells and fresh weight was plotted as a growth curve (Fig. 15A). It can be seen that the suspension culture had a slow growth in the first four days before entering a rapid growth rate from day 5 to day 8 to obtain almost 5 fold increase of the cell fresh weight. After that the growth started to decline and reached their stationary phase at day 10.

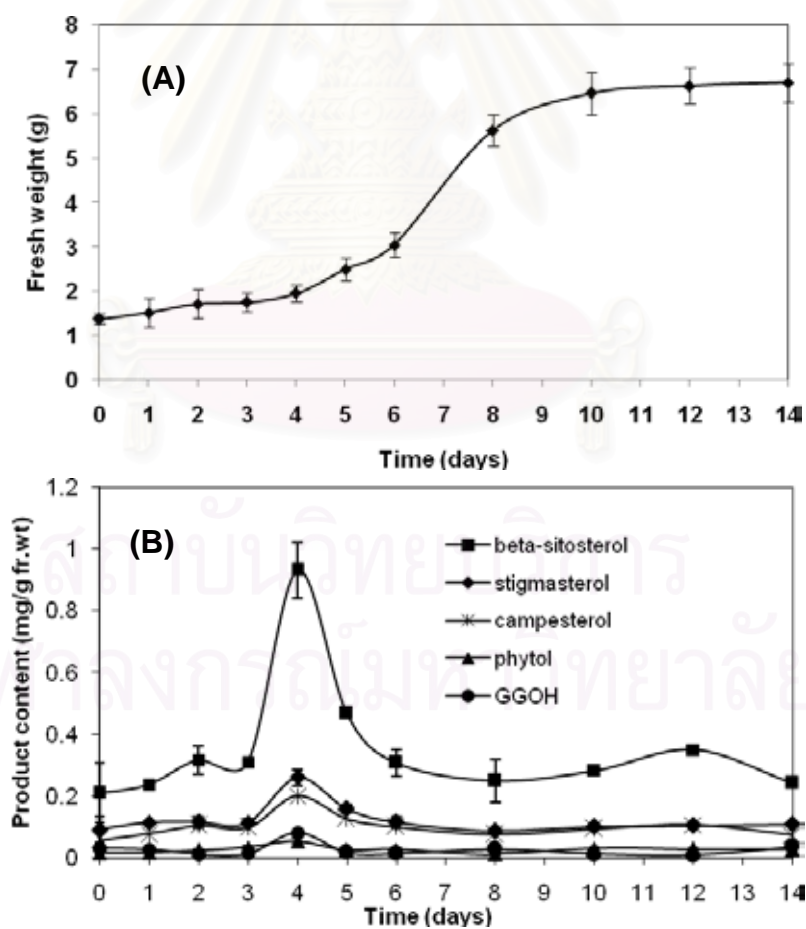


Figure 15 Growth curve (A) and product formation curves (B) during a 14-day culture cycle of *C. stellatopilosus* cell suspension culture.

For the analysis of secondary metabolite formation during the culture cycle, calibration curves were first constructed using authentic phytol, GGOH campesterol, stigmasterol and β -sitosterol as standards (Fig. 16). It can be seen that the concentration range of 0.039-0.312 mg/ml and 0.084-0.67 mg/ml were obtained for the calibration curves of phytol and GGOH with the linear regression of 0.9965 and 0.9989, respectively, (Figs. 16A and 16B) whereas the concentration range of campesterol, stigmasterol and β -sitosterol appeared to be 0.05-0.40 mg/ml, 0.075-0.60 mg/ml, and 0.25-2.0 mg/ml with the linear regression of 0.9989, 0.9985 and 0.9984, respectively (Figs. 16C, 16D and 16E). Based on this GC analysis, the time-course of product formation in *C. stellatopilosus* cell suspension cultures was obtained (Fig. 15B). It can be seen that the cultured cells produced relatively high contents of β -sitosterol, stigmasterol and campesterol compared with the very low levels of GGOH and phytol. Absolutely no plaunotol was detected in the cell culture although its immediate precursor, GGOH, was formed during the culture cycle. Interestingly, the maximal formation of all the products was at day 4, when the cultured cells were entering their rapid growth phase (Fig. 15B and Table 3). This suggested that these compounds are involved in the primary metabolism relating to the cell growth, especially the phytosterols which are known to be the components of plant cell membranes. The results were in agreement with previous report (Wungsintaweekul *et al*, 2007). Kitaoka and co-worker in 1989 showed that GGOH was observed to accumulate in the lag and stationary phases of cell growth (Kitaoka *et al.*, 1989)

Table 3 Contents of secondary metabolites in the crude extract of suspension culture of *C. stellatopilosus* on day 4

	Compound amount (mg/g.fw)				
	Phytol	GGOH	Campesterol	Stigmasterol	β -Sitosterol
Crude extract	0.054 \pm 0.01	0.081 \pm 0.004	0.200 \pm 0.009	0.260 \pm 0.025	0.931 \pm 0.091

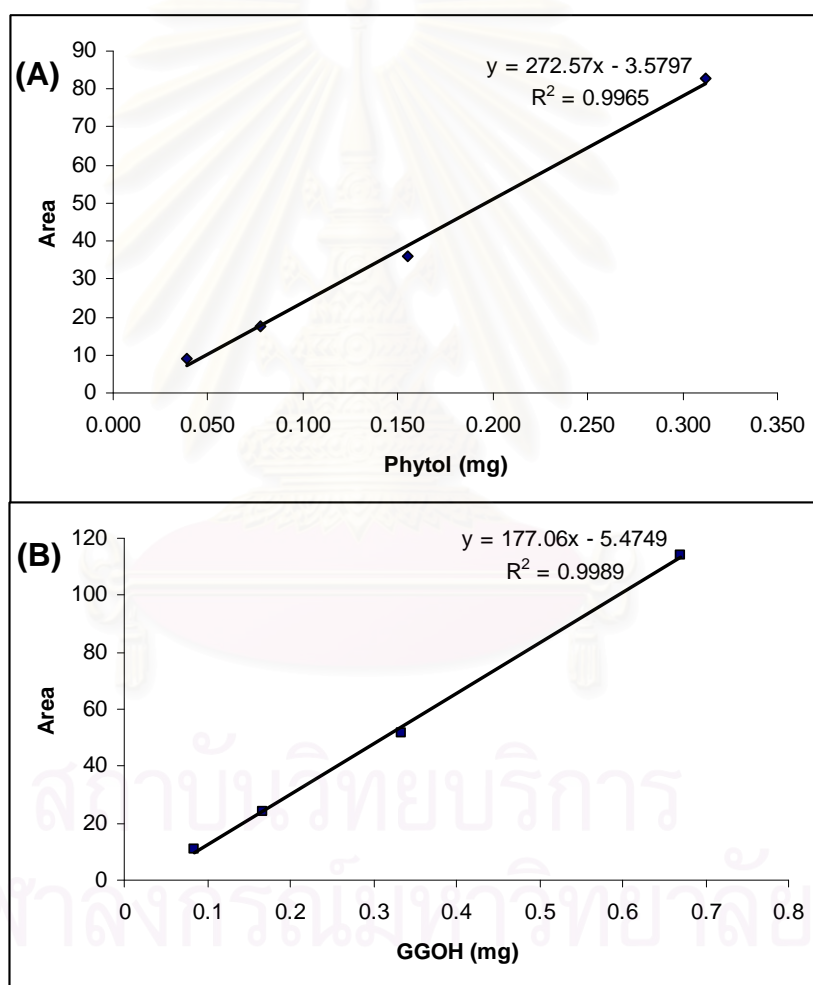


Figure 16 Calibration curves of authentic phytol (A) and GGOH (B)

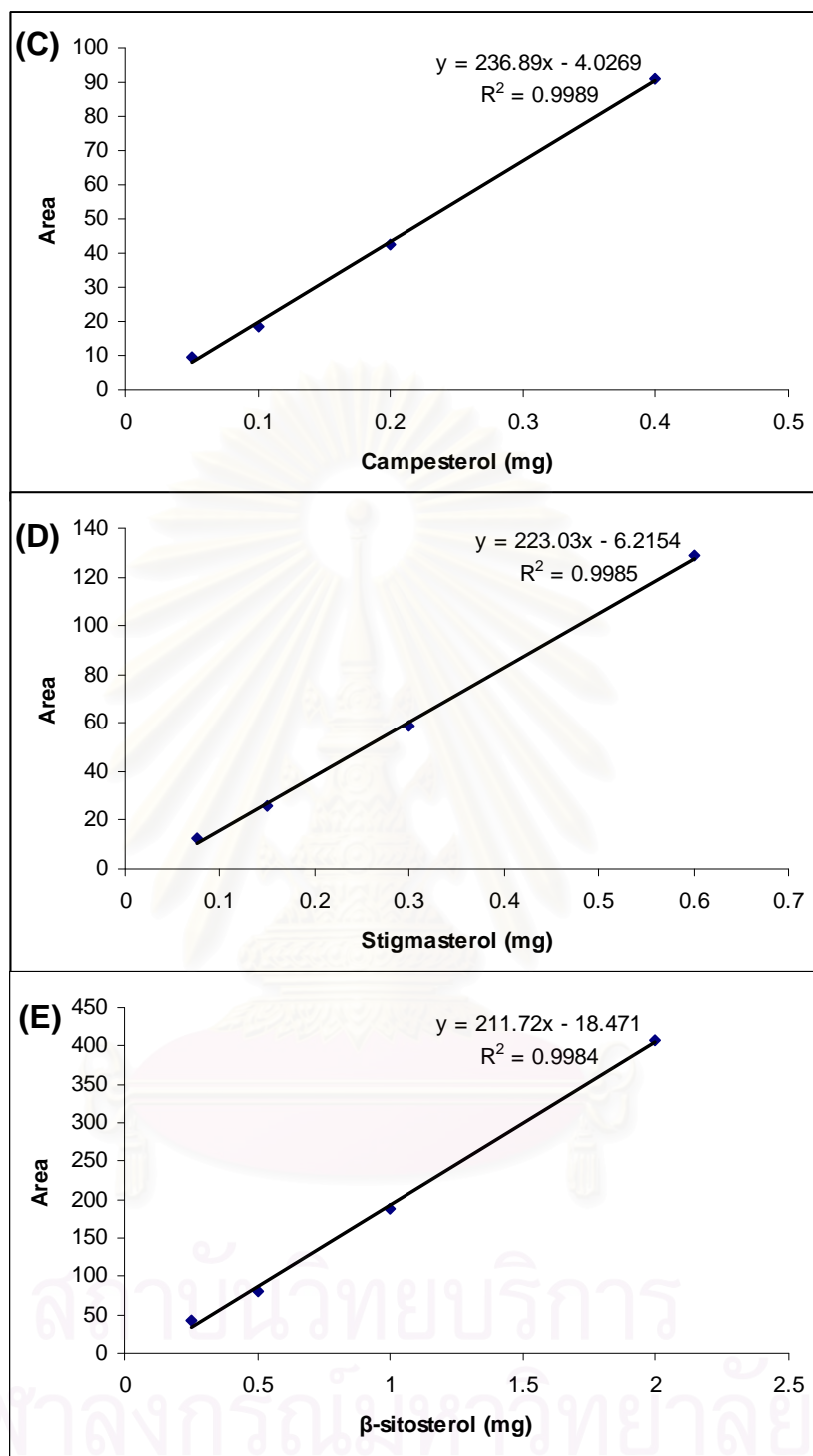


Figure 16 (continued) Calibration curves of authentic campesterol (C), stigmasterol (D) and β -sitosterol (E)

Figure 17 showed GC chromatograms of crude hexane extract of cell suspension cultures of *C. stellatopilosus* on day 0 – day 14 after subculturing. The chromatogram on day 4 showed the highest peaks of phytol, GGOH and phytosterols (β -sitosterol, campesterol, stigmasterol) compared with authentic compounds.

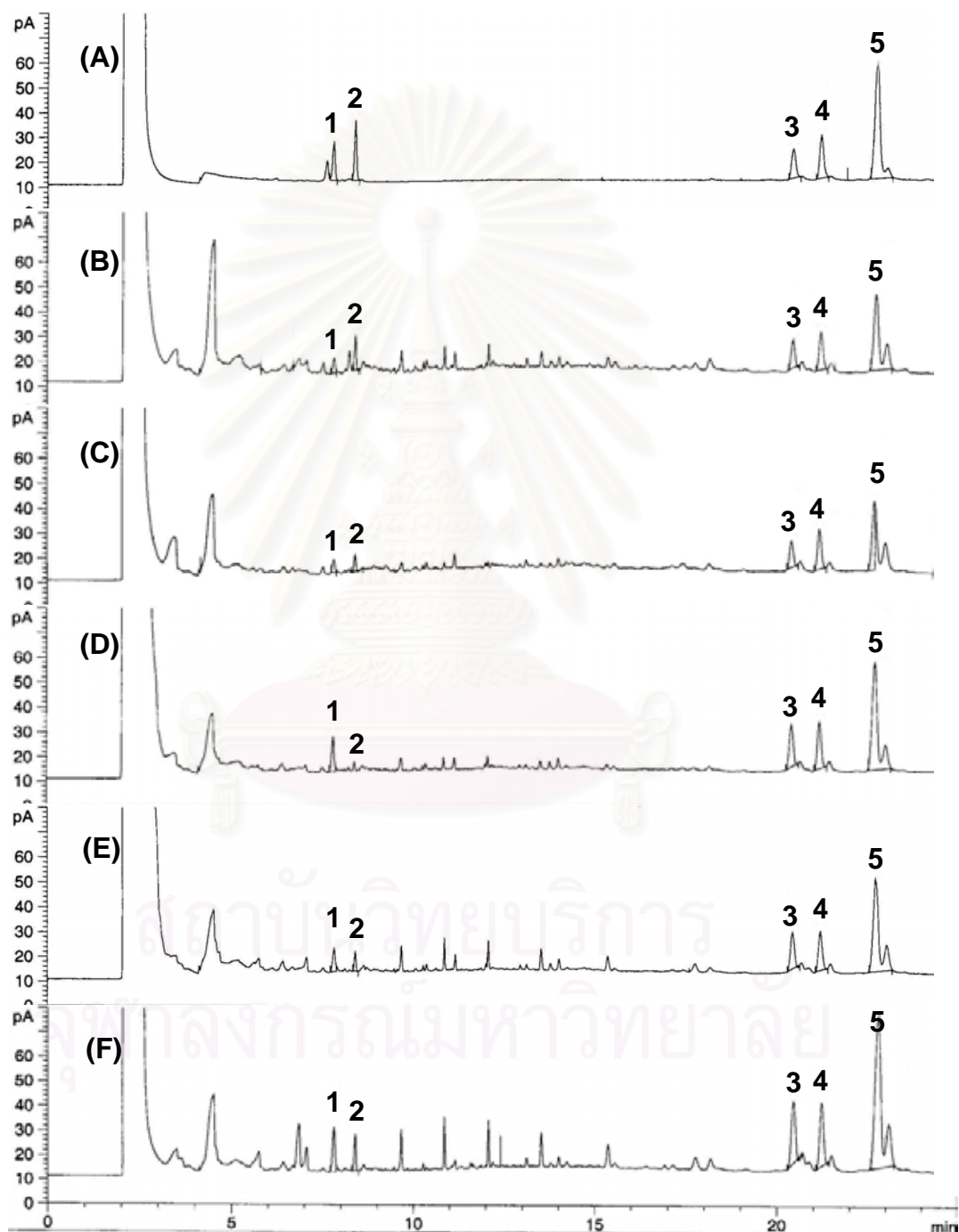


Figure 17 GC chromatograms (A); Authentic compounds, (B-F); crude hexane extract of cell suspension cultures of *C. stellatopilosus* on day0-day4, 1=phytol, 2=GGOH, 3=campesterol, 4=stigmasterol and 5= β -sitosterol

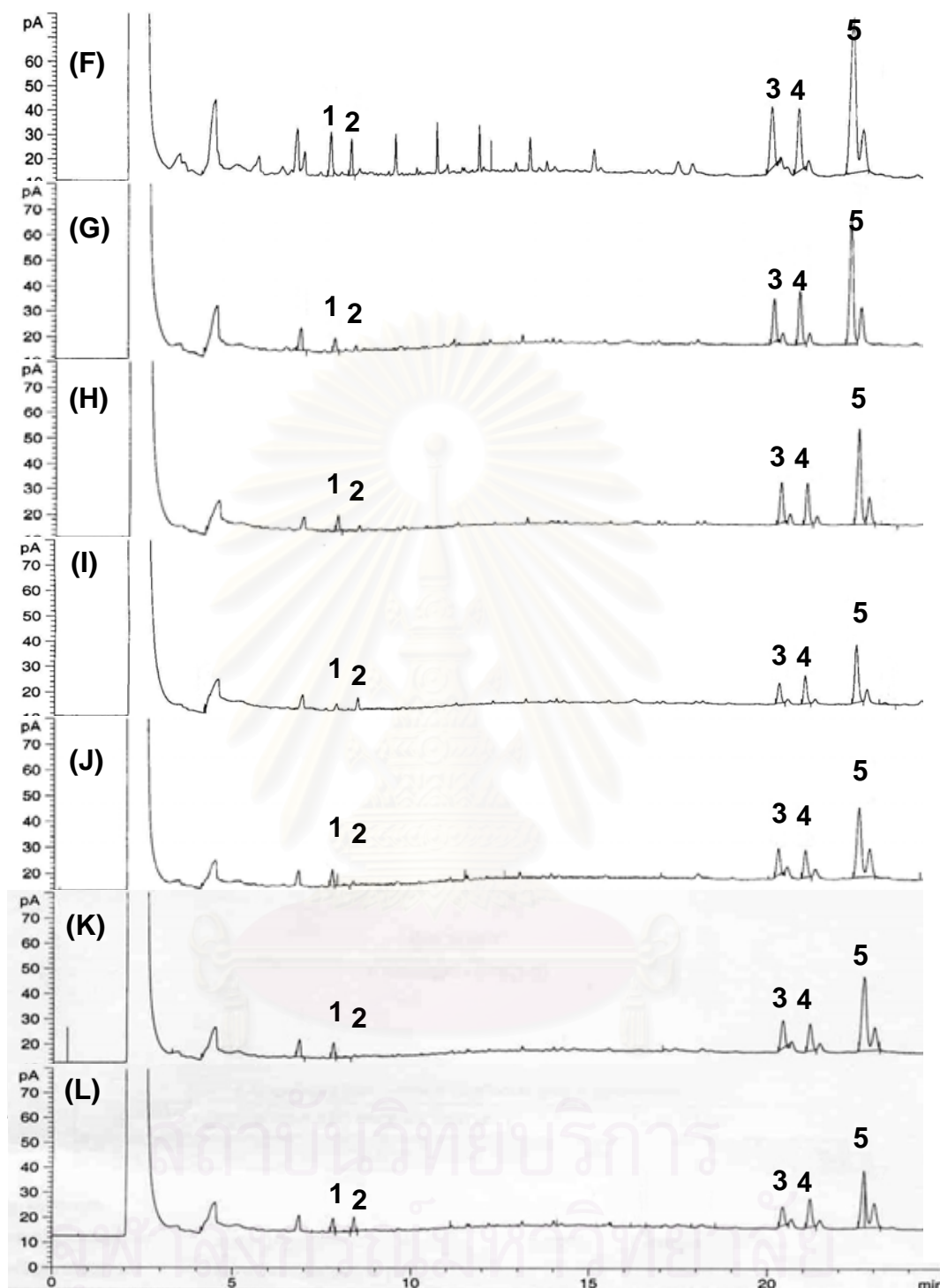


Figure 17 (continued) GC chromatograms of crude hexane extract cell suspension cultures of *C. stellatopilosus* on day4 (F), day5 (G), day6 (H), day8 (I), day10 (J), day12 (K) and day14 (L), 1=phytol, 2=GGOH, 3=campesterol, 4=stigmasterol and 5= β -sitosterol

2. Phytochemical Studies

2.1 Isolation and purification of terpenoids and phytosterols

The crude hexane extracts obtained from both 967 mg of labeled glucose and 915 mg of labeled sodium acetate feedings were purified by column chromatography with silica gel 60 (Scheme 1 and 2). Nine fractions were obtained from the hexane crude of [1-¹³C]glucose feeding (Scheme 1). Fr.4 (26.6 mg) was subsequently purified by analytical normal phase HPLC to give 2 fractions (Fr. 4.1 and Fr. 4.2) (Fig.18). Fr. 4.2 (0.7 mg) was analyzed. By GC-MS and comparison with the mass spectral data of authentic compound, allowed the identification of phytol (Figure 19A and 20A). Fr. 5 and 6 were analyzed by TLC on silica gel 60 F₂₅₄ using dichloromethane/methanol (100:2, v/v) as mobile phase (anisaldehyde/H₂SO₄ as visualization reagent). The *R_f* value of these fractions were 0.42. The fractions were combined and re-crystallized with chloroform/methanol (7:3, v/v) to afford 120.2 mg of phytosterols (Table 4). The presence of these compounds was confirmed by analysis of GC-MS, ¹H NMR and ¹³C NMR spectral data and comparison with these in the literature (Arigoni *et al.*, 1997; Adam *et al.*, 1998). As the crude hexane extract of [1-¹³C]glucose feeding, obtained 0.5 mg phytol (Fig. 19B and 20B) and 102.6 mg phytosterols (Table 4) from the crude hexane extract of [2-¹³C]sodium acetate feeding. However, the unlabeled compounds were prepared using either glucose or sodium acetate as cold precursors. Phytosterols were isolated with the same procedure. Unfortunately in final, we could not isolated GGOH from the crude extract of [1-¹³C]glucose and [2-¹³C]sodium acetate feeding experiments.

Table 4 Contents of terpenoids and phytosterols isolated from feeding experiment of suspension cultures of *C. stellatopilosus*.

Compound	Amount (mg)		Confirmed with
	Feeding with [1- ¹³ C]glucose	Feeding with [2- ¹³ C]acetate	
Phytol	0.7	0.5	GC-MS
Phytosterols	120.2	102.6	GC-MS, ¹ H NMR, ¹³ C NMR

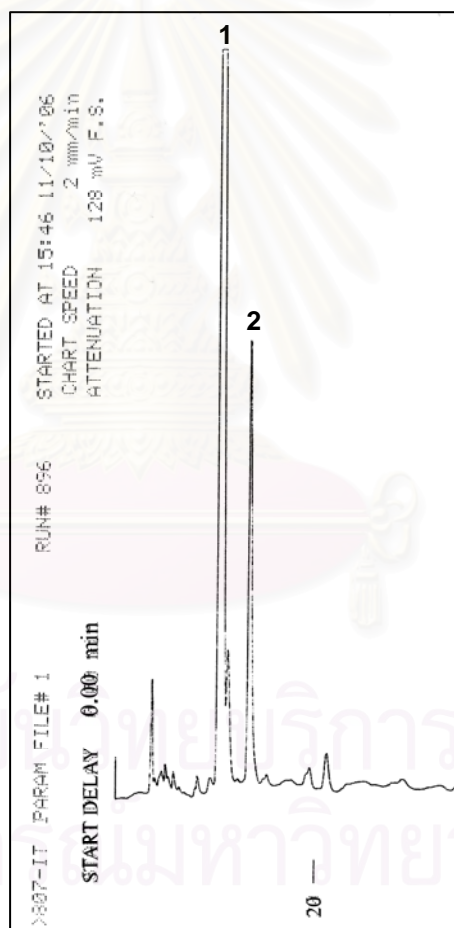


Figure 18 HPLC chromatograms of terpenoids isolated from cell suspension cultures of *C. stellatopilosus* feeding with [1-¹³C]glucose, 1=Fr. 4.1 and 2=Fr. 4.2.

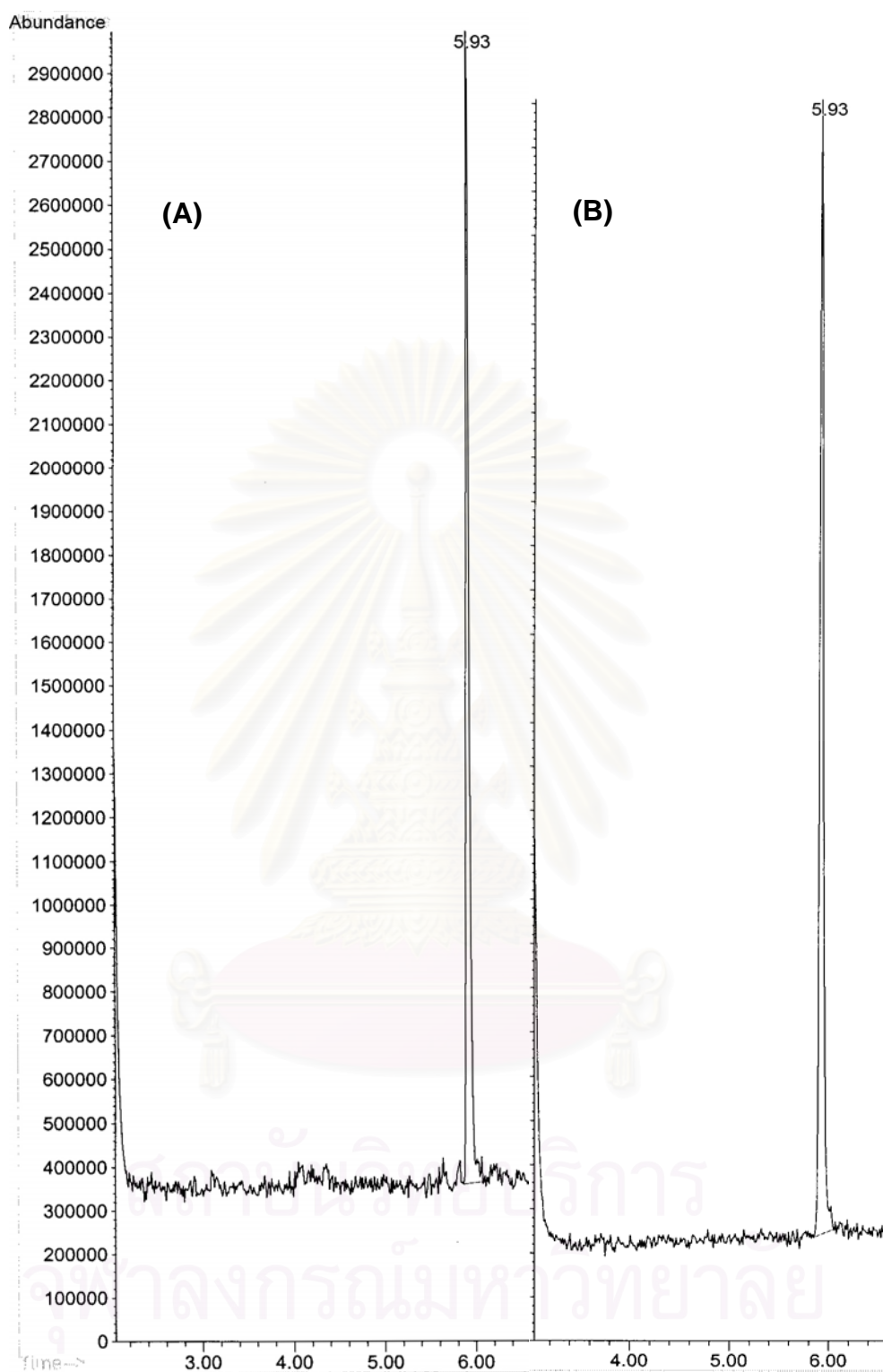


Figure 19 GC-MS chromatograms of phytol isolated from cell suspension cultures of *C. stellatopilosus*, feeding experiment with $[1-^{13}\text{C}]$ glucose (A) and $[2-^{13}\text{C}]$ sodium acetate (B)

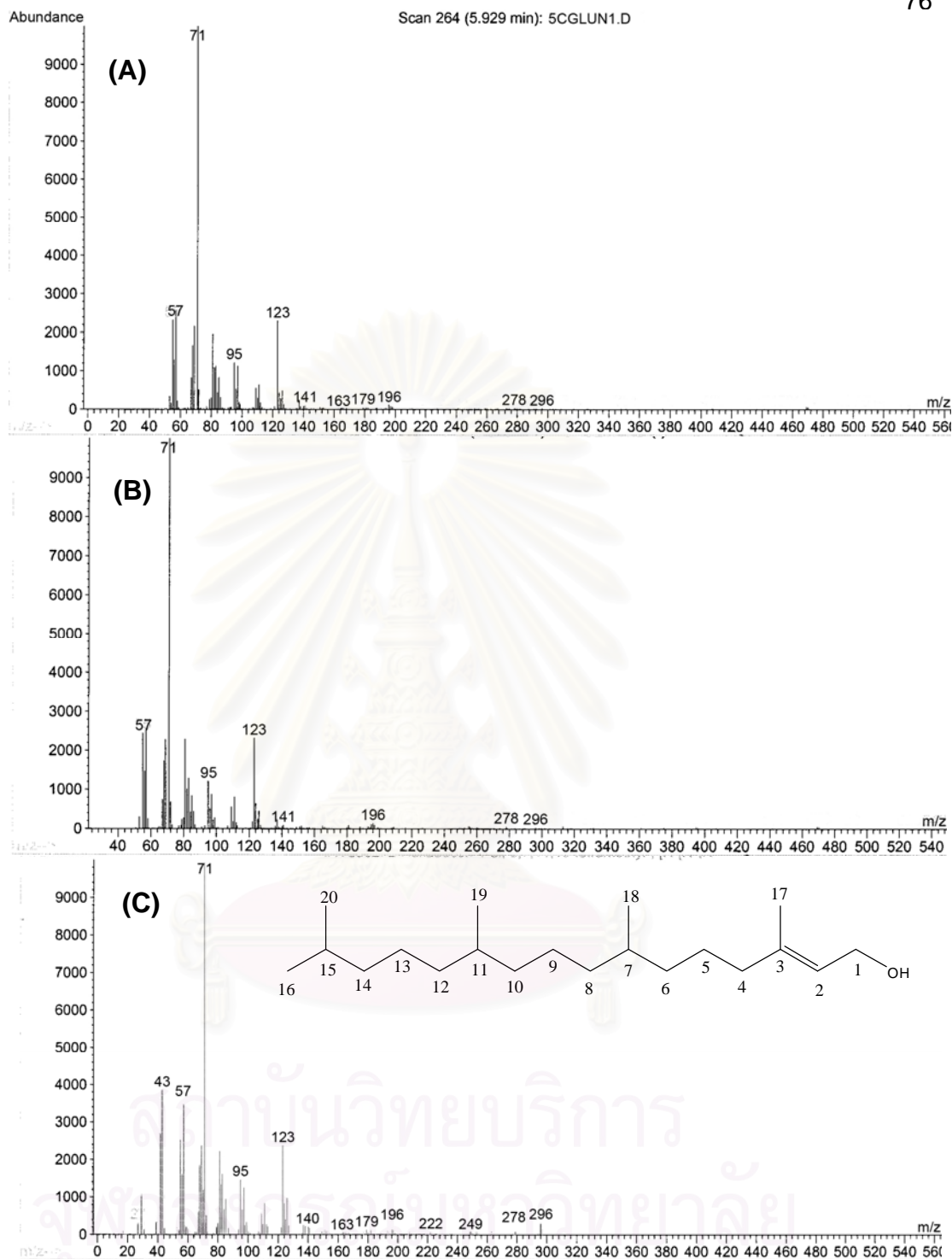


Figure 20 Mass spectral data of (A) phytol isolated from cell suspension cultures of *C. stellatopilosus*, feeding experiment with $[1-^{13}\text{C}]$ glucose, (B) with $[2-^{13}\text{C}]$ sodium acetate, (C) standard phytol

2.2 Identification of phytosterols

By column chromatography as described in Chapter III, major compounds could be isolated from the cell suspension cultures of *C. stellatopilosus* as white amorphous solid. The isolated compounds gave one spot on TLC but after being subjected to extensive spectroscopic studies, including GC-MS and NMR, they were found to be phytosterols. These phytosterols were identified as campesterol, stigmasterol and β -sitosterol (Fig. 21) by GC at the retention time of 12.51, 12.81 and 13.42 min, corresponding to the molecular-ion peaks of m/z 400, 412 and 414, respectively (Figs. 22 and 23). The $^1\text{H-NMR}$ and $^{13}\text{C-NMR}$ spectroscopic analysis showed that the isolated compound was a mixture of stigmasterol and β -sitosterol which could not be separated from each other by column chromatography. The $^1\text{H-NMR}$ (Fig. 24) and $^{13}\text{C-NMR}$ (Figs. 25-26) spectra of the mixture unequivocally corresponded with the data of the mixture reported previously (Wright *et al.*, 1978; Boonyaratavej and Petsom, 1991). The ^{13}C NMR spectrum showed a total of 46 signals. Among them four were olefinic carbon signals (δ 140.72, 138.32, 129.22 and 121.71), and one oxygen-attached carbon signal (δ 71.80) was observed. The remaining carbons showed signals with chemical shifts between 11 and 142 ppm. Comparison of these data with the reported values of β -sitosterol and stigmasterol is summarized in Table 5.

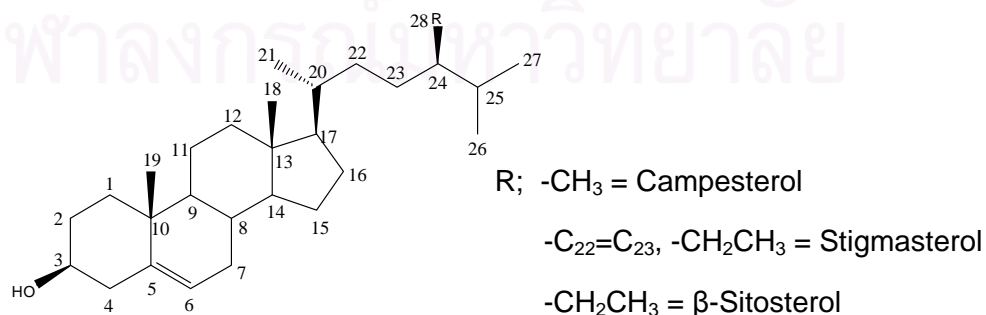


Figure 21 Chemical structures of campesterol, stigmasterol and β -sitosterol

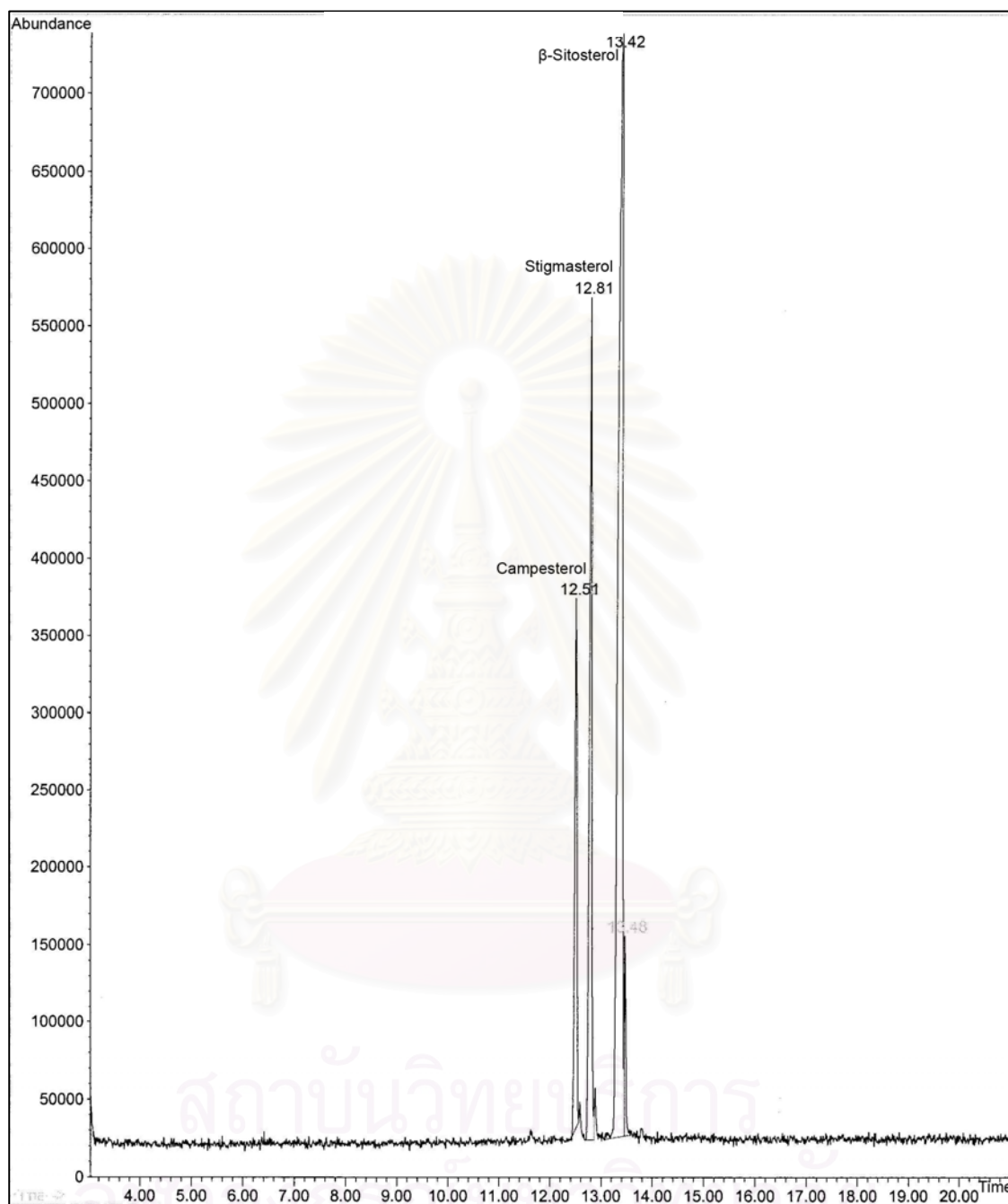


Figure 22 GC-MS chromatogram of phytosterols isolated from cell suspension cultures of *C. stellatopilosus*

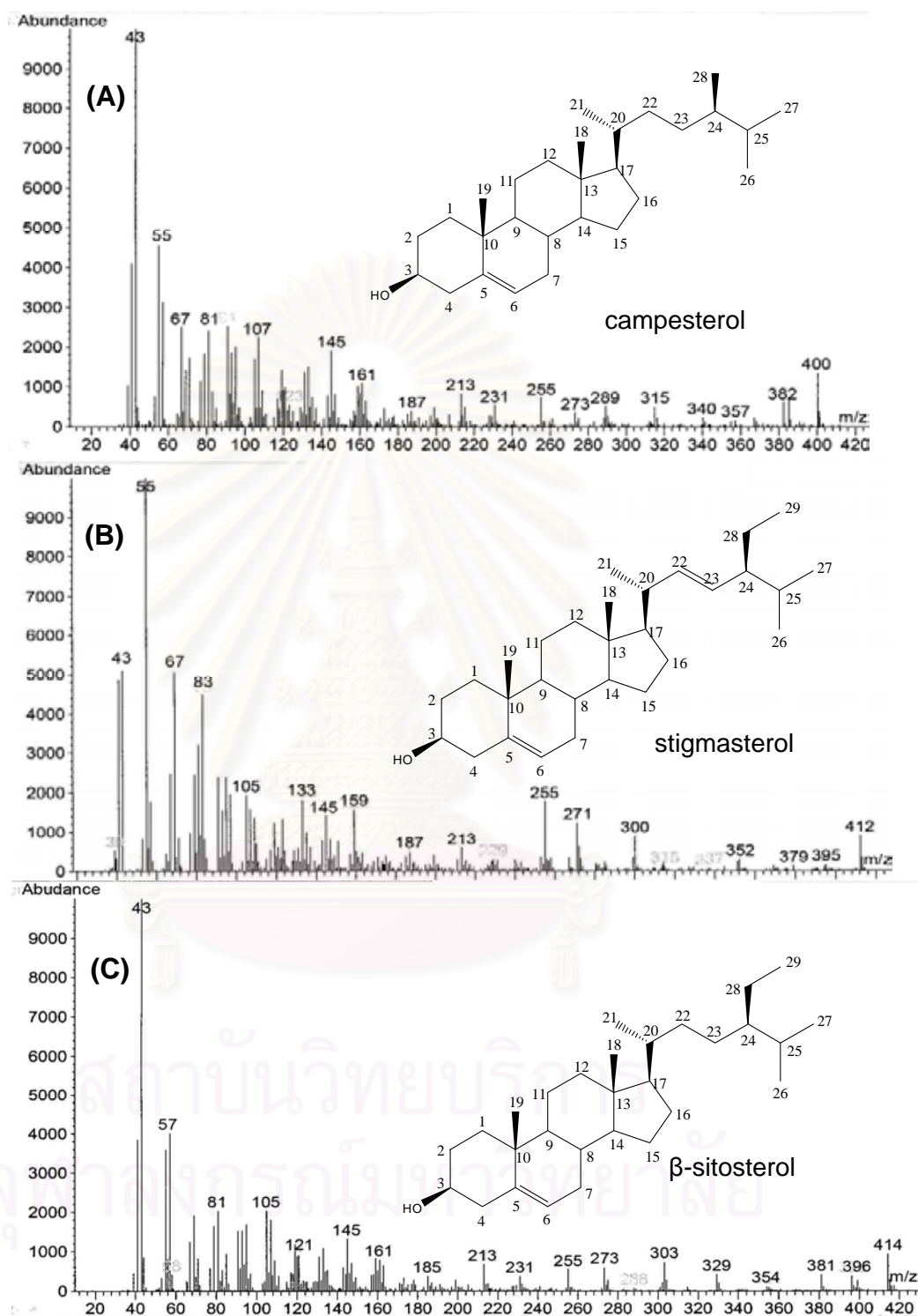


Figure 23 Mass spectral data of phytosterols isolated from the cell suspension cultures of *C. stellatopilosus*. (A) campesterol, (B) stigmasterol and (C) β -sitosterol

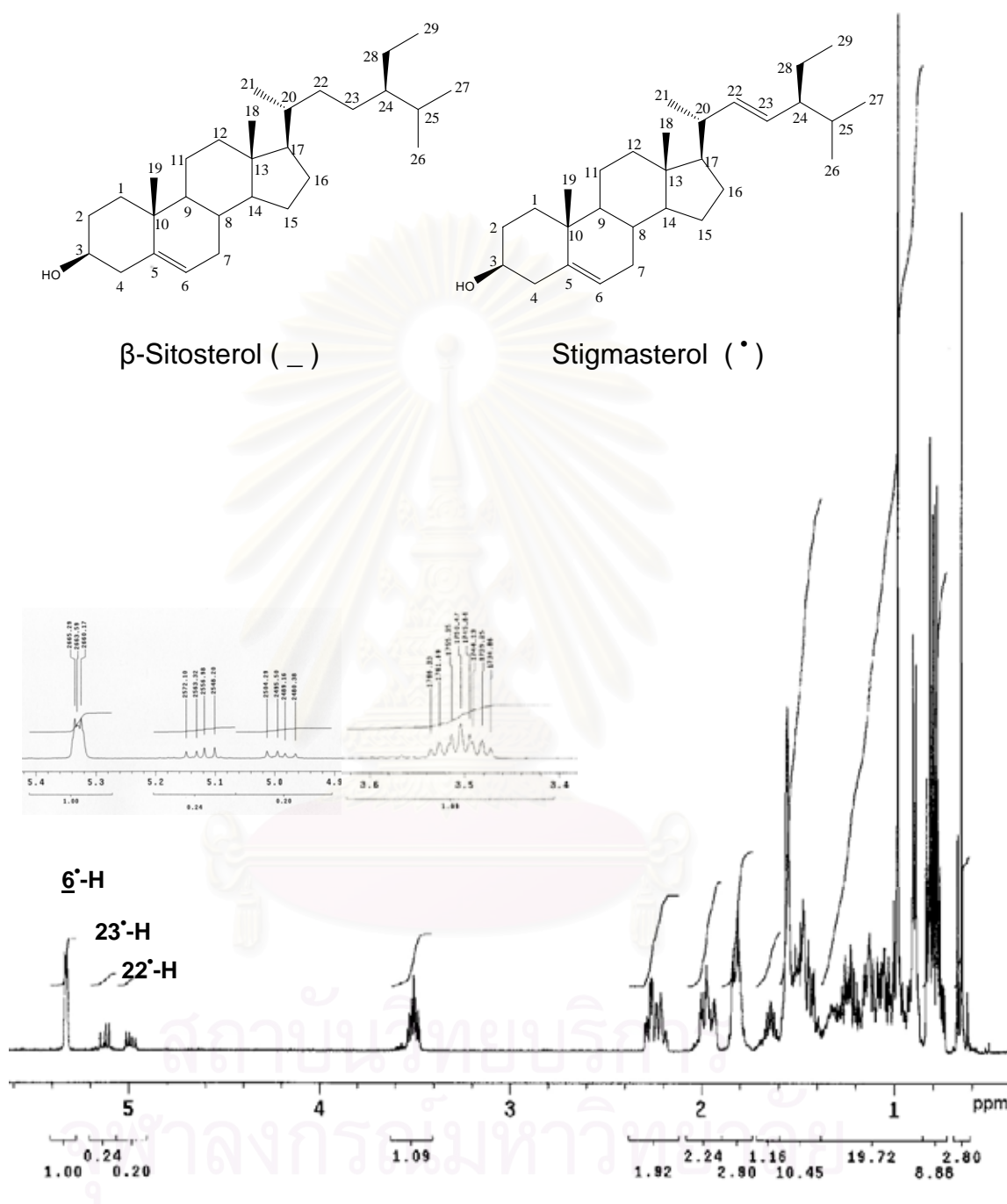


Figure 24 500 MHz ^1H NMR spectrum (in CDCl_3) of the major compounds found in suspension cultures of *C. stellatopilosus*.

The ^1H NMR spectrum (Fig. 24) revealed signals of two singlet methyls at δ 0.98 (H-19) and 0.66 (H-18), three doublet methyls at δ 0.90 (d, $J = 6.6$ Hz, H-21), 0.81 (d, $J = 6.8$ Hz, H-26), and 0.79 (d, $J = 7.1$ Hz, H-27) and a triplet methyl at δ 0.83 (t, $J = 7.6$ Hz, H-29). There were three vinylic proton signals at δ 5.33 (1H, d, H-6), 4.99 (1H, dd, $J = 15.1, 8.8$ Hz, H-22) and 5.12 (1H, dd, $J = 15.1, 8.8$ Hz, H-23) and a proton signal at δ 3.50 (2H, m, H-3). The remaining proton signals were at δ 0.8-2.4. The signals at δ 4.99 (0.20 H, dd, $J=15.1, 8.8\text{Hz}$) and δ 5.12 (0.24 H, dd, $J=15.1, 8.8$ Hz) were assigned to H-22 and H-23 of stigmasterol and δ 5.33 (1.00 H, d, $J=5.1$ Hz) was assigned to H-6 of both β -sitosterol and stigmasterol. The integration of H-6, H-22 and H-23 appeared to be in the ratio of 1.00:0.20:0.24. Therefore, based on the NMR data, the isolated phytosterols could be deduced that the mixture of β -sitosterol and stigmasterol with the ratio of 4:1.

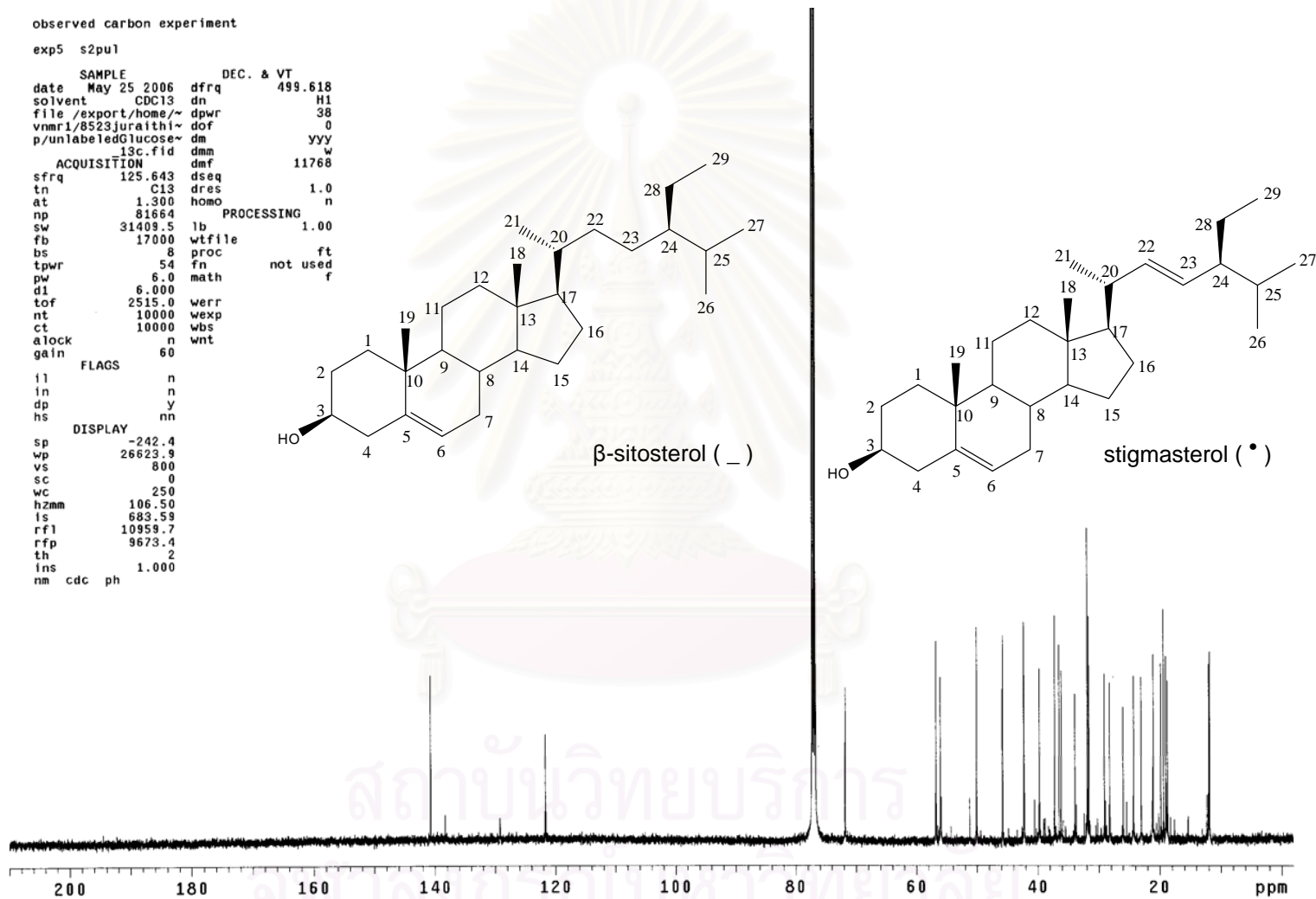


Figure 25 125 MHz ^{13}C NMR spectrum (in CDCl_3) of the major compound found in suspension cultures of *C. stellatopilosus*.

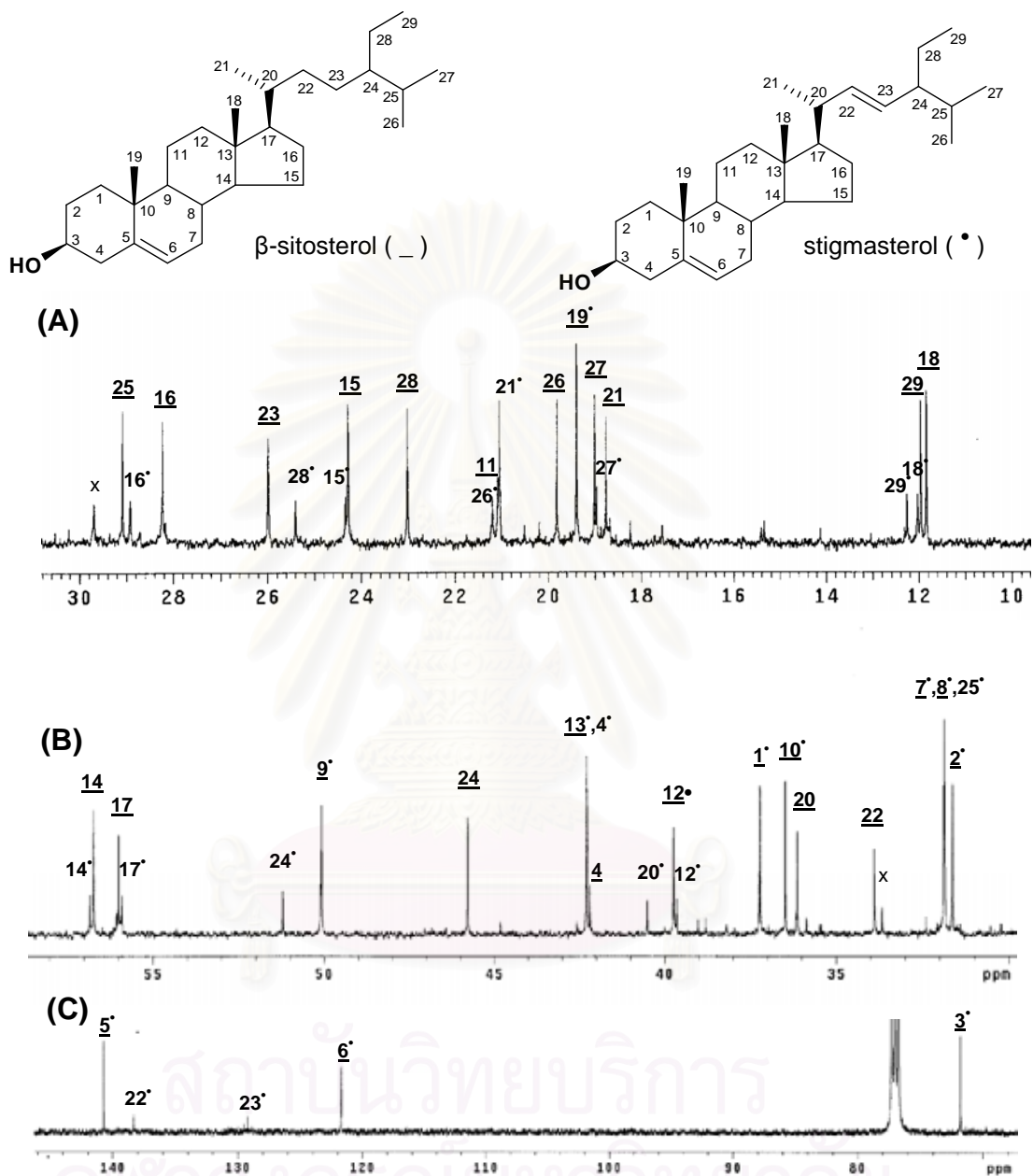


Figure 26 125 MHz ^{13}C NMR spectrum (in CDCl_3) of the major compound found in suspension cultures of *C. stellatopilosus* expanded from 10 to 31 ppm (A), 31 to 58 ppm (B) and 68-146 ppm (C).

Table 5 125 MHz ^{13}C NMR spectral data of the isolated major labeled compound (in CDCl_3) in comparison with reported values (Wright *et al.*, 1978) of β -sitosterol and stigmasterol.

Carbon position	Chemical shift (ppm)				Assignments
	β -sitosterol	Stigmasterol	Isolated compound		
1	37.31	37.31	37.21		-CH ₂ -
2	31.57	31.69	31.62		-CH ₂ -
3	71.69	71.81	71.80		-CH-OH
4	42.25	42.35	42.18	42.29	-CH ₂ -
5	140.76	140.80	140.72		=C<
6	121.59	121.69	121.71		=CH-
7	31.92	31.94	31.87		-CH ₂ -
8	31.92	31.94	31.87		>CH-
9	50.17	50.20	50.08		>CH-
10	36.51	36.56	36.48		>C<
11	21.11	21.11	21.07		-CH ₂ -
12	39.81	39.74	39.73	39.64	-CH ₂ -
13	42.33	42.35	42.29		>C<
14	56.79	56.91	56.73	56.83	>CH-
15	24.32	24.39	24.28	24.34	-CH ₂ -
16	28.26	28.96	28.23	28.92	-CH ₂ -
17	56.11	56.06	56.00	55.90	>CH-
18	11.87	12.07	11.84	12.03	-CH ₃
19	19.40	19.42	19.38		-CH ₃
20	36.17	40.54	36.12	40.50	>CH-
21	18.82	21.11	18.75	21.05	-CH ₃
22	33.95	138.37	33.90	138.32	-CH ₂ -; =CH-
23	26.13	129.32	25.99	129.22	-CH ₂ -; =CH-
24	45.85	51.29	45.78	51.21	>CH-
25	29.18	31.94	29.08	31.87	>CH-
26	19.84	21.26	19.81	21.20	-CH ₃
27	19.07	19.02	19.00	18.95	-CH ₃
28	23.09	25.44	23.02	25.40	-CH ₂ -
29	12.32	12.27	11.96	12.25	-CH ₃

3. Feeding and Incorporation Experiments

3.1 Feeding with radioactively labeled [1-¹⁴C]glucose for system optimization

Feedings of [1-¹⁴C]glucose into the cell suspension cultures of *C. stellatopilosus* were first investigated. The major advantage of using radioactive precursor is that the radioactivity can be easily monitored and thus the incorporation rate can be calculated readily based on the results of radioactivity present in the cells and in the medium. In this study, [1-¹⁴C]glucose was added after transferring cells into fresh medium in the subculturing. Aliquots of the suspension cultures were collected daily. The cells were harvested and extracted as described in the section 2.2.1.1. The radioactivities of both the cells and the medium were then measured using liquid scintillation counter. The results showed that the uptake of [1-¹⁴C]glucose by the cells was highest (17 to 20%) from day 2 to day 4 compared with less than 7% for the other period of cell growth (Fig. 27).

The extracts were then applied onto TLC plate and radioscanned in order to observe the target compounds with label incorporation. The resulting radiochromatograms showed that the radioactive peaks of GGOH and β -sitosterol increased continuously from day 1 and reached a maximum point on day 4 (Fig. 28). This was in agreement with the percentage of incorporation (Fig. 27). Based on these results and also the time-course of the product formation, labeling experiments were performed with the freshly cultured cells, and the uptake and metabolic conversion of the labeled precursors were allowed to take place for 4 days. Two kinds of stable isotopic precursors, [1-¹³C]glucose and [2-¹³C]sodium acetate, were used in the experiments for comparison of their label incorporation. After the feedings, the

cultured cells were harvested and the phytosterols were isolated for the analysis of their ^{13}C -labeling patterns.

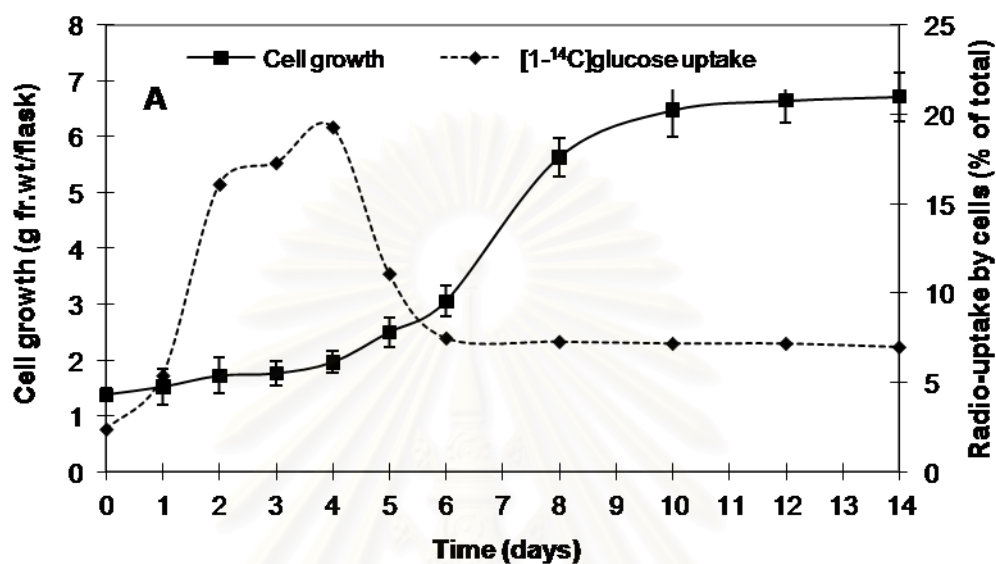


Figure 27 Radio-uptake of $[1-^{14}\text{C}]$ glucose and growth curve during a 14-day culture cycle of *C. stellatopilosus* cell suspension cultures.

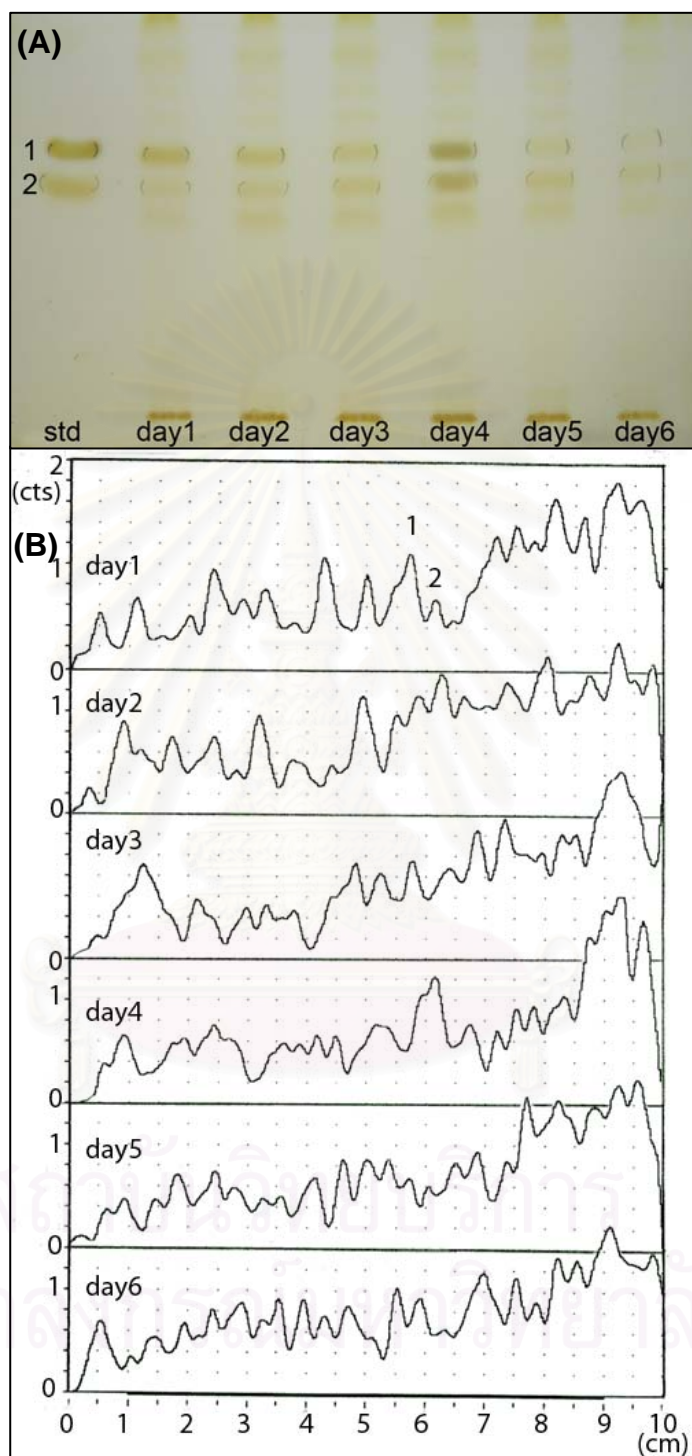


Figure 28 Preliminary studies on feeding of [1-¹⁴C]glucose into *C. stellatopilosus* suspension cultures: (A). TLC plate detected under I₂ vapor, (B). TLC radiochromatograms using TLC-radioscanner, 1, 2 indicate the positions of GGOH and β-sitosterol, respectively.

3.2 Feeding with [U-¹³C]glucose and analysis by GC-MS

Based on the results from the feedings of the radioactively labeled [1-¹⁴C]glucose, the cell suspension cultures of *C. stellatopilosus* (7-day old) were then fed with the isotopically labeled [U-¹³C]glucose (25% w/v, 99% ¹³C enrichment in 75% w/v of unlabeled D-glucose) using the same procedure. Fresh cells (2.6 g) was harvested and extracted as described in the section 2.2.1.1. The crude hexane extract (0.5 mg) was dissolved in 100 µl of *n*-hexane and subjected to gas chromatograph-mass spectrometer for ¹³C enrichment analysis. Unfortunately, we could not detect ¹³C enrichment on this study (data not shown).

3.3 Feeding with [1-¹³C]glucose and quantitative analysis by ¹³C NMR

For quantitative ¹³C NMR analysis the suspension culture was transferred to one hundred flasks in 250-ml erlenmeyer flasks with the culture medium and fed with [1-¹³C]glucose (20% in unlabeled D-glucose). After 4 days the cells were harvested (approximately 835 g) for extraction and isolation of phytosterols (see sections 2.2.1 and 2.2.3).

The structures of both unlabeled and labeled phytosterols were analyzed by ¹³C NMR spectroscopy. ¹³C-NMR spectra 125 MHz were recorded in CDCl₃ using INOVA-500 spectrometer (Varian, CA, USA) with the relaxing time of 6.0 s and 10,000 scans. The ¹³C NMR spectra of the isolated compounds were identical to those of β-sitosterol and stigmasterol. The chemical shift value for each carbon in the ¹³C-NMR spectra could be completely assigned from the incorporation experiments using [1-¹³C]glucose. The NMR signals were separately integrated in each carbon atoms. These values of relative ¹³C-signal intensity were normalized with the peak

intensity of C20 of β -sitosterol since this carbon is not involved in any labeling process either by the MVA pathway or the DXP pathway.

Figure 29 shows the comparison of the ^{13}C -NMR spectra between the phytosterol mixture obtained from the unlabeled glucose incorporation and from $[1-^{13}\text{C}]$ glucose incorporation. It can be seen in general that there were an increase in the peak intensity of many carbons in the phytosterols obtained from the $[1-^{13}\text{C}]$ glucose incorporated suspension culture. Particularly, there were ^{13}C -enrichment at the carbon positions 1, 3, 5, 9, 13, 15, 17, 18, 19, 21, 22, 24, 26, 27, 28 and 29 of β -sitosterol. On the other hand, other carbon atoms of number 2, 4, 6, 10, 11, 12, 14, 16, 20, 23 and 25 were virtually not labeled.

The degree of ^{13}C -enrichment was calculated based on the ^{13}C peak intensity values of the unlabeled glucose feeding. As shown in Table 6, the intensity ratio of $[1-^{13}\text{C}]$ glucose (L)/ unlabeled glucose (U) for the enriched carbons were generally higher than 1.0, whereas the L/U ratio of the non-enriched carbons were approximately 1.0 or lower. Based on the results in Table 6, the pattern of ^{13}C -enrichment in the molecules of β -sitosterol and stigmasterol could be summarized as shown in Figure 30.

สถาบันวิทยบริการ
จุฬาลงกรณ์มหาวิทยาลัย

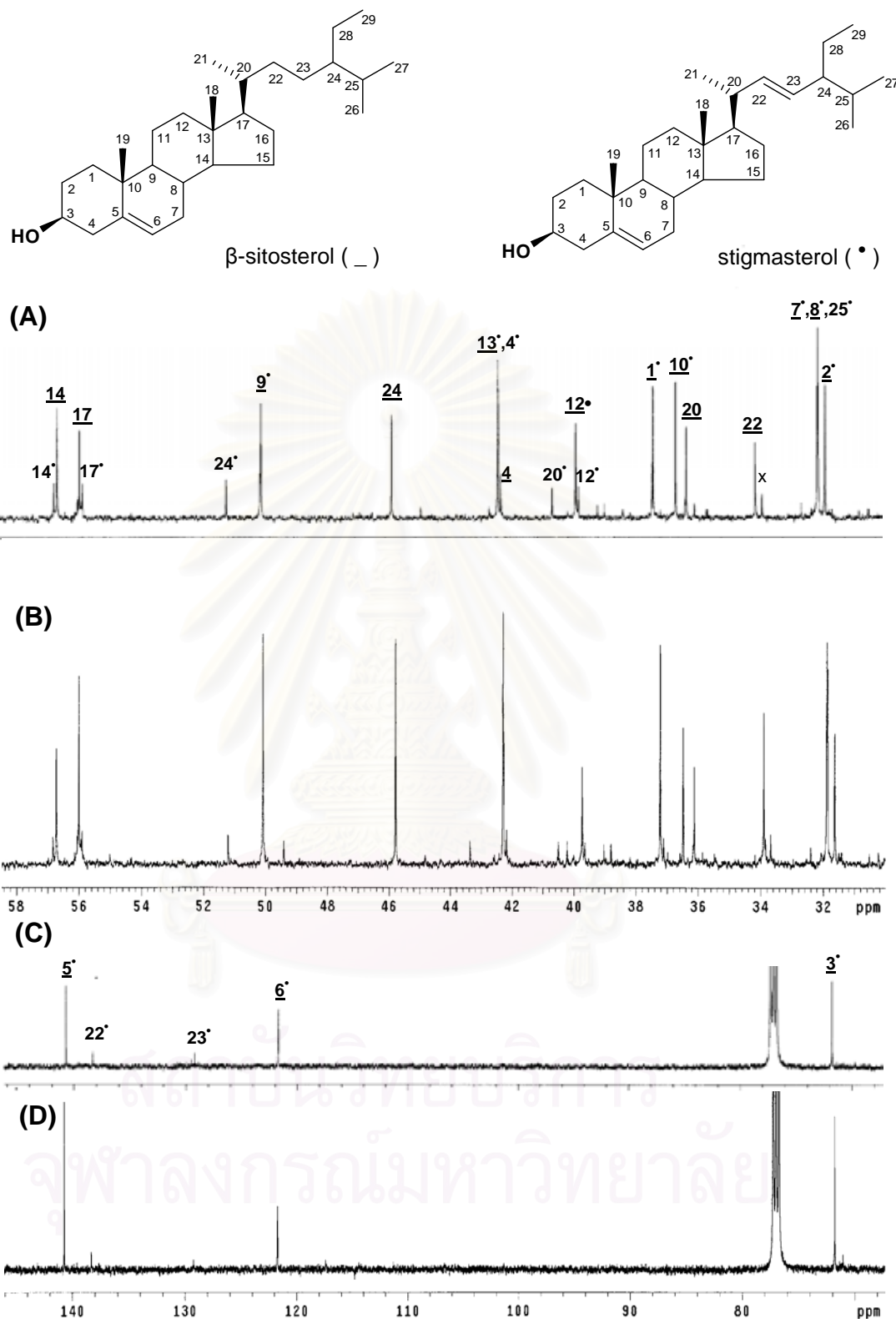


Figure 29 (continued) Comparison of 125 MHz ^{13}C NMR spectra (expanded from 31 to 58 ppm and 70 to 146 ppm) of a mixture of phytosterols (β -sitosterol and stigmasterol) obtained from suspension cultures of *C. stellatopilosus*: (A, C) unlabeled glucose incorporation, and (B, D) $[1-^{13}\text{C}]$ glucose incorporation.

Table 6 ^{13}C NMR analysis and relative ^{13}C -enrichment of β -sitosterol and stigmasterol from *C. stellatopilosus* cell suspension cultures fed with $[1-^{13}\text{C}]$ glucose and unlabeled glucose (control) under the same condition

Carbon No ^a	Chemical shift (ppm)		^{13}C -signal intensity ^b				Enrichment ratio	
	β -Sito-sterol	Stigma-sterol	$[1-^{13}\text{C}]$ Glucose		Unlabeled glucose		β -Sito-sterol L/U	Stigma-sterol L/U
			β -Sito-sterol (L)	Stigma-sterol (L)	β -Sito-sterol (U)	Stigma-sterol (U)		
1*	37.21		2.05		1.22		1.68	1.68
2*	31.62		1.16		1.36		0.85	0.85
3*	71.80		2.27		1.57		1.45	1.45
4	42.18	42.29*	0.32	2.45	0.32	2.04	1.00	1.20
5*	140.72		1.21		0.74		1.64	1.64
6*	121.71		1.18		1.34		0.88	0.88
7*	31.87		3.72		3.01		1.24	1.24
8*	31.87		3.72		3.01		1.24	1.24
9*	50.08		2.28		1.48		1.54	1.54
10*	36.48		0.83		0.90		0.92	0.92
11*	21.07		0.29		0.28		1.03	1.03
12	39.73	39.64	0.92	0.33	1.06	0.35	0.87	0.94
13*	42.29		2.45		2.04		1.20	1.20
14	56.73	56.83	0.93	0.15	1.04	0.25	0.89	0.60
15	24.28	24.34	1.62	0.35	0.98	0.28	1.65	1.25
16	28.23	28.92	1.06	0.18	1.13	0.28	0.94	0.64
17	56.00	55.90	1.27	0.28	0.70	0.22	1.81	1.27
18	11.84	12.03	1.85	0.40	1.10	0.34	1.68	1.18
19*	19.38		1.93		1.21		1.60	1.60
20	36.12	40.50	1.00	0.18	1.00	0.19	1.00	0.95
21	18.75	21.05	1.31	1.34	0.76	1.10	1.72	1.22
22	33.90	138.32	1.76	0.33	0.98	0.23	1.80	1.43
23	25.99	129.22	0.77	0.16	0.84	0.22	0.92	0.73
24	45.78	51.21	1.84	0.32	1.07	0.22	1.72	1.46
25	29.08	31.87*	0.88	3.72	0.97	3.01	0.91	1.24
26	19.81	21.20	1.71	0.42	0.92	0.31	1.86	1.35
27	19.00	18.95	1.99	0.44	0.86	0.31	2.31	1.42
28	23.02	25.40	1.39	0.17	0.90	0.16	1.54	1.06
29	11.96	12.25*	1.49	0.27	0.90	0.20	1.65	1.35

^aAssignments are based on Wright *et al.*, 1978. ^bEach intensity values was obtained based on the intensity (set to 1.0) of C20 of β -sitosterol which is not involved in the label incorporation either from the MVA pathway or DXP pathway. * The carbon with signal overlapping of either the same carbon of the two phytosterols (carbon no. 1-3,5-11, 13 and 19) or of different carbons (carbon no. 4 and 25 of stigmasterol with carbon no. 13 and 7+8 of both phytosterols, respectively).

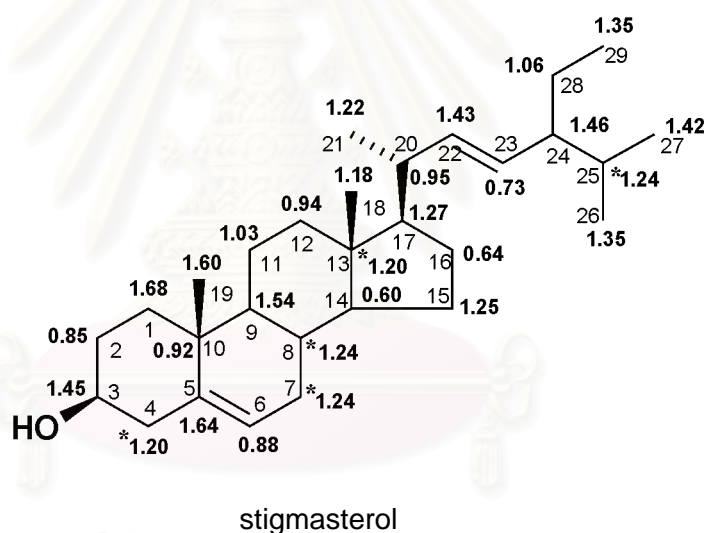
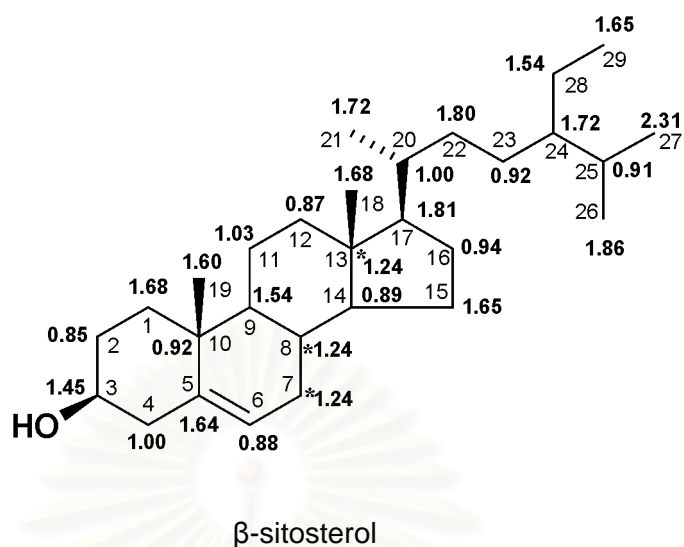


Figure 30 ^{13}C -labeling patterns of *C. stellatopilosus* phytosterols obtained from the incorporation experiments using $[1-^{13}\text{C}]$ glucose. The value indicated at a particular carbon is the ^{13}C -enrichment ratio obtained from Table 6. The value of the carbon with * is the summation of NMR-signal overlapping of different carbons.

3.4 Feeding with [2-¹³C]sodium acetate and quantitative ¹³C NMR analysis of phytosterols

[2-¹³C]Sodium acetate (50% w/v in unlabeled sodium acetate) was fed into the suspension cultures. Again, after the culture condition of 4 days, cells (750 g fr.wt) were harvested to extract for the two phytosterols. As described in section 3.3, the structures of the unlabeled and labeled phytosterols as a mixture of β -sitosterol and stigmasterol were analyzed by ¹³C NMR spectroscopy. Figure 31 compares the ¹³C-NMR spectra of the compounds obtained from the unlabeled sodium acetate and [2-¹³C]sodium acetate incorporation. It can be seen again that there were an increase in the peak intensity of many carbons in the phytosterol molecules obtained from the [2-¹³C]sodium acetate incorporated suspension culture. Particularly, there were ¹³C-enrichment at carbon positions 1, 3, 5, 7, 8, 9, 11, 13, 15, 17, 18, 19, 21, 22, 24, 25, 26, 27, 28 and 29. On the other hand, other carbon atoms of number 2, 4, 6, 10, 12, 14, 16, 20 and 23 were virtually not labeled.

The degree of ¹³C-enrichment was calculated based on the ¹³C peak intensity values of the unlabeled glucose feeding. As shown in Table 7, the intensity ratio of [1-¹³C]glucose (L)/ unlabeled glucose (U) for the enriched carbons were generally higher than 1.0, whereas the L/U ratio of the non-enriched carbons were approximately 1.0 or lower. Based on the results in Table 7, the pattern of ¹³C-enrichment in the molecules of β -sitosterol and stigmasterol could be summarized as shown in Figure 32.

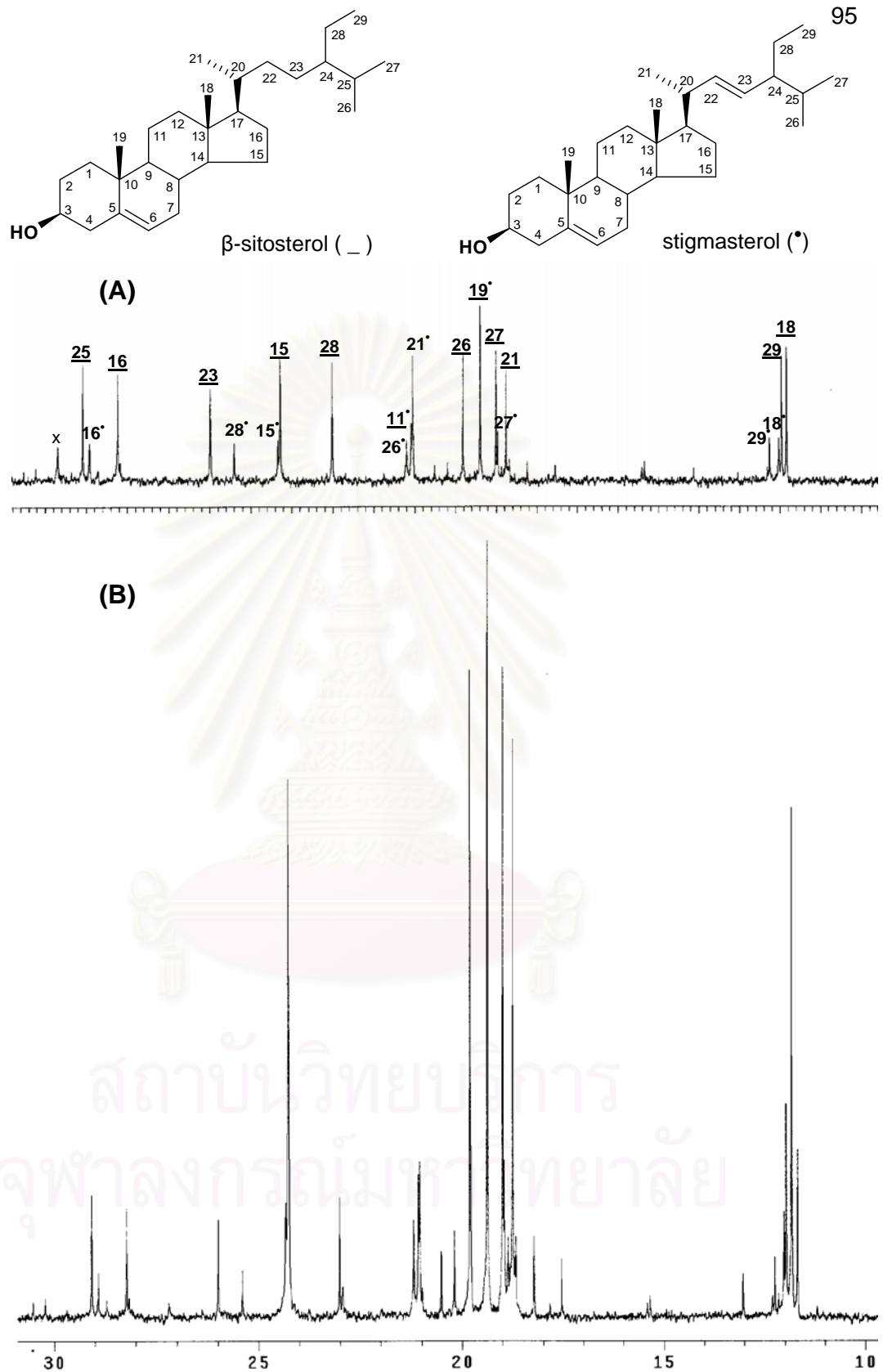


Figure 31 Comparison of 125 MHz ^{13}C NMR spectra (expanded from 10 to 31 ppm) of a mixture of phytosterols (β -sitosterol and stigmasterol) obtained from suspension cultures of *C. stellatopilosus* : (A) unlabeled acetate incorporation, and (B) $[2-^{13}\text{C}]$ sodium acetate incorporation.

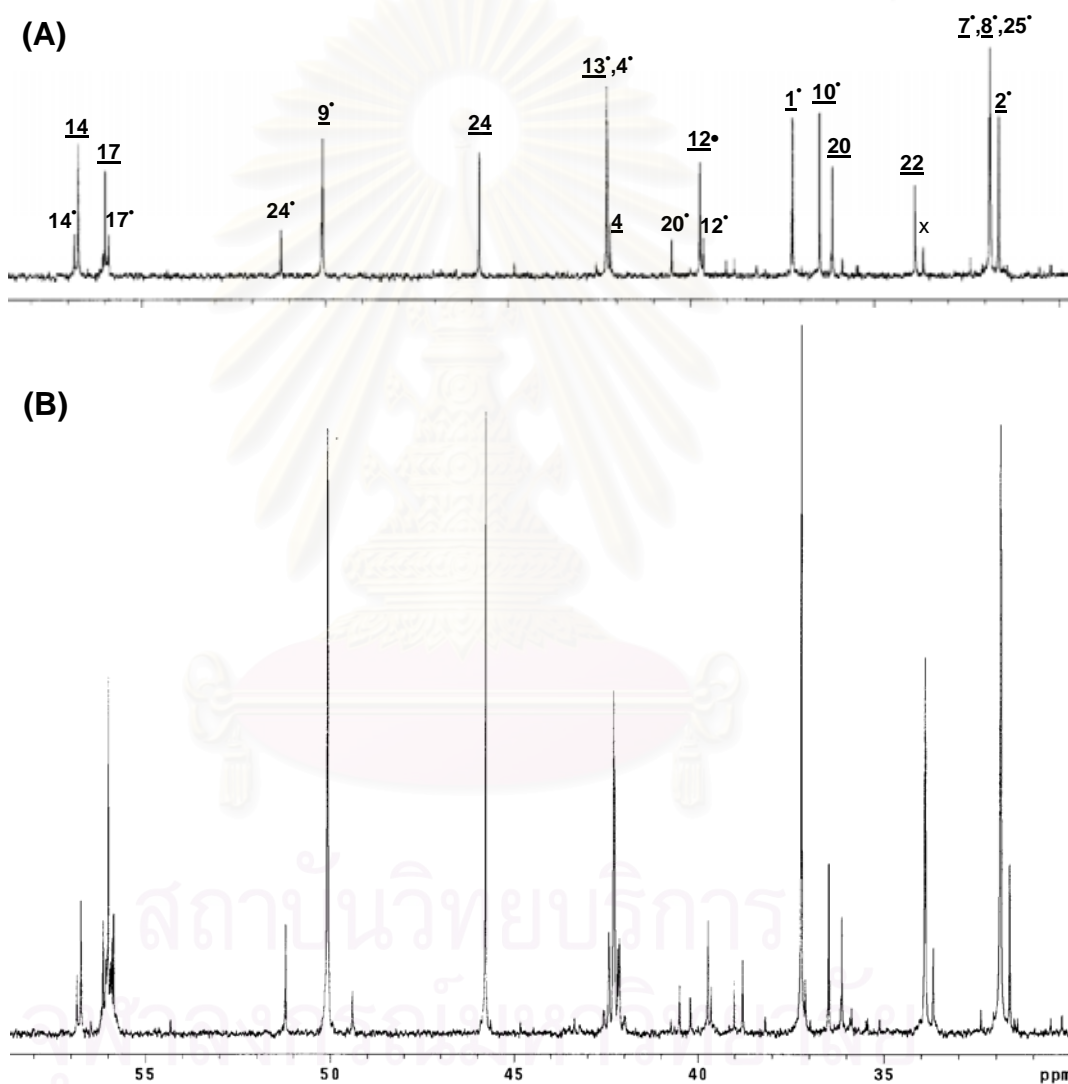
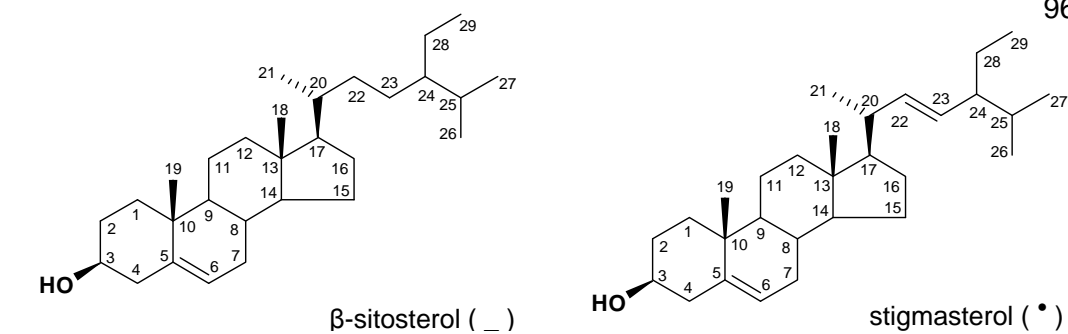


Figure 31(continued) Comparison of 125 MHz ^{13}C NMR spectra (expanded from 31 to 59 ppm) of a mixture of phytoosterols (β -sitosterol and stigmasterol) obtained from suspension cultures of *C. stellatpilosus* : (A) unlabeled acetate incorporation, and (B) $[2-^{13}\text{C}]$ sodium acetate incorporation.

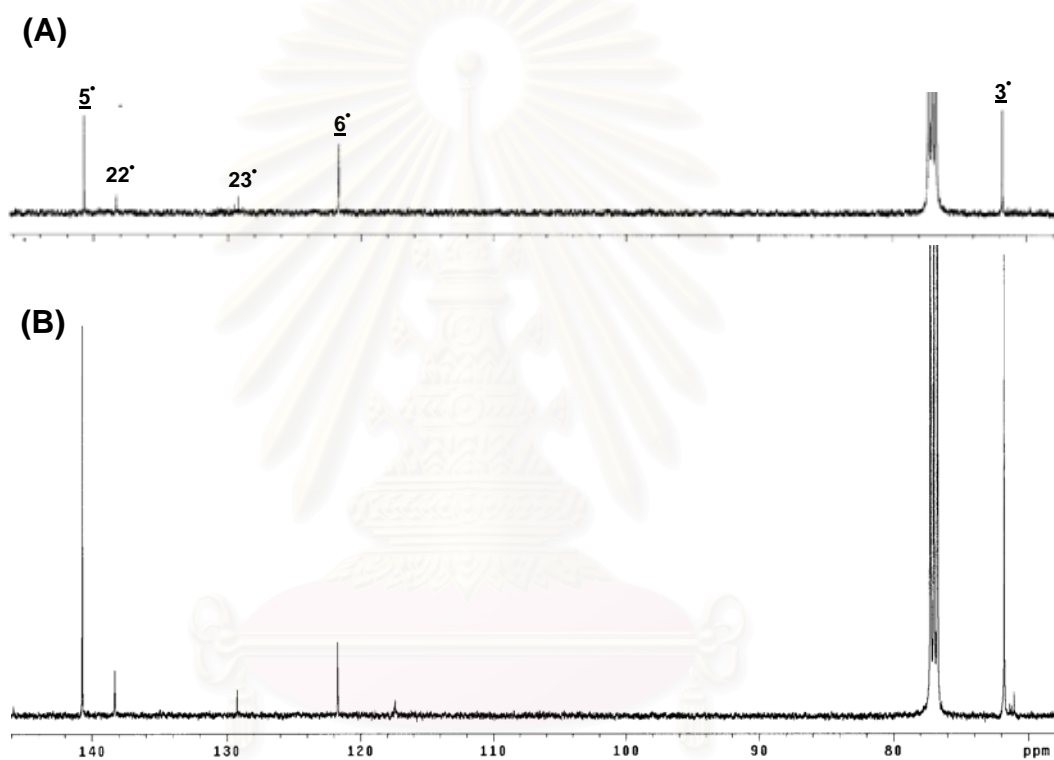
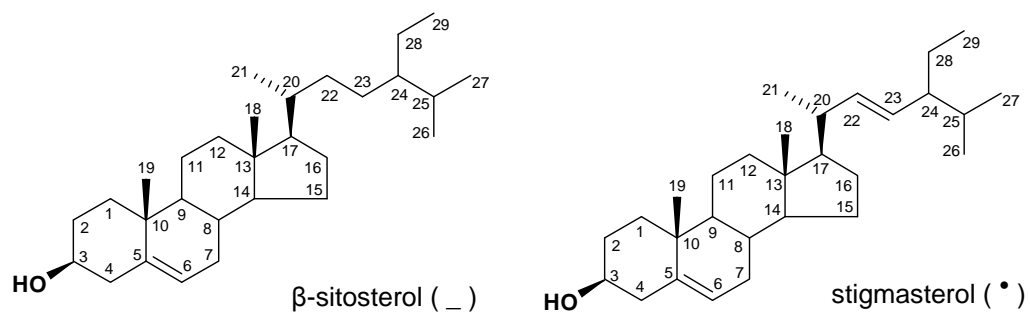


Figure 31(continued) Comparison of 125 MHz ^{13}C NMR spectra (expanded from 70 to 146 ppm) of a mixture of phytosterols (β -sitosterol and stigmasterol) obtained from suspension cultures of *C. stellatopilosus* : (A) unlabeled acetate incorporation, and (B) $[2-^{13}\text{C}]$ sodium acetate incorporation.

Table 7 ^{13}C NMR analysis and relative ^{13}C -enrichment of β -sitosterol and stigmasterol from *C. stellatopilosus* cell suspension cultures fed with $[2-^{13}\text{C}]$ sodium acetate and unlabeled glucose (control) under the same condition

Carbon No ^a	Chemical shift (ppm)		^{13}C -signal intensity ^b				Enrichment ratio	
	β -Sito-sterol	Stigma-sterol	$[2-^{13}\text{C}]$ Acetate		Unlabeled acetate		β -Sito-sterol L/U	Stigma-sterol L/U
			β -Sito-sterol (L)	Stigma-sterol (L)	β -Sito-sterol (U)	Stigma-sterol (U)		
1*	37.21		6.17		1.60		3.86	3.86
2*	31.62		1.36		1.80		0.76	0.76
3*	71.80		6.20		1.62		3.83	3.83
4	42.18	42.29*	0.51	4.30	0.52	2.55	0.98	1.69
5*	140.72		3.62		0.96		3.77	3.77
6*	121.71		1.15		1.51		0.76	0.76
7*	31.87		9.45		3.75		2.52	2.52
8*	31.87		9.45		3.75		2.52	2.52
9*	50.08		7.57		1.63		4.64	4.64
10*	36.48		1.18		1.41		0.84	0.84
11*	21.07		0.46		0.84		0.54	0.54
12	39.73	39.64	0.96	0.38	1.09	0.41	0.88	0.93
13*	42.29		4.30		2.55		1.69	1.69
14	56.73	56.83	0.96	0.43	1.20	0.47	0.80	0.91
15	24.28	24.34	5.47	1.08	1.20	0.51	4.56	2.12
16	28.23	28.92	0.91	0.41	1.32	0.40	0.69	1.02
17	56.00	55.90	2.52	0.85	1.16	0.52	2.17	1.63
18	11.84	12.03	3.71	0.76	1.05	0.42	3.53	1.81
19*	19.38		5.95		1.45		4.10	4.10
20	36.12	40.50	1.00	0.21	1.00	0.22	1.00	0.95
21	18.75	21.05	4.17	1.31	1.26	1.12	3.31	1.17
22	33.90	138.32	4.53	0.73	0.97	0.31	4.67	2.35
23	25.99	129.22	0.63	0.37	0.97	0.35	0.65	1.05
24	45.78	51.21	4.58	0.82	1.02	0.35	4.49	2.34
25	29.08	31.87*	0.81	9.45	1.03	3.75	0.79	2.52
26	19.81	21.20	4.48	0.99	0.97	0.57	4.62	1.74
27	19.00	18.95	3.98	1.06	0.91	0.41	4.37	2.59
28	23.02	25.40	0.77	0.29	1.08	0.38	0.71	0.76
29	11.96	12.25	1.90	0.32	0.89	0.43	2.13	0.74

^aAssignments are based on Wright *et al.*, 1978. ^bEach intensity values was obtained based on the intensity (set to 1.0) of C20 of β -sitosterol which is not involved in the label incorporation either from the MVA pathway or DXP pathway. * The carbon with signal overlapping of either the same carbon of the two phytosterols (carbon no. 1-3,5-11, 13 and 19) or of different carbons (carbon no. 4 and 25 of stigmasterol with carbon no. 13 and 7+8 of both phytosterols, respectively).

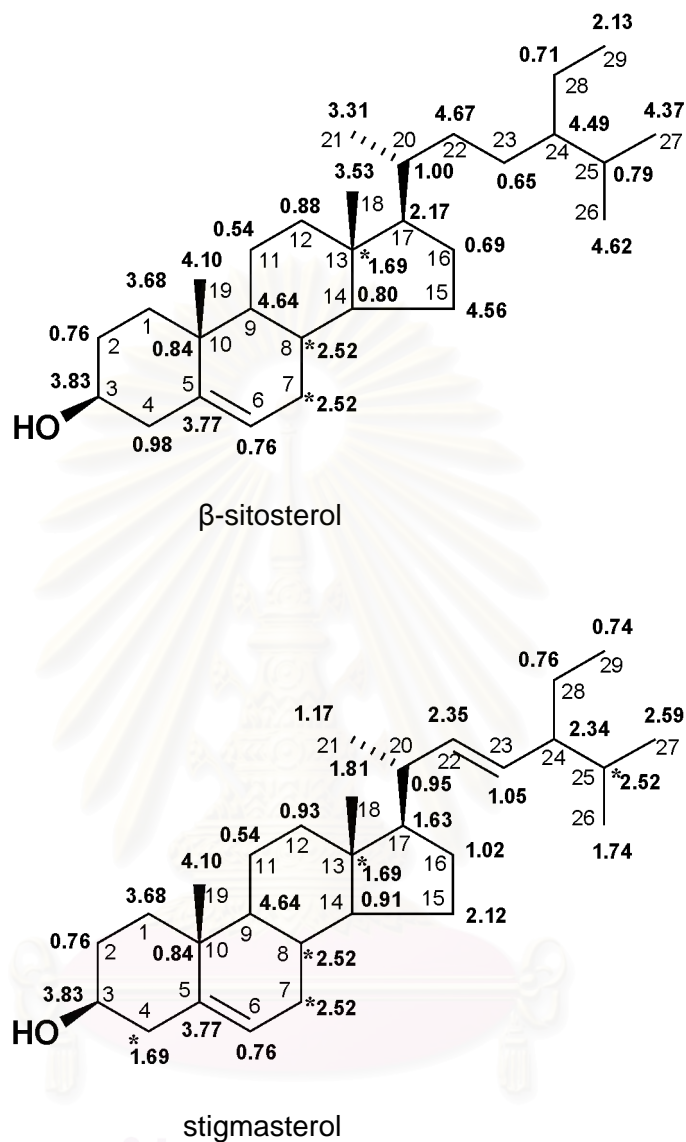


Figure 32 ^{13}C -labeling patterns of *C. stellatopilosus* phytosterols obtained from the incorporation experiments using $[2-^{13}\text{C}]$ sodium acetate. The value indicated at a particular carbon is the ^{13}C -enrichment ratio obtained from Table 7. The value of the carbon with * is the summation of NMR-signal overlapping of different carbons.

3.5 Summary of quantitative ^{13}C NMR analysis of phytosterols

Table 8 shows the values of relative ^{13}C -abundance of β -sitosterol and stigmasterol after being fed with $[1-^{13}\text{C}]$ glucose and $[2-^{13}\text{C}]$ sodium acetate in the format of isoprene unit. Therefore, feeding of $[1-^{13}\text{C}]$ glucose and $[2-^{13}\text{C}]$ sodium acetate could answer the possibility of utilizing the isoprene units in the skeleton of phytosterols. The results showed that the labeling patterns of β -sitosterol obtained either from $[1-^{13}\text{C}]$ glucose or $[2-^{13}\text{C}]$ sodium acetate feeding exhibit quite clearly its origin from the MVA pathway. Total incorporation of $[1-^{13}\text{C}]$ glucose and $[2-^{13}\text{C}]$ sodium acetate into phytosterols are summarized in Table 9 which showed the average of ^{13}C enrichment in the C_5 isoprenic skeleton of stigmasterol and β -sitosterol. From Table 10, it can be seen that the ratio of the labeled and unlabeled carbons for feeding with $[2-^{13}\text{C}]$ sodium acetate were relatively high with the value of 4.95 and 3.30 for β -sitosterol and stigmasterol, respectively, whereas the ratio of the labeled and unlabeled carbons for feeding with $[1-^{13}\text{C}]$ glucose appeared to be significantly lower (1.84 and 1.65 of β -sitosterol and stigmasterol, respectively).

Table 8 Relative ^{13}C enrichment in carbons of β -sitosterol and stigmasterol derived from suspension cultures of *C. stellatopilosus* administered with $[1-^{13}\text{C}]$ glucose and $[2-^{13}\text{C}]$ acetate

Carbon atom in IPP units	Carbon atom	Relative ^{13}C enrichment			
		Feeding with $[1-^{13}\text{C}]$ glucose		Feeding with $[2-^{13}\text{C}]$ acetate	
		β -Sitosterol	Stigmasterol	β -Sitosterol	Stigmasterol
1 ^I	2*	0.85	0.85	0.76	0.76
2 ^I	3*	1.45	1.45	3.83	3.83
3 ^I	4*	1.00	1.20	0.98	1.69
1 ^{II}	6*	0.88	0.88	0.76	0.76
2 ^{II}	5*	1.64	1.64	3.77	3.77
3 ^{II}	10*	0.92	0.92	0.84	0.84
4 ^{II}	1*	1.68	1.68	3.86	3.86
5 ^{II}	19*	1.60	1.60	4.10	4.10
1 ^{III}	11*	1.03	1.03	0.54	0.54
2 ^{III}	9*	1.54	1.54	4.64	4.64
3 ^{III}	8*	1.24	1.24	2.52	2.52
4 ^{III}	7*	1.24	1.24	2.52	2.52
1 ^{IV}	12	0.87	0.94	0.88	0.93
2 ^{IV}	13*	1.20	1.20	1.69	1.69
3 ^{IV}	14	0.89	0.60	0.80	0.91
4 ^{IV}	15	1.65	1.25	4.56	2.12
5 ^{IV}	18	1.68	1.18	3.53	1.81
1 ^V	16	0.94	0.64	0.69	1.02
2 ^V	17	1.81	1.27	2.17	1.63
3 ^V	20	1.00	0.95	1.00	0.95
4 ^V	22	1.80	1.43	4.67	2.35
5 ^V	21	1.72	1.22	3.31	1.17
1 ^{VI}	23	0.92	0.73	0.65	1.05
2 ^{VI}	24	1.72	1.46	4.49	2.34
3 ^{VI}	25*	0.91	1.24	0.79	2.52
4 ^{VI}	26	1.86	1.35	4.62	1.74
5 ^{VI}	27	2.31	1.42	4.37	2.59
a	28	1.54	1.06	0.71	0.76
a	29	1.65	1.35	2.13	0.74

^aNonmevalonoid origin

*Signal overlapping

Table 9 Average ^{13}C enrichment in carbon atom of the C_5 isoprenic skeleton of stigmasterol and β -sitosterol incorporating $[1-^{13}\text{C}]$ glucose and $[2-^{13}\text{C}]$ sodium acetate (data not include signal overlapping)

Carbon atom in IPP units	Average ^{13}C enrichment			
	Feeding with $[1-^{13}\text{C}]$ glucose		Feeding with $[2-^{13}\text{C}]$ acetate	
	β -Sitosterol	Stigmasterol	β -Sitosterol	Stigmasterol
C-1	0.89±0.04	0.90±0.04	0.75±0.08	0.90±0.14
C-2	1.63±0.14	1.47±0.14	3.78±0.98	3.24±1.22
C-3	0.94±0.05	0.82±0.19	0.88±0.10	0.90±0.05
C-4	1.75±0.10	1.43±0.18	4.43±0.38	2.52±0.93
C-5	1.83±0.33	1.40±0.21	3.83±0.409	2.83±0.16

Table 10 Average relative ^{13}C -abundance of β -sitosterol and stigmasterol after feeding with $[1-^{13}\text{C}]$ glucose and $[2-^{13}\text{C}]$ sodium acetate (data not include signal overlapping)

	Feeding with $[1-^{13}\text{C}]$ glucose		Feeding with $[2-^{13}\text{C}]$ acetate		Ratio	
	Labeled ^a carbon (A)	Unlabeled ^b carbon (B)	Labeled ^a carbon (C)	Unlabeled ^b carbon (D)	A/B	C/D
	β -sitosterol	1.71±0.19	0.93±0.05	3.86±0.83	0.78±0.12	1.84
stigmasterol	1.42±0.11	0.86±0.15	2.77±1.10	0.84±0.14	1.65	3.30

^acarbon atom number 1, 3, 5, 9, 15, 17, 18, 19, 21, 22, 24, 26, 27, 28 and 29

^bcarbon atom number 2, 4, 6, 10, 12, 14, 16, 20, 23 and 25

According to the enrichment values shown in Figure 33, it was obvious that all carbons in the above labeling pattern were enriched from the $[1-^{13}\text{C}]$ glucose and $[2-^{13}\text{C}]$ sodium acetate incorporation. These suggested that the isoprene units used for the phytosterols formation were biosynthesized predominantly *via* the mevalonate pathway. However, in order to obtain information on the average values of the ^{13}C

enrichment based on L/U ratio, the carbons number 15, 17, 21, 22, 24, 26 and 27 of both stigmasterol and β -sitosterol were chosen for averaging their L/U ratio values. These carbons gave ^{13}C -NMR signals that were not overlapped with other carbon signals and therefore gave accurate values of ^{13}C enrichment of both sterols based on the mevalonate pathway of isoprene biosynthesis. As shown in Tables 11 and 12, it was found that the ^{13}C -enrichment of the labeled carbons in β -sitosterol were relatively high with the average L/U values of 1.82 ± 0.20 and 3.97 ± 0.86 for feeding with $[1-^{13}\text{C}]$ glucose and $[2-^{13}\text{C}]$ sodium acetate respectively, whereas the values of the same labeled carbons of stigmasterol appeared to be lower significantly (average values of 1.32 ± 0.10 and 1.97 ± 0.45 for feeding with $[1-^{13}\text{C}]$ glucose and $[2-^{13}\text{C}]$ sodium, acetate respectively). For the carbons number 1, 3, 5, 9 and 19 in which their signals represented the combined effect of the two sterols, the averages value of 1.58 ± 0.09 and 4.04 ± 0.30 were obtained.

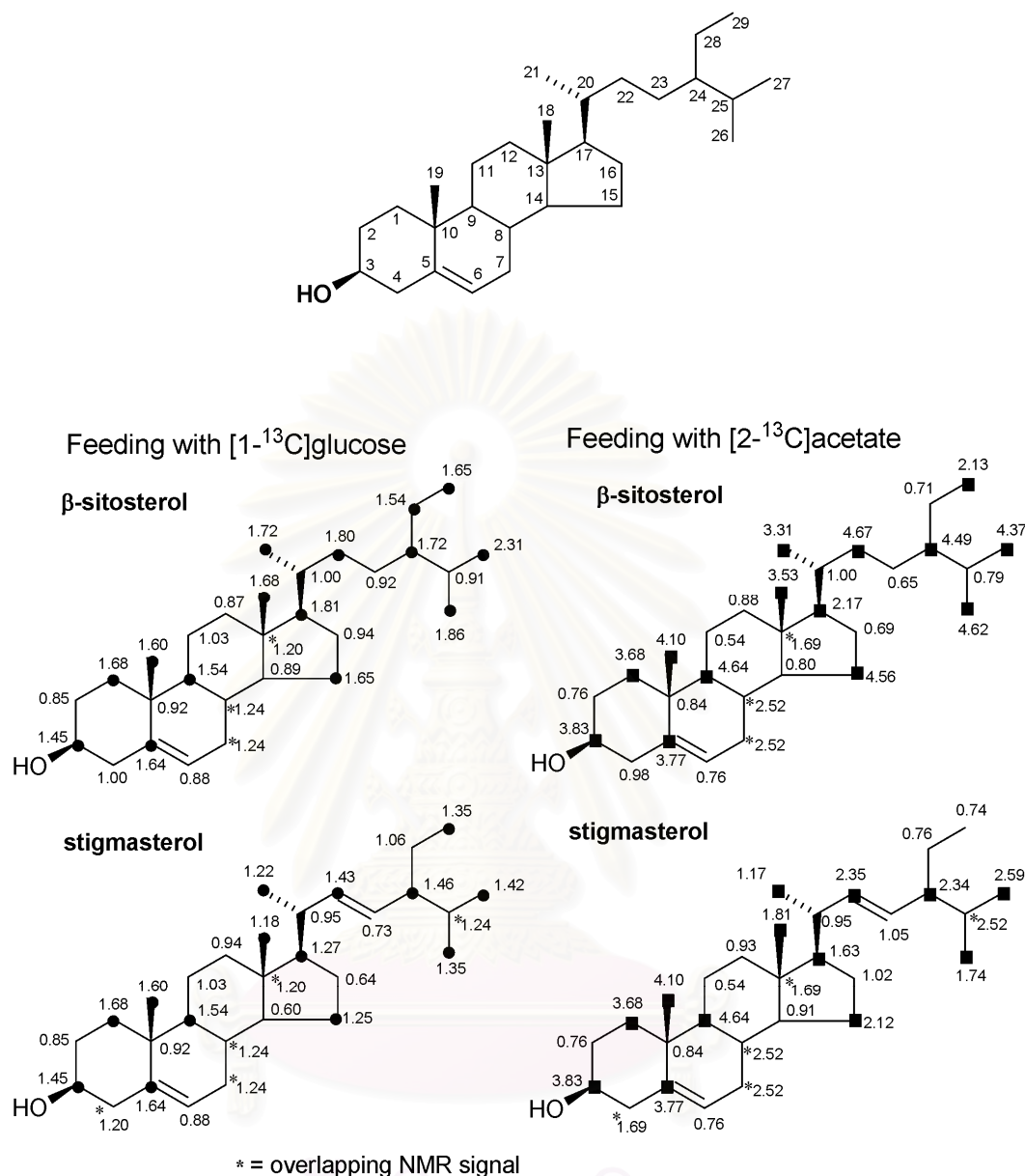


Figure 33 Summary of the degree of ¹³C-enrichment at various carbon atoms of β-sitosterol and stigmasterol. Both phytosterols were obtained as a mixture from *C. stellatopilosus* suspension cultures which had been incorporated with [1-¹³C]glucose and [2-¹³C]sodium acetate. A control incorporation experiment was also carried out in parallel with unlabeled glucose. The value indicated at a particular carbon is the ratio of ¹³C-NMR signal intensity of the ¹³C-labeled/the non-labeled (L/U). ●, ■ The observed labeled carbon from the MVA pathway feeding with [1-¹³C]glucose and [2-¹³C]sodium acetate, respectively; * the overlapping signal; numbers indicated the relative ¹³C-abundance.

Table 11 ^{13}C -Enrichment of some carbon atoms in the molecules of stigmasterol and β -sitosterol fed with $[1-^{13}\text{C}]$ glucose *via* the mevalonate pathway.

Carbon atom	Relative ^{13}C -abundance		
	β -Sitosterol	Stigmasterol	Signal overlapping
15	1.65	1.25	-
17	1.81	1.27	-
18	1.68	1.18	-
21	1.72	1.22	-
22	1.80	1.43	-
24	1.72	1.46	-
26	1.86	1.35	-
27	2.31	1.42	-
1	-	-	1.69
3	-	-	1.45
5	-	-	1.64
9	-	-	1.54
19	-	-	1.60
Average	1.82±0.20	1.32±0.10	1.58±0.09

Table 12 ^{13}C -Enrichment of some carbon atoms in the molecules of stigmasterol and β -sitosterol fed with $[2-^{13}\text{C}]$ sodium acetate *via* the mevalonate pathway.

Carbon atom	Relative ^{13}C -abundance		
	β -Sitosterol	Stigmasterol	Signal overlapping
15	4.56	2.12	-
17	2.17	1.63	-
18	3.53	1.81	-
21	3.31	1.17	-
22	4.67	2.35	-
24	4.49	2.34	-
26	4.62	1.74	-
27	4.37	2.59	-
1	-	-	3.86
3	-	-	3.83
5	-	-	3.77
9	-	-	4.64
19	-	-	4.10
Average	3.97±0.86	1.97±0.45	4.04±0.30

Table 13 shows that the relative enrichment rates of the two sterols were consistent. The value of 1.38 (L/U ratio of β -sitosterol : L/U ratio of stigmasterol) was obtained based on feeding experiment with $[1-^{13}\text{C}]$ glucose and the value of 2.02 was obtained based on the feeding experiment with $[2-^{13}\text{C}]$ sodium acetate. It can be interpreted that the ^{13}C -enrichment of β -sitosterol is slightly faster than that of stigmasterol by a factor of 1.38 and 2.02 depending on the L/U ratio of β -sitosterol and stigmasterol.

Table 13 The relative ^{13}C -enrichment of the two sterols. The values were calculated based on ^{13}C -NMR signal intensities of some relevant carbon atoms. (data from Tables 11 and 12)

Phytosterol	Relative ^{13}C -abundance	
	Feeding with $[1-^{13}\text{C}]$ glucose (L/U)	Feeding with $[2-^{13}\text{C}]$ acetate (L/U)
β -Sitosterol (A)	1.82 \pm 0.20	3.97 \pm 0.86
Stigmasterol (B)	1.32 \pm 0.10	1.97 \pm 0.45
Relative enrichment of the two sterols (A/B)	1.38	2.02

4. Transmission Electron Microscopic Analysis

Since the fact that the level of cell differentiation could affect the source of primary metabolites, plant cells from leaf, green callus and suspension cultures were prepared for electron micrograph to inspect the cell organelles. Transmission electron microscopy (TEM) indicated a different scattering of chloroplasts in plant cells (Fig. 34). In leaf, it was clear that the chloroplasts were densely present in palisade cells. On the other hand, the green callus contained a few chloroplasts, whereas the cell culture was lacking in the chloroplasts. Screening for plant cell-containing cells has been performed with green callus and suspension culture. The

results indicated that artificial cultures lost their capability for plaunotol production. It can be hypothesized that the absence of some organelles leads to the lack of essential enzymes for plaunotol biosynthesis.

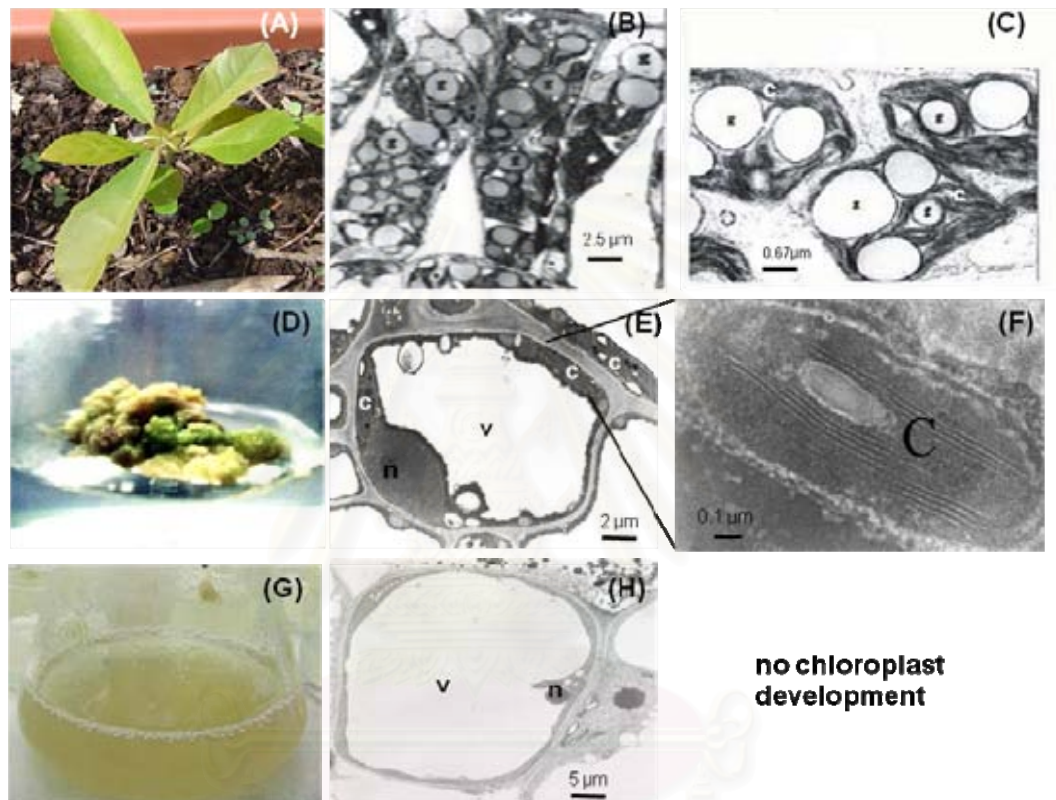


Figure 34 Electron micrograph images of different tissues of *C. stellatopilosus*: (A) leaves, (B) palisade mesophyll cells in leaf, (x 3,800) and (C) its magnified palisade mesophyll cells in chloroplast, (x 15,200), (D) green callus, (E) a callus cell, (x 4,000) and (F) its magnified chloroplast (x 60,000), (G) cell suspension cultures and (H) suspension cultured cells (x 1,500). v=vacuole, n=nucleus, c=chloroplast and g=oil globule.

5. Comparative Analysis of *dxs*, *dxr* and *ggpps* Gene Expression Profiles of *C. stellatopilosus* Plant and Cell Cultures

5.1 cDNA preparation of *C. stellatopilosus* leaf, green callus and suspension cultures

Total RNA from *C. stellatopilosus* young leaf, green callus and suspension cultures were isolated according to method described in 2.4.1. An aliquot of RNA (2 μ l) from leaves, green callus and suspension cultures were diluted in 500 μ l of DEPC water. Concentration of the RNA was determined by measuring the absorbance at 260 nm (A_{260}) in a spectrophotometer and calculated according to the equation (2.4.1). The concentration and purity the RNAs from leaves, green callus and suspension cultures were shown in Table 14. Analysis of the total RNA on 1.2% (w/v) agarose gel electrophoresis was performed (Fig. 35). The cDNAs were synthesized from 0.24 (leaves), 0.08 (green callus) and 1.68 μ g (suspension cultures) of total RNA using SuperScriptTM III RT (Invitrogen) with the random primers as described in 2.4.2.

Table 14 The concentration and purity of the isolated total RNA

Tissue	A_{260}	A_{280}	Total RNA (μ g/ μ l)	Purity [A_{260}/A_{280}]
Leaves	3.402	2.385	0.03	1.426
Green callus culture	3.408	2.402	0.01	1.419
Cell suspension culture	3.424	2.401	0.21	1.426



Figure 35 Agarose gel electrophoresis of total RNA from leaves (L), green callus (C) and suspension cultures (S) of *C. stellatopilosus*, M; DNA ladder (SibEnzyme)

5.2 Transcription profiles analyses of *dxs*, *dxr* and *ggpps* genes

Semiquantitative RT-PCR was carried out to investigate the transcription profiles of *dxs*, *dxr* and *ggpps* genes in organized cells such as leaves and disorganized cells such as green callus and suspension cultures. The cDNAs obtained from reverse-transcription of each sample were used as templates in two-step RT-PCR reactions. The amplification products of *dxs*, *dxr* and *ggpps* on the agarose gel electrophoresis were ca. 700, 300 and 600 bp., respectively. For the control, *18S rRNA* of the housekeeping gene, fragment was parallel amplified for ca.530 bp. All PCR products containing samples and the housekeeping gene were separated by 1.2% (w/v) agarose gel electrophoresis. After ethidium bromide staining, band intensity was measured by Gel documentation model 1000 (Bio-Rad, USA) equipped with Bio-Rad's Image Analysis Systems, version 1.4. The relative intensity was calculated as the ratio of band intensity of sample to *18S rRNA*.

The PCR cycles were optimized dependent upon the feature of each gene. The intensity of bands of the PCR products were, therefore, related to transcription levels of the genes. As shown in Table 15, the abundance of genes was different in various sources of plant. The results showed that the abundance of genes in green callus was higher than in leaves and in cell suspension. These may reflect physiological roles of the genes in the plant organelles, within the cells. In comparison to the housekeeping gene, the results indicated that *dxs*, *dxr* and *ggpps* genes were strongly expressed in plant leaves and green callus culture, but rarely found in cell suspension culture (Fig. 36)

Table 15 Expression profiles of genes from different sources of *C. stellatopilosus*

Target genes	Band intensity			Relative intensity to <i>18SrRNA</i>		
	Leaf	Green callus culture	Suspension culture	Leaf	Green callus culture	Suspension culture
<i>dxs</i>	3.77±0.65	8.63±1.64	0.67±0.14	0.36±0.07	0.73±0.05	0.05±0.01
<i>dxr</i>	4.20±0.37	10.17±1.12	0.40±0.09	0.40±0.07	0.86±0.06	0.03±0.01
<i>ggpps</i>	4.94±0.10	9.18±1.35	0.67±0.02	0.47±0.02	0.78±0.04	0.05±0.02
<i>18SrRNA</i>	10.50±0.45	11.82±0.58	13.40±0.85			

Figure 36 illustrates the transcription levels of investigated genes as well as the relative intensity compared to *18S rRNA*. The results indicated that *dxs*, *dxr* and *ggpps* genes were strongly expressed in plant leaf and green callus culture, but rarely found in suspension culture.

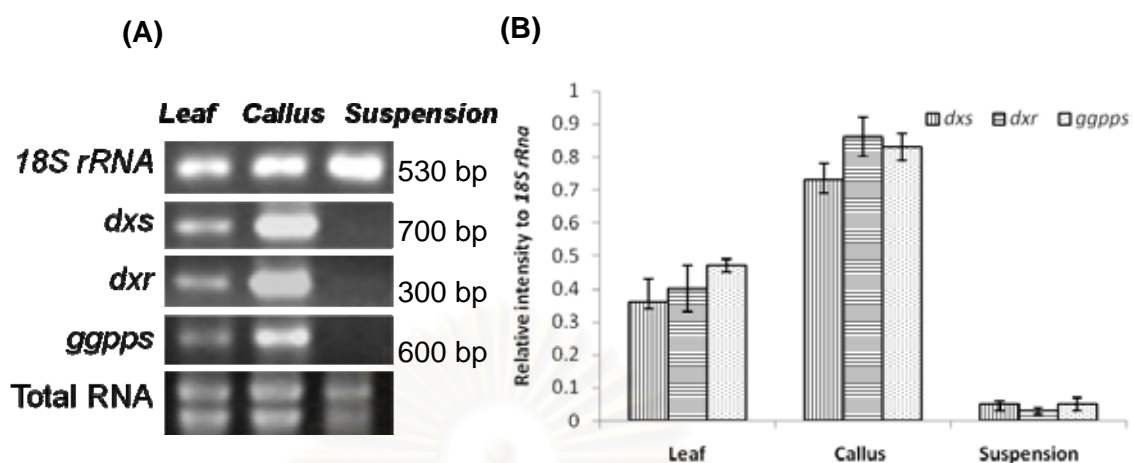


Figure 36 The mRNA expression profiles of *dxs*, *dxr* and *ggpps* genes in plant leaves, green callus and suspension cultures: (A). 1.2% agarose gel electrophoresis of gene transcripts in comparison with the *18S rRNA*; (B). relative intensity to *18S rRNA* of genes after gel documentation.

CHAPTER V

DISCUSSION

1. *Croton stellatopilosus* Cell Suspension Cultures

1.1 Establishment of cell suspension cultures of *C. stellatopilosus*

A callus culture of *C. stellatopilosus* was established successfully from the leaf segments. The medium that induced callus formation was MS agar medium containing 2.0 mg/l 2,4-D and 1.0 mg/l kinetin. In subsequent subculture, this callus culture appeared to grow well on MS agar medium containing 1.0 mg/l 2,4-D and 1.0 mg/l BA to form soft, friable, yellow tissues. Cell suspension cultures of *C. stellatopilosus* were initiated from the established callus cultures on MS liquid medium supplemented with 1.0 mg/l 2,4-D, 0.1 mg/l BA and 0.1 mg/l NAA. The undifferentiated cultured cells appeared to be friable, homogeneous, yellowish aggregates.

Charlwood and Rhodes (1990) have explained that the dedifferentiation of plant tissue *in vitro* to produce callus or suspension culture is usually accompanied by an apparent loss of ability to accumulate secondary compounds. This has been shown to be true in many cases. This study, therefore, tried to increase the degree of differentiation by inducing normal callus to be green callus. This was done by subculturing the normal callus on MS medium containing 1% (w/v) sucrose, 2.0 mg/l NAA, 2.0 mg/l BA and 2 g/l gellan gum, and by inducing the green callus into suspension culture using the MS liquid medium supplemented with 2.0 mg/l 2,4-D, 2.0 mg/l BA and 3% (w/v) sucrose (Wungsintaweekul *et al.*, 2007). The cell cultures appeared as small, pale yellow aggregates.

1.2 Detection of terpenoids and phytosterols by gas chromatography and gas chromatography – mass spectrometry

Detection of terpenoids and phytosterols in cell suspension cultures of *C. stellatopilosus* was carried out by using gas chromatography and gas chromatography – mass spectrometry. Phytol, GGOH, β -sitosterol, stigmasterol and campesterol were detected in the crude hexane extracts. These compounds have been found previously in cell suspension cultures of various plants, for example phytol in the cyanobacterium *Synechocystis* sp. (Disch *et al.*, 1998; Proteau *et al.* 1998), green algae *Scenedesmus obliquus* (Schwender *et al.*, 1996), phytol and β -sitosterol in cell suspension culture of *Catharanthus roseus* (Arigoni *et al.*, 1997, 1999), phytol, β -sitosterol and stigmasterol in cell suspension culture of *Lemna gibba*, *Hordeum vulgare* and *Daucus carota* (Lichtenthaler *et al.*, 1997). Unfortunately, plaunotol, the antipeptic ulcer substance of *C. stellatopilosus*, could not be found in this cell suspension culture.

It has been reported that plaunotol accumulation is observed in callus cultures of *C. stellatopilosus* grown on media containing gelling agents, especially gellan gum and agarose. Increased chlorophyll content, slow growth and light were found to stimulate plaunotol accumulation in *C. stellatopilosus* callus cultures (Morimoto and Murai, 1989). These results, however, could not be repeated in my laboratory and, thus, plaunotol accumulation in either the callus or cell suspension has not yet been observed.

In literature, there has been only one report on the study of plaunotol production in *in vitro* cultures of *C. stellatopilosus* (Morimoto, 1989). The report was on the callus cultures that showed plaunotol accumulation up to 0.17% of dry weight. Geranylgeraniol has also been found to accumulate in the suspension cultures of *C.*

stellatopilosus in the lag or stationary phase of cell growth at 0.05% of dry weight (Kitaoka *et al.*, 1989). Wungsintaweekul and coworkers have found that GGOH is produced in the lag phase of the culture cycle of *C. stellatopilosus* cell suspension culture (Wungsintaweekul *et al.*, 2007). In terms of plaunotol formation, however, both callus and cell suspension cultures failed to produce plaunotol under various conditions tested in this study. It is possible that the composition of medium, type and concentration of growth regulators and other supplements were not suitable for plaunotol formation in both cultures.

The resulting suspension culture appeared to produce phytosterols as its major metabolites. This was shown by a time-course study which exhibited a major peak of the phytosterol mixture during the 14-day-culture cycle of the suspension culture. The phytosterols were produced rapidly during the 4 days old of the culture age. Structure identification confirmed that the phytosterols were actually a mixture of stigmasterol and β -sitosterol. The formation of phytol, GGOH, β -sitosterol, stigmasterol and campesterol in the cell suspension allowed us to study the biosynthesis of these compounds, especially the origin of the isoprene units of their molecules by feeding experiments.

1.3 [1-¹³C]Glucose and [2-¹³C]sodium acetate feeding experiments on cell suspension cultures of *C. stellatopilosus*

The presence of both sterols in high amount in the suspension cultures of *C. stellatopilosus* allowed the study the isoprene origin although plaunotol itself was not produced in the cultures. Both phytosterols are commonly known to be biosynthesized from six isoprene units. Therefore, high incorporation of glucose into the phytosterols would be a good sign of success of the study. This was indeed the

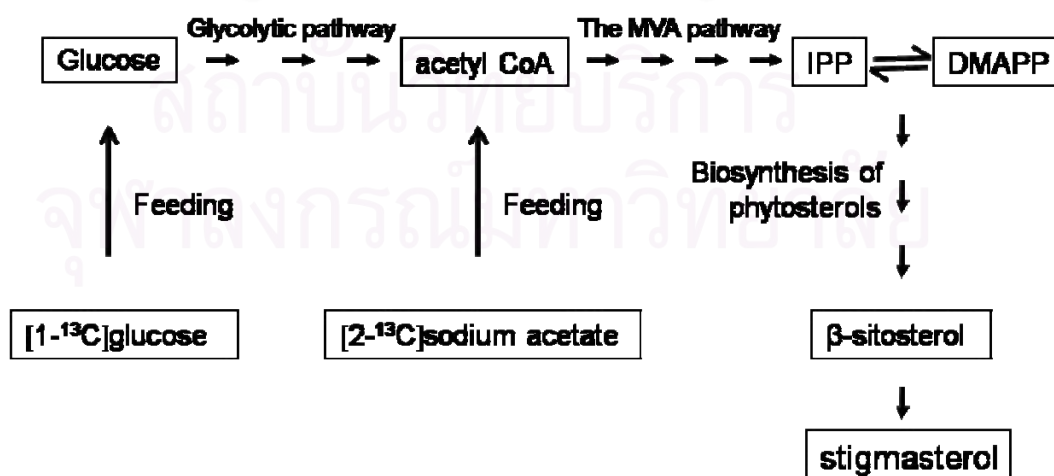
case when it was found that [1-¹⁴C]glucose was rapidly and almost exclusively incorporated into the phytosterols. Incorporation of [1-¹⁴C]glucose reached its maximum on day 4 after feeding, in agreement with the percentage on incorporation, suggesting that feeding experiments of isotopic precursors such as [1-¹³C]glucose and later with [2-¹³C]sodium acetate should be performed right after subculturing and the culture cells should be harvested on day 4.

2. The Origin of Isoprene Blocks of Phytosterol Skeleton

This study has shown that incorporation of [1-¹³C] glucose and [2-¹³C]sodium acetate into *C. stellatopilosus* suspension cultures during their highly active biosynthesis of phytosterols results in ¹³C-enrichment of some particular carbons in the molecules. This ¹³C-enrichment is best expressed as a value of L/U ratio of each carbon, where L (Labeled) is the ¹³C-NMR signal intensity of a phytosterol carbon obtained from the labeled [1-¹³C]glucose or [2-¹³C]sodium acetate incorporation and U (Unlabeled) is that obtained from unlabeled glucose or sodium acetate incorporation. Incorporation of the unlabeled precursors under the same conditions as the labeled precursors is, therefore, a control in which its ¹³C-NMR spectrum comes from the signals of the natural abundance of ¹³C presence in each carbon atom of the phytosterol molecules. Moreover, under this unlabelled control, the relative amount of β -sitosterol/stigmasterol should be the same as in the L condition. Therefore, the expression of L/U would reflect mainly the degree of ¹³C-enrichment of a particular carbon. The value of around 1.0 means there is no ¹³C-enrichment, whereas the value of more than 1.0 indicates ¹³C-enrichment at that particular carbon. However, prior to obtaining the L/U ratio of each ¹³C-peak, it is necessary to work out the relative ¹³C-signal intensity of each peak to be based on a particular

carbon not involved in any labeling process either by the mevalonate or non-mevalonate pathway. In this study, the peak intensity of C20 of β -sitosterol was chosen as having 100% intensity. The intensity of other peaks were then recalculated relative to that of C20. The values of L/U of all ^{13}C -signal peaks were then obtained. The results showed that 37 out of 58 carbons of both phytosterols were labeled by $[1-^{13}\text{C}]$ glucose, 35 out of the 58 carbons of both phytosterols were labeled by $[2-^{13}\text{C}]$ sodium acetate.

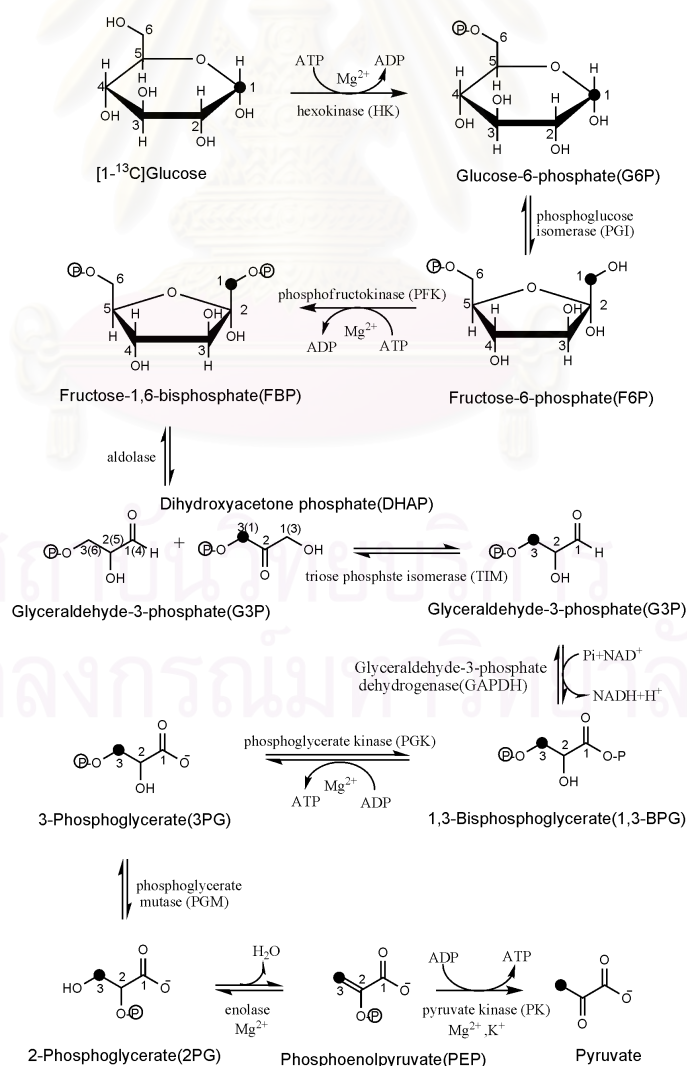
Analysis on various aspects which possibly contributed to the distribution of ^{13}C -labeling in β -sitosterol and stigmasterol led to the following conclusion: First, the isoprene unit used for the formation of β -sitosterol and stigmasterol is biosynthesized exclusively from the mevalonate pathway. Second, the value of 1.38 obtained from L/U ratio of β -sitosterol : L/U ratio of stigmasterol based on the feeding experiments with $[1-^{13}\text{C}]$ glucose calculation means that the ^{13}C -enrichment of β -sitosterol is slightly faster than that of stigmasterol by a factor of 1.38. This is likely to be due to the shorter biosynthetic steps of β -sitosterol compared to that of stigmasterol as follows:



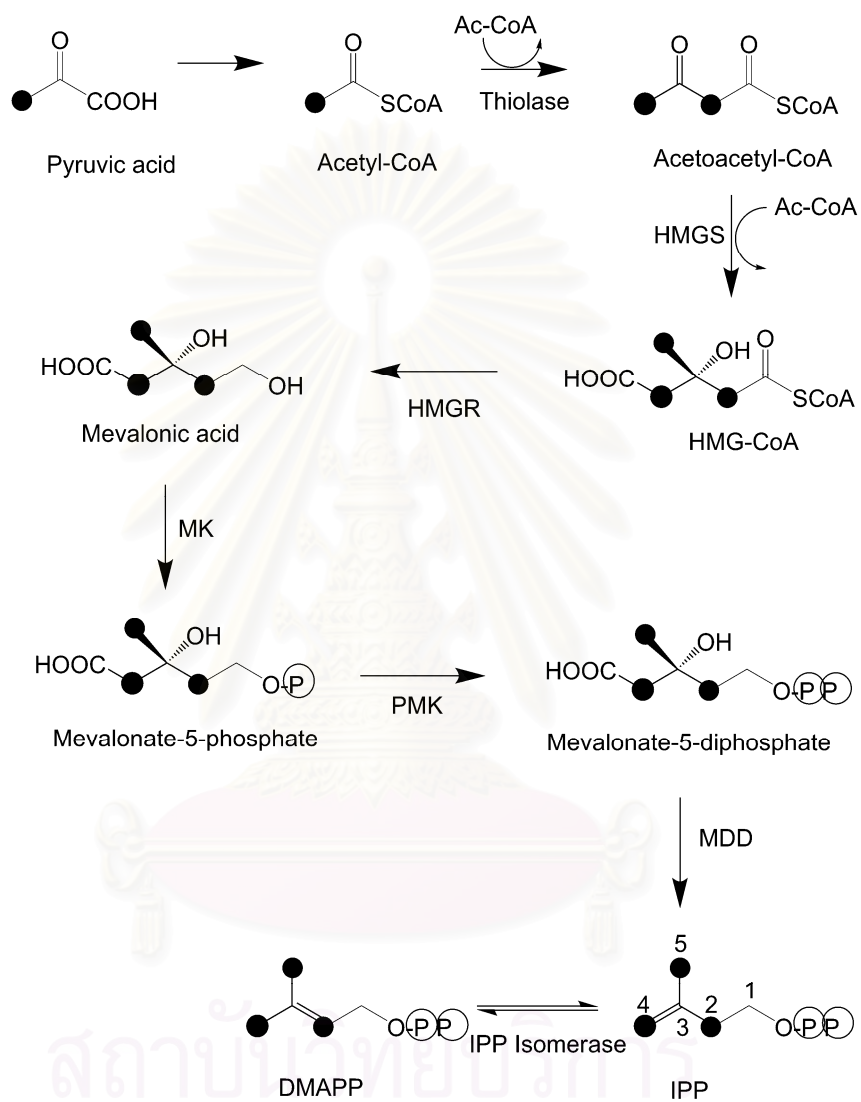
Similar results were also obtained with the [2-¹³C]sodium acetate but with the value of 2.02 (L/U ratio of β -sitosterol : L/U ratio of stigmasterol). Furthermore the higher value of 2.02 for acetate feeding than the 1.38 for glucose feeding also reflects the shorter route of acetate to be biosynthesized into the phytosterols compared to glucose.

The labeling pattern of the phytosterols can be explained by the metabolic sequence of [1-¹³C]glucose after being taken up by *C. stellatopilosus* suspension cultures as follows:

2.1 Conversion of [1-¹³C]glucose to pyruvate by glycolytic pathway

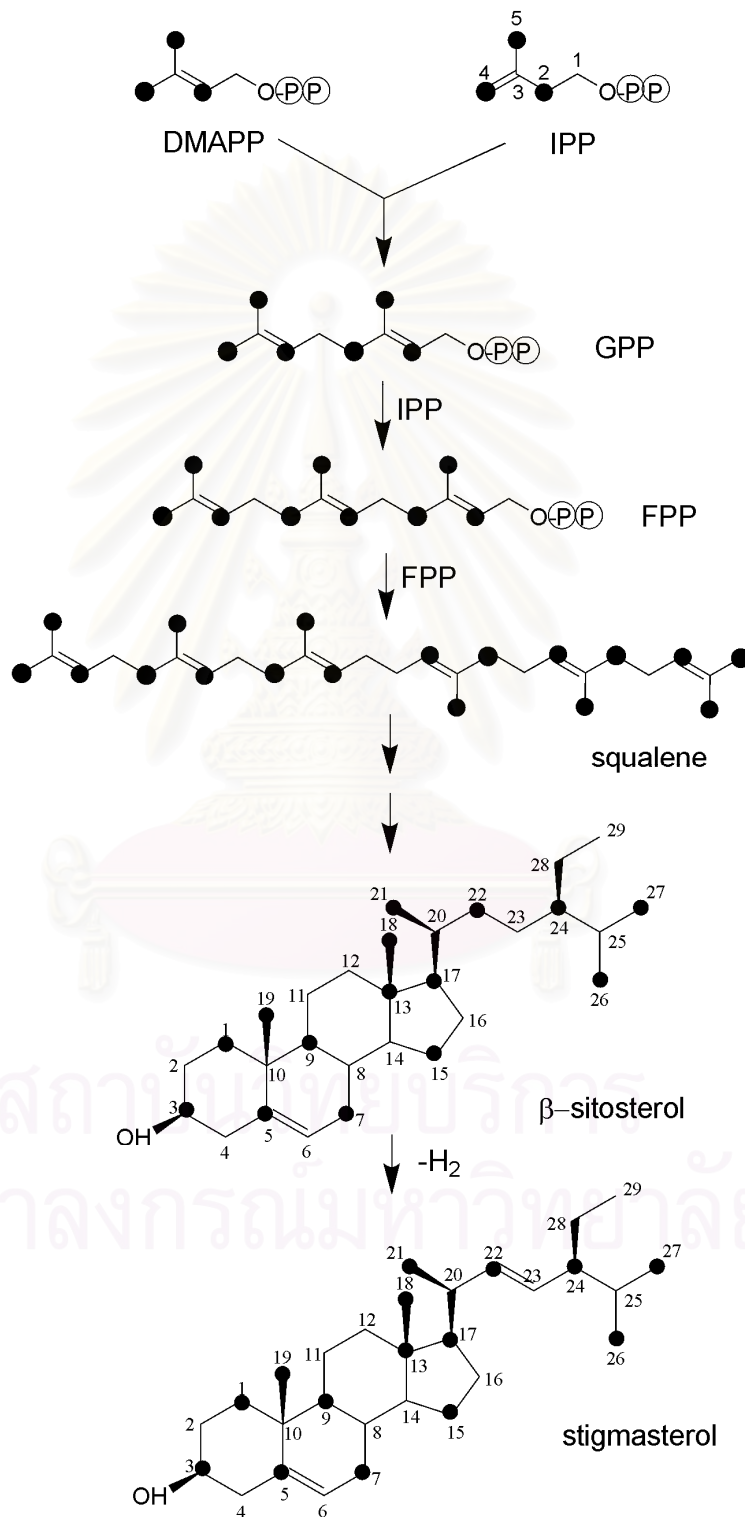


2.2 Biosynthesis of IPP from pyruvate *via* the mevalonate pathway



สถาบันวิจัยการ
จุฬาลงกรณ์มหาวิทยาลัย

2.3 Biosynthesis of β -sitosterol and stigmasterol from IPP



3. Possible Explanation on the Sole Operation of the MVA Pathway in *C. stellatopilosus* Cell Suspension Cultures.

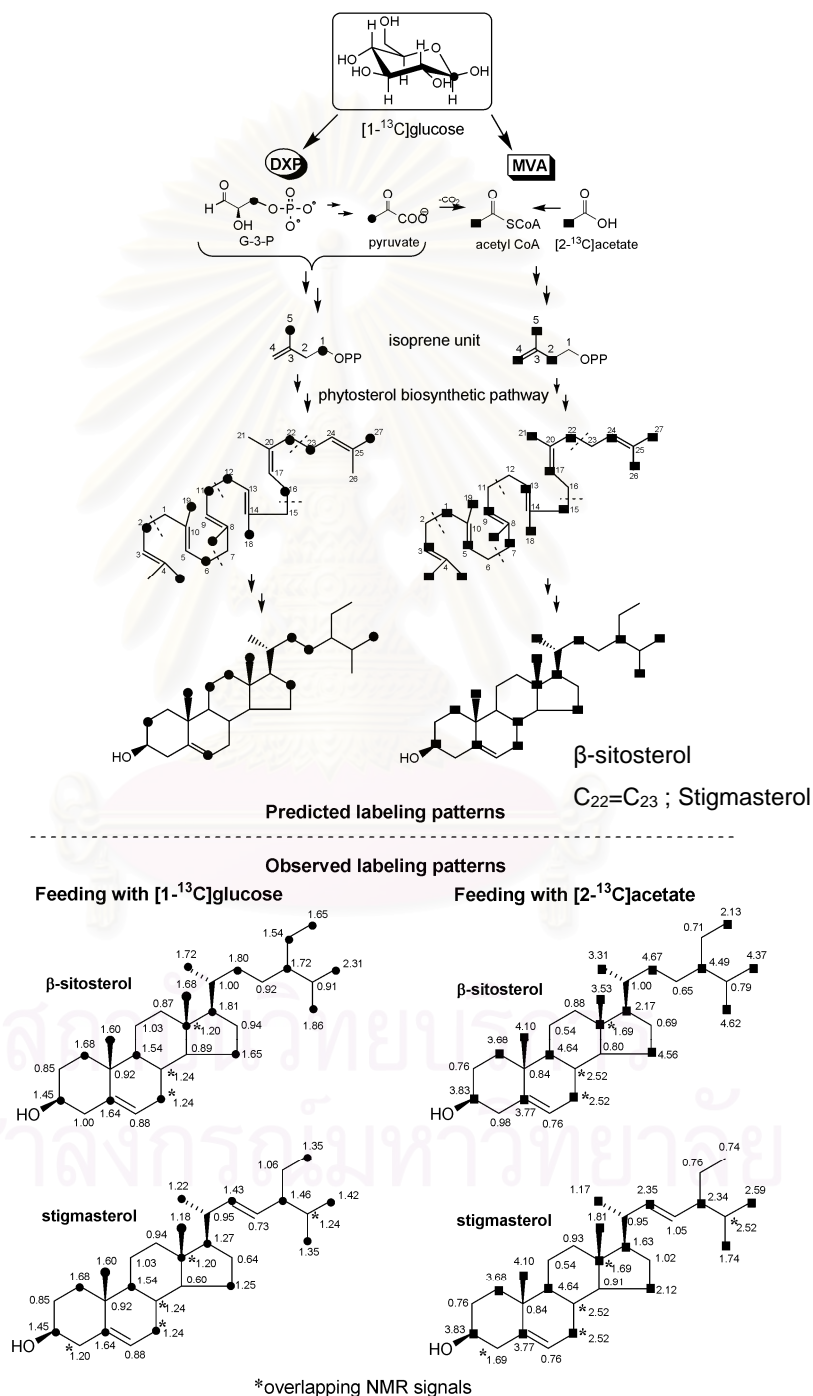


Figure 37 ¹³C-labeling patterns of β-sitosterol and stigmasterol after feeding with [1-¹³C]glucose (●) and [2-¹³C]sodium acetate (■) ; * the overlapping signal. Numbers indicated relative ¹³C-abundance.

Passing through the glycolysis, the molecule of glucose is converted to various glycolytic intermediate including glyceraldehyde 3-phosphate and pyruvate, which act as precursors for the DXP pathway, and acetyl CoA, as precursor for the MVA pathway. Therefore, feeding of [1-¹³C]glucose and [2-¹³C]sodium acetate could answer the question on the origin of isoprene units in the skeleton of β -sitosterol and stigmasterol. β -Sitosterol and stigmasterol formed from labeled glucose via the DXP or MVA pathways can be predicted to have different labeling patterns. [1-¹³C]Glucose feedings showed clearly that the observed labeling patterns of the two phytosterols were consistent with the isoprenoid origin from the MVA pathway. This result was confirmed by another feeding experiment using [2-¹³C]sodium acetate which also showed similar labeling pattern (Fig. 37). It should also be noted that the C28 and C29 of β -sitosterol and stigmasterol, which are not part of the isoprene unit, were also labeled. This was likely to be the results of the removal of the methyl groups of C4 squalene during the phytosterol biosynthesis.

Biosynthesis of plant sterols has been reported to involve the mevalonate pathway, whilst other terpenoids can be formed concurrently *via* the non-mevalonate pathway (Rohmer, 1999). Efficient utilization of mevalonate for sterol biosynthesis has been reported in duckweed (*Lemna gibba*), yet poor incorporation of 1-deoxy-D-xylulose has been noted (Schwender *et al.*, 1997). The use of [1-¹³C]glucose as a precursor has shown that three higher plants, i.e. duckweed, barley (*Hordeum vulgare*), and carrot (*Daucus carota*), possess two distinct routes for isoprene biosynthesis, producing their cytoplasmic sterols *via* the mevalonate pathway, but their chloroplast-bound terpenoids *via* the non-mevalonate pathway (Lichtenhaler *et al.*, 1997). Thus, phytol, β -carotene, lutein and plastoquinone-9 all displayed the isoprene labeling patterns of non-mevalonate pathway, but β -sitosterol and

stigmasterol had the isoprene labeling patterns of mevalonate pathway. This dichotomy in higher plants allows reasonable explanation for the many unexpected and inconclusive results concerning the biosynthesis of chloroplast isoprenoids which had mainly been interpreted *via* models involving compartmentation of the mevalonate pathway. The different pathways displayed may reflect the subcellular location of the terpenoid in question. Studies using plantlets and shoot cultures of *Marrubium vulgare* also indicated that these plant sterols were produced by the mevalonate pathway, whilst labdane diterpenes arose *via* the non-mevalonate pathway (Knoss *et al.*, 1997).

Study on the diterpenoid biosynthesis in *C. stellatopilosus* has shown earlier that plaunotol is biosynthesized from the DXP pathway associated with plastid compartment (Wungsintaweekul and De-Eknamkul, 2005) (Fig 38A). That evidence is in agreement with the finding of the oil globule of plaunotol in the plastid compartment. (Sitthithaworn, Potduang and De-Eknamkul, 2006) For phytosterol biosynthesis, a study in *C. stellatopilosus* green callus culture concluded that the isoprene units of these phytosterols are supplied from mixed pathway (De-Eknamkul and Potduang, 2003) (Fig 38B). This might result from the chloroplast which was differentiated in the green callus culture. In this study, feedings of isotopic glucose and sodium acetate into *C. stellatopilosus* suspension culture reveal that the source of IPP in the skeleton of phytosterols is exclusively from the MVA pathway (Fig 38C). The electron micrograph of *C. stellatopilosus* cells from suspension culture showed only the simple compartments which are essential for survival such as nucleus, cell membrane and large vacuoles (Fig. 34F). The absence of chloroplast in suspension culture limits the origin of the carbon blocks in phytosterol skeleton. It is, therefore, likely that cellular differentiation toward chloroplast development is a prerequisite for

expression of the DXP pathway, and might be the reason of the observed mixed isoprene origin in the callus and the sole mevalonate pathway in the cell suspension cultures. To confirm this conclusion, comparative studies with respect to gene expression of the DXP pathway in various cell types with different degree of differentiations (e.g. cell suspension, callus culture, and whole plant tissues), and their chloroplast development are necessary.

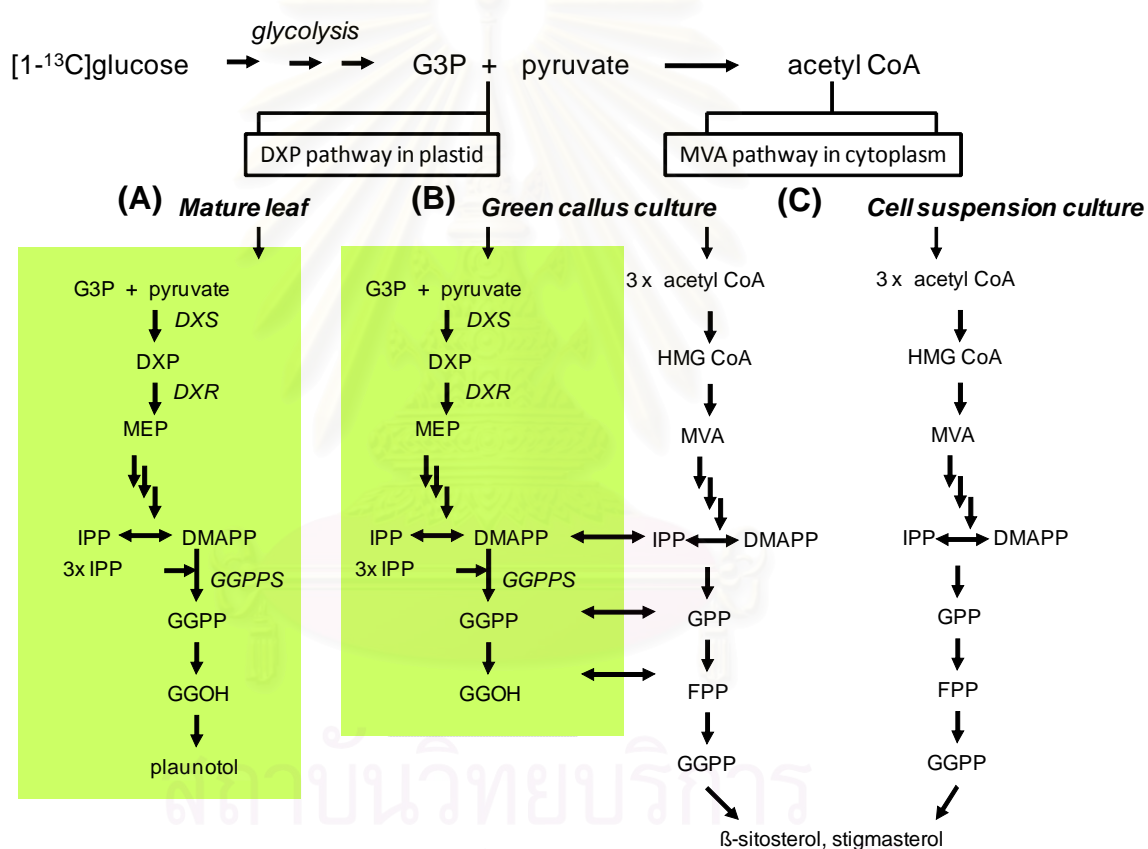


Figure 38 Proposed relationship between the DXP pathway and MVA pathway occurring in whole leaf (A), callus culture (B) and cell suspension cultures (C) of *C. stellatopilosus*

4. Comparative Analysis of *dxs*, *dxr* and *ggpps* Gene Expression Profiles of *C. stellatopilosus* Plant and Cell Cultures

The expression profiles of chloroplastic genes involved in the DXP pathway, i.e. *dxs*, *dxr* and *ggpps*, were investigated in different plant cells using semi-quantitative RT-PCR technique and compared with the housekeeping gene (*18S rRNA*). The *dxs*, *dxr* and *ggpps* genes were shown to locate in chloroplast (Wungsintaweekul, 2004; Sirisuntipong, 2007; Sitthithaworn *et al.*, 2001).

The *dxr* gene has been cloned from cDNA of young leaves of *C. stellatopilosus*. The full-length cDNA cloning encoding *dxr* by the RACE (rapid amplification of cDNA ends) method was performed. The results demonstrated that the cDNA of *dxr* contained an open reading frame of 1,404 bp encoding a deduced peptide of 467 amino acid residues with a predicted molecular mass of 50.6 kDa and isoelectric point of 5.64. The chloroplast transit peptides and a thiamine diphosphate-binding domain are presented in N-terminus amino acids. The amino acid sequence shares high homology (more than 70%) with amino acid sequences of Dxr from other higher plants. Expression of *dxr* transcripts in *C. stellatopilosus* from various parts were analyzed by semiquantitative RT-PCR method. The expression of *dxr* mRNA were unchanged in leaf 1st-5th but decreased in shoot while the amount of plaunotol are different, therefore *dxr* gene is not involved with the rate-limiting step enzyme of plaunotol biosynthesis (Sirisuntipong, 2007).

cDNAs encoding geranylgeranyl diphosphate synthase (GGPPS) of *C. stellatopilosus* have been isolated using the homology-based polymerase chain reaction (PCR) method. Its clones contained highly conserved aspartate-rich motifs (*DDXX(XX)D*) and its N-terminal residues exhibited the characteristics of chloroplast

targeting sequence. The result showed that the cloned GGPPS is a chloroplast protein (Sitthithaworn *et al.*, 2001).

The level of cell differentiation could affect the source of primary metabolites. Transmission electron microscopy (TEM) indicated different scattering of chloroplasts in plant cells from leaf, green callus and suspension cultures (Fig. 34). In leaf, it was clear that the chloroplasts were present densely in palisade cells. On the other hand, the green callus contained a few chloroplasts, whereas no chloroplasts were found in the cell culture. Screening of plaunotol containing cells including green callus and suspension culture indicated that artificial cultures lost their capability for plaunotol production. It can be hypothesized that the absence of some organelles causes the lack of essential enzymes for plaunotol biosynthesis. This result is related to the presence/absence of chloroplast from electron micrographs. This is probably a reason why suspension culture could produce high content of phytosterols and fatty acids but unable to produce the diterpenoid compounds such as plaunotol. Figure 36 illustrated the transcription levels of investigated genes as well as the relative intensities in correlation with *18S rRNA*. The results indicated that three genes were strongly expressed in plant leaf and green callus culture, but rarely found in suspension culture.

5. Conclusions

Cell suspension cultures of *Croton stellatopilosus* were fed with [1-¹³C]glucose and [2-¹³C]sodium acetate and cultured under control conditions. β -Sitosterol and stigmasterol were isolated and elucidated for their ¹³C-labeling patterns using quantitative NMR spectroscopy. Analysis of the patterns of ¹³C-enrichment revealed that all the isoprene units in the molecules of both phytosterols

were originated exclusively from the mevalonate pathway. These results were in contrast with a previous study using green callus cultures of *C. stellatopilosus* which showed that the isoprene units of β -sitosterol and stigmasterol were supplied equally from both the deoxyxylulose phosphate (DXP) and the mevalonate pathways (De-Eknamkul and Potduang, 2003). Observation by transmission electron microscope of sub-cellular structures of both cell types revealed that the callus cells contained partially differentiated chloroplasts, whereas the suspension cultured cells did not. Since the DXP pathway is known to be located in the chloroplasts, it is suggested that the presence of chloroplast structure is absolutely required for the expression of the DXP pathway.

Comparative analyses of mRNA expression of *dxs*, *dxr*, *ggpps* genes was investigated in leaf, green callus and suspension cultures cells in parallel with the transmission electron micrograph of these cells. The results indicated that those genes were strongly expressed in plant leaf and green callus culture, but rarely in cell suspension culture. Transcription of genes was related to the presence/absence of chloroplast compartment. This study demonstrated that the operation of two possible pathways of isoprene formation for *C. stellatopilosus* is dependent upon the type of cultures and the ability of chloroplast-forming cells.

References

Thai

- จุฬาลงกรณ์มหาวิทยาลัย. คณะเภสัชศาสตร์, ภาควิชาเภสัชพฤกษศาสตร์. 2530. **ชื่อสมุนไพรและประโยชน์.** กรุงเทพมหานคร : ภาควิชาเภสัชพฤกษศาสตร์ คณะเภสัชศาสตร์ จุฬาลงกรณ์มหาวิทยาลัย.
- ธราธร บุญแก้ว, 2534 การเพาะเลี้ยงเนื้อเยื่อต้นเปล้าน้อย (*Croton sublyratus*) เพื่อผลิตสารเปลาโนทอล. วิทยานิพนธ์ปริญญามหาบัณฑิต. สาขาเทคโนโลยีชีวภาพ บัณฑิตวิทยาลัย จุฬาลงกรณ์มหาวิทยาลัย.
- นันทวัน บุญยะประภัศร, บรรณานิการ. 2532. เปล้าน้อย. **จุลสารโครงการศูนย์ข้อมูลสมุนไพร มหาวิทยาลัยมหิดล 6:1-6.**
- ประเสริฐ พรหมมณี และคณะ. 2531. ตำราเภสัชกรรมไทยแผนโบราณ. กรุงเทพมหานคร: โรงพิมพ์จุฬาลงกรณ์ราชวิทยาลัย.
- เปรมจิต นาคประสิทธิ์, บรรณานิการ. 2526. เปล้าน้อย. **ข่าวสารเภสัชพาณิชย์ 34:4.** มหิดล, มหาวิทยาลัย คณะเภสัชศาสตร์. 2523. **สมุนไพรสวนสิริรุกชาติ.** กรุงเทพมหานคร: คณะเภสัชศาสตร์ มหาวิทยาลัยมหิดล.

English

- Adam, K.P., Thiel, R., and Zapp, J. 1999. Incorporation of [1-¹³C]deoxy-D-xylulose in chamomile sesquiterpenes. **Arch. Biochem. Biophys.** 369:127–132.
- Adam, K.P., Thiel, R., Zapp, J., and Becker, H. 1998. Involvement of the mevalonic acid pathway in terpenoid biosynthesis of the liverwort *Conocephalum conicum* and *Ricciocarpos natans*. **Arch. Biochem. Biophys.** 354:181–187.
- Adam, K.P., and Zapp, J. 1998. Biosynthesis of the isoprene units of chamomile sesquiterpenes. **Phytochemistry** 48:953–959.
- Airy Shaw, H.K. 1972. The Euphorbiaceae of Siam. **Kew Bull.** 26:191-363.
- Arigoni, D., Eisenreich, W., Latzel, C., Sagner, S., Radykewicz, T., Zenk, MH., and Bacher, A. 1999. Dimethylallyl pyrophosphate is not the committed precursor of isopentenyl pyrophosphate during terpenoid biosynthesis from 1-deoxyxylulose in higher plants. **Proc. Natl. Acad. Sci. USA** 96:1309-1314.

- Arigoni, D., Sagner, S., Latzel, C., Eisenreich, W., Bacher, A., and Zenk, M.H. 1997. Terpenoid biosynthesis from 1-deoxy-D-xylulose in higher plants by intramolecular skeletal rearrangement. **Proc. Natl. Acad. Sci. USA** 94:10600-10605.
- Barlow, A.J., Becker, H., and Adam, K.P. 2001. Biosynthesis of the hemi and monoterpene moieties of isoprenyl phenyl ethers from the liverwort *Trichocolea tomentella*. **Phytochemistry** 57:7–14.
- Bergamo, D.C.B., Kato, M.J., Bolzani, V. da S., and Furlan, M. 2005. Biosynthetic origins of the isoprene units of 4-nerolidylcatechol in *Potomorphe umbellata*. **J. Braz. Chem. Soc.** 16:1406–1409.
- Bonetti, P.O., Lerman, L.O., Napoli, C., and Lerman, A. 2003. Statin effects beyond lipid lowering – are they clinically relevant? **Eur. Heart J.** 24(3):225–248.
- Boonyaratavej, S., and Petsom, A. 1991. Chemical constituents of the roots of *Bridelia tomentosa* BL. **J. Sci. Soc. Thailand** 17:61-69.
- Bouvier, F., Rahier, A., and Camara, B. 2005. Biogenesis, molecular regulation and function of plant isoprenoids. **Prog. Lipid Res.** 44: 357–429.
- Broers, S.T.J. 1994. **Über die frühen Stufen der Biosynthese von Isoprenoiden in *Escherichia coli*. [On the early stages of isoprenoid biosynthesis in *E. coli*]**. Doctoral Dissertation. Nr. 10978, Swiss Federal Institute of Technology Zurich, Switzerland.
- Brown, G.D. 1998. The biosynthesis of steroids and triterpenoids. **Nat. Prod. Rep.** 15:653-696.

- Burlat, V., Oudin, A., Courtois, M., Rideau, M., and St-Pierre, B. 2004. Co-expression of three MEP pathway genes and geraniol 10-hydroxylase in internal phloem parenchyma of *Catharanthus roseus* implicates multicellular translocation of intermediates during the biosynthesis of monoterpene indole alkaloids and isoprenoid-derived primary metabolites. **Plant J.** 38:131-141.
- Charlwood, B.V., and Rhodes, M.J.C., ed. 1990. **Secondary production from plant tissue culture.** Oxford: Clarendon Press.
- Chikaraishi, Y., Naraoka, H., and Poulson, S.R. 2004. Carbon and hydrogen isotopic fractionation during lipid biosynthesis in a higher plant (*Cryptomeria japonica*). **Phytochemistry** 65:323–330.
- Coates, R.M., and Robinson, W.H. 1971. Stereoselective total synthesis of presqualene alcohol. **J. Am. Chem. Soc.** 93:1785-1786.
- Corey, E.J., and Yamamoto, H. 1970. New stereospecific synthetic routes to farnesol and its derivatives. **J. Am. Chem. Soc.** 92:6637-6638.
- De-Eknamkul, W., and Potduang, B., 2003. Biosynthesis of β -sitosterol and stigmasterol in *Croton sublyratus* proceeds via a mixed origin of isoprene units. **Phytochemistry** 62:389-398.
- Department of medical information, Sankyo Co., Ltd.1993. **Mucosal protective antiulcer drug: Kelnac capsules Kelnac fine granules.** Tokyo: Sankyo Co., Ltd.
- Dewick, P.M. 2002. **Medicinal natural product: a biosynthetic approach.** 2nd. John Wiley & Son. UK, pp. 167-225.

- Disch, A., Schwender, J., Müller, C., Lichtenthaler, H.K., and Rohmer, M. 1998. Distribution of the mevalonate and glyceraldehyde phosphate/pyruvate pathways for isoprenoid biosynthesis in unicellular algae and the cyanobacterium *Synechocystis* PCC6714. **Biochem. J.** 381-388.
- Duvold, T., Cali, P., Bravo, J.M., and Rohmer, M. 1997. Incorporation of 2-C-methyl-D-erythritol, a putative isoprenoid precursor in the mevalonate-independent pathway, into ubiquinone and menaquinone of *Escherichia coli*. **Tetrahedron Lett.** 38:6181–6184.
- Eisenreich, W., Bacher, A., Arigoni, D., and Rohdich, F. 2004. Biosynthesis of isoprenoids via the non-mevalonate pathway. **Cell. Mol. Life Sci.** 61:1401-1426.
- Enfissi, E.M.A., Frase, P.D., Lois, L., Boronat, A., Schuch, W., and Bramley, P.M. 2005. Metabolic engineering of the mevalonate and nonmevalonate isopentenyl diphosphate-forming pathways for the production of health-promoting isoprenoids in tomato. **Plant Biotech. J.** 3:17–27.
- Esser, J., and Chayamarit, K. 2001. Two new species and a new name in Thai *Croton* (Euphorbiaceae). **Thai For. Bull. (Bot.)** 29:51-57.
- Flesch, G., and Rohmer, M. 1988. Prokaryotic hopanoids: the biosynthesis of the bacteriohopane skeleton. **Eur. J. Biochem.** 175:405–411.
- Glauert A. M. 1984. **Fixation, Dehydration and Embedding of Biological Specimens: Practical Methods in Electron Microscopy**. pp 208. North-Holland Publishing Company, Amsterdam.
- Goldstein, J.L., and Brown, M.S. 1990. Regulation of the mevalonate pathway. **Nature** 343(6257):425–30.

- Hertewich, U., Zapp, J., Becker, H., and Adam, K.P. 2001. Biosynthesis of a hopane triterpene and three diterpenes in the liverwort *Fossombronia alaskana*. **Phytochemistry** 58:1049–1054.
- Herz, S., Wungsintaweekul, J., Schuhr, C.A., Hecht, S., Lüttgen, H., Sagner, S., Fellermeier, M., Eisenreich, W., Zenk, M.H., Bacher, A., and Rohdich, F. 2000. Biosynthesis of terpenoids: YgbB protein converts 4-diphosphocytidyl-2C-methyl-D-erythritol 2-phosphate to 2C-methyl-D-erythritol 2, 4-cyclodiphosphate. **Proc. Natl. Acad. Sci. USA** 97, 2486-2490.
- Hill, R.A. 2002. **Dictionary of Natural Products**. Version 9.1[CD-Rom]. Chapman and Hall, CRC Press, London, NY.
- Hinson, D.D., Chambliss, K.L., Toth, M.J., Tanaka, R.D., and Gibson, K.M. 1997. Posttranslational regulation of mevalonate kinase by intermediates of the cholesterol and nonsterol isoprene biosynthetic pathways. **J. Lipid Res.** 38(11):2216–2223.
- Hirai, N., Yoshida, R., Todoroki, Y., and Ohigashi, H. 2000. Biosynthesis of abscisic acid by the non-mevalonate pathway in plants, and by the mevalonate pathway in fungi. **Biosci. Biotech. Biochem.** 64:1148–1458.
- Horton, J.D. 2002. Sterol regulatory element-binding proteins: transcriptional activators of lipid synthesis. **Biochem. Soc. Trans.** 30(6):1091–1095.
- Kitaoka, M., Nagashima, H., and Kamimura, S. 1989. Accumulation of geranylgeraniol in cell suspension culture of *Croton sublyratus* Kurz. (Euphorbiaceae). **Sankyo Kenkyosho Nenpo** 41 : 169-173.
- Kitazawa, E., Kurabayashi, M., Kasuga, S., Oda, O., and Ogiso, A. 1982. New Ester of Diterpene Alcohol from *Croton sublyratus*. **Ann. Rep. Sankyo Res. Lab.** 34:39-41.

- Kitazawa, E., and Ogiso, A. 1981. Two diterpene alcohols from *Croton sublyratus*. **Phytochemistry** 20:287-289.
- Kitazawa, E., Ogiso, A., Sato, A., Kurabayashi, M., Kuwano, H., Hata, T., and Tamura, C. 1979. Plaunol A and B, new antiulcer diterpenelactones from *Croton sublyratus*. **Tetrahedron Lett.** 13:1117-1120.
- Kitazawa, E., Sato, A., Tanahashi, S., Kuwano, H., and Ogiso, A. 1980. Novel diterpene lactones with anti-peptic ulcer activity from *Croton sublyratus*. **Chem. Pharm. Bull.** 28:227-234.
- Knoss, W., Reuter, B., and Zapp, J. 1997. Biosynthesis of the labdane diterpene marrubiin in *Marrubium vulgare* via a non-mevalonate pathway. **Biochem. J.** 326:449–454.
- Koga, T., Inoue, H., Toshii, C., Okazaki, Y., Domon, H., and Utsui, Y. 2002. Effect of plaunotol in combination with clarithromycin or amoxicillin on *Helicobacter pylori* *in vitro* and *in vivo*. **J. Antimicrob. Chemother.** 50:133-136.
- Koga, T., Kawada, H., Utsui, Y., Domon, H., Tshii, C., and Yasuda, H. 1996. *In vitro* and *in vivo* antibacterial activity of plaunotol, a cytoprotective antiulcer agent, against *Helicobacter pylori*. **J. Antimicrob. Chemother.** 37:919-929.
- Kuzuyama, T., and Seto, H. 2003. Diversity of the biosynthesis of the isoprene units. **Nat. Prod. Rep.** 20:171–183.
- Lago, J.H.G., Ramos, C.S., Casanova, D.C.C., Morandim, A.A., Bergamo, D.C.B., Cavalheiro, A.J., Bolzani, V.da S., Furlan, M., Guimaraes, E.F., Young, M.C.M., and Kato, M.J. 2004. Benzoic acid derivatives from Piper species and their fungi toxic activity against *Cladosporium cladosporioides* and *C. sphaerospermum*. **J. Nat. Prod.** 67:1783–1790.

- Lange, B.M., and Croteau, R. 1999. Isoprenoid biosynthesis via a mevalonate-independent pathway in plants: cloning and heterologous expression of 1-deoxy-D-xylulose-5-phosphate reductoisomerase from peppermint. **Arch. Biochem. Biophys.** 365:170–174.
- Lange, B.M., Wildung, M.R., McCaskill, D., and Croteau, R. 1998. A family of transketolases that directs isoprenoid biosynthesis via a mevalonate independent pathway. **Proc. Natl. Acad. Sci. USA** 95:2100–2104.
- Lichtenthaler, H.K. 1999. The 1-deoxy-D-xylulose-5-phosphate pathway of isoprenoid biosynthesis in plants. **Ann. Rev. Plant Physiol. Plant Mol. Biol.** 50:47-65.
- Lichtenthaler, H.K., Schwender, J., Disch, A., and Rohmer, M. 1997. Biosynthesis of isoprenoids in higher plant chloroplasts proceeds via a mevalonate-independent pathway. **FEBS Lett.** 400:271-274.
- Lois, L.M., Campos, N., Putra, S.R., Danielsen, K., Rohmer, M., and Boronat, A. 1998. Cloning and characterization of a gene from *Escherichia coli* encoding a transketolase-like enzyme that catalyses the synthesis of 1-deoxy-D-xylulose 5-phosphate, a common precursor for isoprenoid, thiamin, and pyridoxol biosynthesis. **Proc. Natl. Acad. Sci. USA** 95, 2105-2110.
- Luckner, M. 1984. **Secondary metabolism in microorganisms, plants, and animals.** Springer-Verlag, Berlin, pp. 211-213.
- Lüttgen, H., Rohdich, F., Herz, S., Wungsintaweekul, J., Hecht, S., Schuhr, C.A., Fellermeier, M., Sagner, S., Zenk, M.H., Bacher, A., and Eisenreich, W. 2000. Biosynthesis of terpenoids: YchB protein of *Escherichia coli* phosphorylates the 2-hydroxy group of 4-diphosphocytidyl-2C-methyl-D-erythritol. **Proc. Natl. Acad. Sci. USA** 97, 1062-1067.

- Masse, G., Belt, S.T., and Rowland, S.J. 2004. Biosynthesis of unusual monocyclic alkenes by the diatom *Rhizosolenia setigera*. **Phytochemistry** 65:1101–1106.
- McCaskill, D., and Croteau, R. 1998. Some caveats for bioengineering terpenoid metabolism in plants. **TIBTECH** 16:349-355.
- McGarvey, D.J., and Croteau, R. 1995. Terpenoid metabolism. **Plant Cell** 7:1015–1026.
- Morimoto, H. 1989. Plaunotol manufactured by plant tissue cultures of *Croton* species. Jpn. Kokai Tokkyo Koho JP 63, 317,090 [88, 317, 090] (Cl.C12P7/18), 26 Dec 1988, Appl. 87/152, 920, 19 Jun 1987:**Chemical Abstracts** 110:Abstract No. 171823q.
- Morimoto, H., and Murai, F. 1989. The effect of gelling agents on plaunotol accumulation in callus cultures of *Croton sublyratus* Kurz. **Plant Cell Rep.** 8:210-213.
- Murakami, K., Okajima, K., Harada, N., Isobe, H., Liu, W., Johno, M., and Okabe, H. 1999. Plaunotol prevents indomethacin-induced gastric mucosal injury in rats by inhibiting neutrophil activation. **Ailment. Pharmacol. Ther.** 13:521-530.
- Murashige, T., and Skoog, F., 1962. A revised medium for rapid growth and bioassays. with tobacco tissue culture. **Physiol. Plant** 15:473-497.
- Nilubol, N. 1992. Process for extraction and purification of plaunotol. **United States patent.** No. 826702.
- Nualkaew, N., De-Eknamkul, W., Kutchan, T.M., and Zenk, M.H. 2005. Geranylgeraniol formation in *Croton stellatopilosus* proceeds via successive monodephosphorylations of geranylgeranyl diphosphate. **Tetrahedron Lett.** 46:8727-8731.

- Nualkaew, N., De-Eknamkul, W., Kutchan, T.M., and Zenk, M.H. 2006. Membrane-bound geranylgeranyl diphosphatases: purification and characterization from *Croton stellatopilosus* leaves. **Phytochemistry**. 67(15):1613-1620.
- Ogiso, A., Kitasawa, E., Kobayashi, S., Komai, N., Matsunuma, N., and Kataumi, S. 1985. (CS-684), A new antipeptic ulcer agent. **Sankyo Kenkyusho Nempo** 37:1-39.
- Ogiso, A., Kitazawa, E., Kurabayashi, M., Sato, A., Takahashi, S., Noguchi, H., Kuwano, H., Kobayashi, S., and Mishima, H. 1978. Isolation and structure of antipeptic ulcer diterpene from Thai medicinal plant. **Chem. Pharm. Bull.** 26: 3117-3123.
- Ogiso, A., Kitazawa, E., Mikuriya, I., and Promdej, C. 1981. Original plant of Thai crude drug, Plau-noi. **Shoyakugaku Zasshi**. 35(4):287-290.
- Ponglux, D., Wongseripipatana, S., Phadungcharoen, T., Ruangrunsi, N., and Likhitwitayawuid, K.. 1987. **Medicinal Plants**. Bangkok : Victory Power Point Corp.
- Potduang, B. 2000. **Isoprenoid biosynthesis in callus cultures of *Croton sublyratus***. Doctoral dissertation, Pharmaceutical Chemistry and Natural Products, Graduate School, Chulalongkorn University.
- Proteau, P.J. 1998. Biosynthesis of phytol in the cyanobacterium *Synechocystis* sp. UTEX 2470: utilization of the non-mevalonate pathway. **J. Nat. Prod.** 61: 841-843.
- Rodriguez-Concepcion, M., and Boronat, A. 2002. Elucidation of the methylerythritol phosphate pathway for isoprenoid biosynthesis in bacteria and plastids. A metabolic milestone achieved through genomics. **Plant Physiol.** 130:1079-1089.

- Rohdich, F., Lauw, S., Kaiser, J., Feicht, R., Köhler, P., Bacher, A., and Eisenreich, W. 2006. Isoprenoid biosynthesis in plants 2C-methyl-d-erythritol-4-phosphate synthase (IspC protein) of *Arabidopsis thaliana*. **FEBS J.** 273:4446-4458.
- Rohdich, F., Wungsintaweekul, J., Lüttgen, H., Fischer, M., Eisenreich, W., Schuhr, CA., Fellermeier, M., Schramek, N., Zenk, MH., and Bacher, A. 2000. Biosynthesis of terpenoids: 4-diphosphocytidyl-2-C-methyl-D-erythritol kinase from tomato. **Proc. Natl. Acad. Sci. USA** 97:8251–8256.
- Rohdich, F., Wungsintaweekul, J., Fellermeier, M., Sagner, S., Herz, S., Kis, K., Eisenreich, W., Bacher, A., and Zenk, M.H. 1999. Cytidine 5'-triphosphate-dependent biosynthesis of isoprenoids: YgbP protein of *Escherichia coli* catalyzes the formation of 4-diphosphocytidyl-2-C-methylerythritol. **Proc. Natl. Acad. Sci. USA** 96:11758-11763.
- Rohdich, F., Zepeck, F., Adam, P., Hecht, S., Kaiser, J., Laupitz, R., Grawert, T., Amslinger, S., Eisenreich, W., Bacher, A., and Arigoni, D. 2003. The deoxyxylulose phosphate pathway of isoprenoid biosynthesis: studies on the mechanisms of the reactions catalyzed by IspG and IspH protein. **Proc. Natl. Acad. Sci. USA** 100(4):1586-1591.
- Rohmer, M. 1999. The discovery of a mevalonate independent pathway for isoprenoid biosynthesis in bacteria, algae and higher plants. **Nat. Prod. Rep.** 16:565-574.
- Rohmer, M., Knani, M., Simonin, P., Sutter, B., and Sahm, H. 1993. Isoprenoid biosynthesis in bacteria : a novel pathway for the early steps leading to isopentenyl diphosphate. **Biochem. J.** 295:517-524.

- Rohmer, M., Seeman, M., Horbach, S., Bringer-Meyer, S., and Sahn, H. 1996. Glyceraldehyde 3-phosphate and pyruvate as precursors of isoprenic units in an alternative non-mevalonate pathway for terpenoid biosynthesis. **J. Am. Chem. Soc.** 118:2564-2566.
- Sakakura, Y., Shimano, H., and Sone, H. 2001. Sterol regulatory element-binding proteins induce an entire pathway of cholesterol synthesis. **Biochem. Biophys. Res. Commun.** 286(1):176–183.
- Schuhr, C.A., Radykewicz, T., Sagner, S., Latzel, C., Zenk, M.H., and Arigoni, D. 2003. Quantitative assessment of crosstalk between the two isoprenoid biosynthesis pathways in plants by NMR spectroscopy. **Phytochem. Rev.** 2:3-16.
- Schwarz, M.K. 1994. **Terpene biosynthesis in *Ginkgo biloba*: a surprise story**. Doctoral Dissertation. Nr.10951, Swiss Federal Institute of Technology Zurich, Switzerland.
- Schwender, J., Seemann, M., Lichtenthaler, H.K, and Rohmer, M. 1996. Biosynthesis of isoprenoids (carotenoids, sterols, prenyl side-chains of chlorophyll and plastoquinone) via a novel pyruvate/glycero-aldehyde-3-phosphate non-mevalonate pathway in the green alga *Scenedesmus obliquus*. **Biochem. J.** 316:73-80.
- Schwender, J., Zeidler, J., Groner, R., Muller, C., Focke, M., Braun, S., Lichtenthaler, FW., and Lichtenthaler, HK. 1997. Incorporation of 1-deoxy-D-xylulose into isoprene and phytol by higher plants and algae. **FEBS Lett.** 414:129-134.

- Seemann, M., Tse Sum Bui, B., Wolff, M., Miginiac-Maslow, M., and Rohmer, M. 2006. Isoprenoid biosynthesis in plant chloroplasts via the MEP pathway: direct thylakoid/ferredoxin-dependent photoreduction of GcpE/IspG. **FEBS Lett.** 580:1547–1552.
- Shiratori, K., Watanabe, S., and Takeuchi, T. 1993. Role of endogenous prostaglandins in secretin and plaunotol-induced inhibition of gastric acid secretion in the rat. **Am. J. Gastroenterol.** 88:84-89.
- Sirisuntipong, T. 2007. **cDNA Cloning of 1-deoxy-D-xylulose 5-phosphate reductoisomerase from *Croton stellatopilosus* Ohba leaves.** Master's Thesis. Programme of Pharmaceutical Sciences, Graduate School, Prince of Songkla University.
- Sitthithaworn, W., Kojima, N., Viroonchatapan, E., Suh, D.Y., Iwanami, N., Hayashi, T., Noji, M., Saito, K, Niwa, Y., and Sankawa, U. 2001. Geranylgeranyl diphosphate synthase from *Scoparia dulcis* and *Croton sublyratus* plastid localization and conversion to a farnesyl diphosphate synthase by mutagenesis. **Chem. Pharm. Bull.** 49:197-202.
- Sitthithaworn, W, Potduang, B., and De-Eknamkul, W. 2006. Localization of Plaunotol in the leaf of *Croton stellatopilosus* ohba. **ScienceAsia** 32:17-20.
- Sprenger, G.A., Schörken, U., Wiegert, T., Grolle, S., De Graaf, A.A., Taylor, S.V., Begley, T.P., Bringer-Meyer, S., and Sahm, H. 1997. Identification of a thiamin-dependent synthase in *Escherichia coli* required for the formation of the 1-deoxy-D-xylulose 5-phosphate precursor to isoprenoids, thiamin, and pyridoxol. **Proc. Natl. Acad. Sci. USA** 94:12857-12862.

- Spurgeon, S. L., and Porter, J. W. 1981. **Biosynthesis of Isoprenoid Compounds**.
Porter, J. W., Spurgeon, S. L., Eds.; John Wiley and Sons: New York, pp. 1–53.
- Stefan, B., Andreas J., Gerd G., and Wilhelm B. 2006. Dynamic pathway allocation in early terpenoid biosynthesis of stress-induced lima bean leaves
Phytochemistry 67:1661-1672.
- Takagi, A., Koga, Y., Aiba, Y., Kabir, A.M., Watanabe, S., Ohta-Tada, U., Osaki, T. Kamiya, S., and Miwa, T. 2000. Plaunotol suppresses interleukin-8 secretion induced by *Helicobacter pylori*: therapeutic effect of plaunotol on *H. pylori* infection. **J. Gastroenterol. Hepatol.** 15:374-380.
- Takahashi, S., Kurabayashi, M., Kitazawa, E, Haruyama, H., and Ogiso, A. 1983. Plaunolide, a furanoid diterpene from *Croton sublyratus*. **Phytochemistry** 22:302-303.
- Takahashi, S., Kuzuyama, T., Watanabe, H., and Seto, H. 1998. A 1-deoxy-D-xylulose 5-phosphate reductoisomerase catalyzing the formation of 2-C-methyl-D-erythritol 4-phosphate in an alternative nonmevalonate pathway for terpenoid biosynthesis. **Proc. Natl. Acad. Sci. USA** 95:9879–9884.
- Tansakul, P., and De-Eknamkul, W. 1998. Geranylgeraniol-18-hydroxylase : The last enzyme on the plaunotol biosynthetic pathway in *Croton sublyratus*.
Phytochemistry 47 :1241-1246.
- Thiel, R., and Adam, K.P., 2002. Incorporation of [1-¹³C]1-deoxy-D-xylulose into isoprenoids of the liverwort *Conocephalum conicum*. **Phytochemistry** 59: 269–274.
- Thiel, R., Adam, K.P., Zapp, J., and Becker, H. 1997. Isopentenyl diphosphate biosynthesis in liverwort. **Pharmacology Lett.** 7:103–105.

- Umlauf, D., Zapp, J., Becker, H., and Adam, K.P. 2004. Biosynthesis of the irregular monoterpene artemisia ketone, the sesquiterpene germacrene D and other isoprenoids in *Tanacetum vulgare* L. (Asteraceae). **Phytochemistry** 65: 2463–2470.
- Ushiyama, S., Matsuda, K., Asai, F., and Yamazaki, M. 1987. Stimulation of prostaglandin production by (2E,6Z,10E)-7-hydroxymethyl-3, 11, 15-trimethyl-2, 6, 10, 14-hexadecatetraen-1-ol (plaunotol), a new anti ulcer drug, *in vitro* and *in vivo*. **Biochem. Pharmacol.** 36:369-375.
- Vongchareonsathit, A. 1994. **Quantitative analysis of Plaunotol in the leaves and tissue cultures of *Croton sublyratus* Kurz.** Master's Thesis. Programme of Biotechnology, Graduate School, Chulalongkorn University.
- Vongchareonsathit, A., and De-Eknamkul, W. 1998. Rapid TLC-densitometric analysis of plaunotol from *Croton sublyratus* leaves. **Planta Med.**64:279-280.
- Weber, LW., Boll, M., and Stampfl, A. 2004. Maintaining cholesterol homeostasis: sterol regulatory element-binding proteins. **World. J. Gastroenterol.** 10:3081–3087.
- Wungsintaweekul, J. 2004. **Molecular Cloning of 1-Deoxy-D-xylulose 5-Phosphate Synthase from *Croton stellatopilosus* Ohba.** The JSPS-NRCT report.
- Wungsintaweekul, J., and De-Eknamkul, W. 2005. Biosynthesis of plaunotol in *Croton stellatopilosus* proceeds via the deoxyxylulose phosphate pathway. **Tetrahedron Lett.** 46:2125-2128.

Wungsintaweekul, J., Sriyapai, C., Kaewkerd, S., Tewtrakul, S., Kongduang, D, and De-Eknamkul, W., 2007. Establishment of *croton stellatopilosus* suspension culture for geranylgeraniol production and diterpenoid biosynthesis. **Z. Naturforsch.** 62c:389-396.

Welzen, P.C.V. Flora of Thailand Euphorbiaceae. [Online] Available from <http://www.nationaalherbarium.nl/thaieuph/ThSearchSc/ThSearchScT.htm> [cited in 22 June 2007]

Wright, J.L.C., McInnes, A.G., Shimizu, S., Smith, D.G., and Walter, J.A. 1978. Identification of C-24 alkyl epimers of marine sterols by ^{13}C nuclear magnetic resonance spectroscopy. **Can. J. Chem.** 56:1898-1903.



สถาบันวิทยบริการ
จุฬาลงกรณ์มหาวิทยาลัย

VITA

Mr. Damrong Kongduang was born on June, 22, 1976 in Ubonratchathani, Thailand. He received his Bachelor's Degree in Chemistry in 1998 (2nd degree honor) from Mahasarakham University, Thailand. In March-September, 1998, he worked as a Chemist in Khon Kaen Fishing Net Factory Co. Khon Kaen.

During his Ph.D. study, he received a scholarship from The Royal Golden Jubilee (RGJ) Ph.D. Program, Thailand Research Fund (TRF) in 2000 to study in the program of Pharmaceutical Chemistry and Natural Products, Faculty of Pharmaceutical Sciences, Chulalongkorn University.

Publications:

1. Wungsintaweekul, J., Sriyapai, C., Kaewkerd, S., Tewtrakul, S., **Kongduang, D.** and De-Eknamkul, W. 2007. Establishment of *Croton stellatopilosus* suspension culture for geranylgeraniol production and diterpenoid biosynthesis. *Z. Naturforsch.* 62c, 389-396.
2. Wungsintaweekul J, Sirisuntipong T, **Kongduang D**, Losupanporn T, Ounaron A, Tansakul P, and De-Eknamkul W. 2008. Transcription profiles analysis of genes encoding 1-deoxy-D-xylulose 5-phosphate synthase and 2C-methyl-D-erythritol 4-phosphate synthase in plaunotol biosynthesis from *Croton stellatopilosus*. *Biol. Pharm. Bull.* in press.
3. **Kongduang D**, Wungsintaweekul J, and De-Eknamkul W. 2008. Biosynthesis of β -sitosterol and stigmaterol proceeds exclusively via the mevalonate pathway in cell suspension cultures of *Croton stellatopilosus*. *Tetrahedron Lett.* in press.
4. **Kongduang D**, Wungsintaweekul J, and De-Eknamkul W. 2008. Comparative analyses of mRNA expressions of genes involved in the methylerythritol phosphate pathway in both organized and disorganized cells of *Croton stellatopilosus*. *Biotechnology Lett.* (submitted)

Oral presentations:

Kongduang, D. Analysis of Transcription Profiles of Genes Involved in the Non-Mevalonate Pathway in Organized and Disorganized Cells of *Croton stellatopilosus*. RGJ-Ph.D. Congress IX, The Thailand Research Fund April 4-6, 2008, Jomtien Palm Beach Resort Pattaya, Chonburi, Thailand.

Poster presentations:

- Kongduang, D.**, Sriyapai, C., Kaewkerd, S., Wungsintaweekul J. and De-Eknamkul, W. 2005. Geranylgeraniol and β -sitosterol biosynthesis : a preliminary study on the carbon blocks in *Croton stellatopilosus* suspension culture. The Fourth Indochina Conference on Pharmaceutical Sciences (PHARMA INDOCHINA IV) November 10 – 13, 2005, Unification Palace, Ho Chi Minh City, Vietnam.
- Kongduang, D.**, Wungsintaweekul J. and De-Eknamkul, W. 2007. Biosynthesis of β -Sitosterol and stigmaterol proceeds exclusively via mevalonate pathway in the disorganized cell suspension cultures of *Croton stellatopilosus* Annual Meeting of the Phytochemical Society of North America July 21-25, 2007, Donald Danforth Plant Science Center, St. Louis, Missouri, USA.